Energy performance optimization of a CO_2 Booster refrigeration system with parallel compression

Filipe Baganha Ferreira de Lemos

Master's Dissertation

FEUP Supervisor: Prof. José Luís Alexandre

Company Supervisor: Eng. Fábio André Carvalho

U.PORTO

FEUP FACULDADE DE ENGENHARIA
UNIVERSIDADE DO PORTO

Master in mechanical engineering

October 2022

Abstract

The 21st century paradigm forces the thought of engineering from an energy efficiency and environmental impact point of view. Specifically in refrigeration, due to the increasingly pressure from regulations, the usage of CO_2 as a refrigerant is becoming increasingly popular because it significantly contributes to the reduction of greenhouse gas emissions and the destruction of the ozone layer. However, using this refrigerant brings with it some challenges from the energy efficiency point of view, mainly due to its low temperature at the critical point.

Using as an object of study a Booster CO_2 refrigeration system with parallel compression used in a medium-sized supermarket, performance optimization was sought to optimize, measured using EER, without changing the system's components, keeping it always working with no restrictions and fulfilling the refrigeration need of the store at any moment, only using parameterization. It was decided that three parameters of study would be studied: liquid receiver pressure, medium temperature stage suction pressure and medium temperature stage superheat. Having made this decision, the study was carried out not only from a practical point of view, but also with theoretical supports through specific software from the maker of refrigeration compressors that allows simulating the real system with more precision than a traditional numerical calculation model. The reason behind is the fact that, being made from the same manufacturer as the real installation's compressors, the software accounts for variable compressor efficiency with parameter change, data that is not available to consult.

The changes were spaced at least 24h in order to ensure not only the functioning of the system, but also to have a sufficient amount of data for the study. The data used in the analysis were collected at a frequency of 5 minutes, between 00:00 and 05:00 in the morning, when there is no activity in the store. The ambient temperatures were between 18ºC and 22ºC during this period. The experimental results suggest that, under these conditions:

- An increase of 1 bar in the receiver tank pressure is reflected, on average, in a 0.9% increase in the EER, resulting in economic savings of 0.07€/hour in electrical bills, for the supermarket;
- An increase of 1 bar in the MT suction pressure is reflected, on average, in a 0.85% increase in the EER, resulting in an economic savings of 0.07€/hour;
- A 1K reduction in the MT superheat is reflected, on average, in a 0.25% increase in the EER, resulting in an economic savings of 0.02€/hour.

Otimização energética de um sistema de refrigeração Booster a CO_2 com compressão paralela

Resumo

O paradigma atual do século XXI obriga a pensar na engenharia do ponto de vista da eficiência energética e do impacto ambiental. Especificamente na refrigeração, e devido à crescente pressão imposta pelas legislações, o uso de CO_2 como refrigerante é cada vez mais popular devido à sua contribuição significativa para a redução de emissões de gases que provocam efeito de estufa e destruição da camada do ozono. Contudo, o uso deste refrigerante tem associado alguns desafios do ponto de vista da sua rentabilização energética, devido principalmente à sua baixa temperatura no ponto crítico.

Tendo como base uma central de refrigeração *booster* a CO_2 com compressão paralela usado num supermercado de média dimensão, procurou-se otimizar a sua performance energética, medida através do EER, sem recorrer a qualquer alteração de componentes, mantendo a central a funcionar sem qualquer impedimento e cumprindo com os requisitos de frio da loja em qualquer momento, apenas alterando a parametrização do Sistema. Foi decidido que três parâmetros iriam ser estudados: pressão do depósito de líquido, pressão de aspiração do estágio de media temperatura e sobreaquecimento desse mesmo estágio. Tomada esta decisão, procurou-se realizar o estudo não só do ponto de vista prático, mas também com um suporte teórico, através de um *software* específico do fabricante de compressores que permite simular o sistema real de forma mais precisa, quando comparada a uma modelação tradicional em *software* de cálculo numérico. Isto porque, sendo do mesmo fabricante dos compressores utilizados na instalação, prevê as quedas de rendimento energético dos mesmos, informação não acessível para consulta.

Períodos mínimos de 24h entre alterações foram garantidos de modo a assegurar o funcionamento do sistema e a ter uma quantidade de dados suficientes para o estudo. Os dados utilizados na análise foram recolhidos com uma frequência de 5 minutos, entre as 00:00 e as 05:00 da manhã, horário sem atividade na loja. As temperaturas ambientes encontravam-se entre os 18ºC e os 22ºC, neste período. Os resultados sugerem que, nestas condições:

- Um aumento em 1 bar na pressão de depósito reflete-se, em média, num aumento de 0.9% no EER, resultando, do ponto de vista económico para o supermercado, numa poupança 0.07€/hora em gastos de eletricidade;
- Um aumento em 1 bar na pressão de aspiração MT reflete-se, em média, num aumento de 0.85% no EER, resultando numa poupança económica de 0.07€/hora;
- Uma redução em 1K no sobreaquecimento dos postos MT reflete-se, em média, num aumento de 0.25% no EER, resultando numa poupança económica de 0.02€/hora.

Acknowledgments

First of all, I want to formally thank the opportunity that RACE S.A. gave to me, which allowed me to learn among highly experienced engineers and experience the work of a refrigeration engineer. Particularly, I want to thank my supervisor, Eng. Fábio Carvalho, Eng. Vítor Nogueiro and Eng. Bernardo Silva, for the patience, availability and general help during the development of this work. I am very thankful for the information they taught me.

Second of all, I would like to thank my FEUP supervisor, Prof. José Alexandre, and the personnel at FEUP for making this project viable and achievable.

Last but not the least, I would like to express my gratitude towards my parents, for supporting me during my whole academic education and for making me believe everything is possible with hard work and dedication. To my girlfriend Rita, a special thanks for putting up with me during all these years and for the unconditional support during the development of this dissertation. To all my friends that made life a lot more enjoyable during these 5 years, a toast to you.

"I'm speechless… I'm speechless. We have to remember these days, because there is no guarantee they will last forever. Enjoy them as long as the last. I love you guys." -SV

Table of Contents

Nomenclature

$\dot{V}_{Dis}$	Displaced volume	$[m^3/s]$
$\dot{V}_v$	Swept volume	$[m^3/s]$
m	Mass	$[kg]$
η_i	Isentropic efficiency	$[-]$
η_v	Volumetric efficiency	$[-]$
AC	Air-Conditioning	
AVG	Average	
CO_2	Carbon-Dioxide	
DHW	Domestic Hot Water	
EEV	Electronic Expansion Valve	
GWP	Global Warming Potential	
h	Specific entalpy	$[kJ/kg]$
HPC	High-pressure compressor	
IHX	Internal Heat Exchanger	
IT	Intermediate-Temperature	
LPC	Low-pressure compressor	
LR	Load Ratio	
LT	Low-Temperature	
MT	Medium-Temperature	
ODP	Ozone Depletion Potential	
ODS	Ozone Depletion Substances	
P	Electric power	[W]
PWM	Pulse width modulation	

R134a	1,1,1,2-Tetrafluoroethane refrigerant nomenclature	
R404A	Blended hydrofluorocarbon used as a refrigerant	
R744	CO_2 refrigerant nomenclature	
RPRV	Receiver Pressure Release Valve	
COP	Coefficient of Performance	$[-]$
Q	Energy transfer	$[W]$
W	Work	$[W]$
g	Gravitational acceleration	$[m/s^2]$
q	Heat transfer per unit mass	$[kJ/kg]$
w	Work transfer per unit mass	$[kJ/kg]$

Subscripts

amb	Ambient
c	Compressor
f	Fluid
g	Gas
h	From hot source
l	From cold source
LT	Low temperature
MT	Medium temperature
net	Total net
r	refrigeration

Superscripts

$\cdot$	(dot above script) – per unit time

List of figures

List of Tables

1. Introduction

In this first introductory chapter, a brief history of refrigeration and its current global context will be accessed in order to then better understand the importance of the project, always focusing on the use of CO_2 as a refrigerant. Afterwards, a brief introduction of the company where the work was developed and their main object of focus in this study will be presented, as well as the project's main goal. At the end of the chapter, the main structure of the dissertation is presented.

1.1 Brief history of refrigeration

Refrigeration has been a key part of human well-being along with the production of heat, the first being harder and more complex than the second. Its history can be divided, essentially, in two historical times:

- From pre-history until the 19th century;
- Artificial refrigeration, from the 19th century until today.

1.1.1 Pre-history until 19th century

Refrigeration needs appeared as a conservation method for hunting produce. Rapidly, humans understood that fresh meat and other foods stayed fresh for longer when stored in colder places like caves, holes, snow piles or exposing water to the sky, taking advantage of radiation at night, freezing it. An intermediate process in the history of refrigeration consisted in the addition of chemicals to water such as sodium and potassium nitrate, lowering its temperature. This popularized the consumption of cold drinks. [1]

In the end of the 17th century, with the invention of the microscope, bacteria and other living forms were found in abundance in water and foods. Studies made by scientists such as *Louis Pasteur* demonstrated that those living organisms were mostly responsible for the rotting of food and, consequently, the spread of infections and diseases. It was also found that the reproduction bacteria could be prevented by lowering temperatures, highlighting the importance of refrigeration, ramping up the production of ice and, essentially, kicking off the so called "*Ice revolution*". The usage of natural ice, however, had many inconveniences from a geographical standpoint, as well as representing a health hazard due to the pollutants in it. An alternative was needed. [2]

1.1.2 Artificial Refrigeration Era

In 1834, American inventor *Jacob Perkins* developed the first working vapor-compression system, using ether in a closed cycle. Although it showed the potential of vapor-compression usage, the system wasn't commercially successful, and iceboxes made by carpenters designed to take advantage of large ice of blocks for refrigeration became the norm for household refrigeration, despite its disadvantages. [3]

The biggest drive to change came from the proliferation of home electricity in cities in the beginning of the 20^{th} century, which allowed the production of ice by the consumers. In the 1920's the first electric refrigerator appeared and by the 1950's almost 7 million units were produced annually. From then on, household artificial refrigeration became part of daily human activity. An example of one of these early refrigerators can be seen in Figure 1.1. [2]

FIGURE 1.1: GE 'MONITOR TOP' REFRIGERATOR FROM THE 1920'S [4]

Nowadays, cold production is an essential part of many industrial and commercial activities such as the conservation of perishable products, on the chemical industry, construction, metal industry, biology, medicine, and many other areas. In the next section a deeper study of the global context of refrigeration is made. [2]

1.2 Global Context of refrigeration

Today, the refrigeration industry goes well beyond the conservation of perishable foods and its economic, social, and environmental impact is of great importance and should be well understood and taken into account by policy makers and project designers. This sub-chapter will focus on the relationship between refrigeration and economics, energy and environment. [5]

1.2.1 Refrigeration and economics

To better illustrate the dimension of the sector worldwide, an estimation of the number of refrigeration systems in operation was made and the results can be seen in Table 1.

TABLE 1: NUMBER OF REFRIGERATION SYSTEMS IN OPERATION WORLDWIDE PER APPLICATION [5]

Application	Sectors	Equipment	Number of units in operation
Refrigeration and food	Domestic refrigeration	Refrigerators and freezers	2 billion
	Commercial refrigeration	Commercial refrigeration equipment	120 million
	Refrigerated transport	Refrigerated vehicles	5 million
		Refrigerated containers	1.2 million
	Refrigerated storage	Cold stores	50.000
Air conditioning	Air conditioners	Air-cooled systems	1.6 billion
		Water chillers	40 million
	Mobile air-conditioning systems	Air-conditioned vehicles	1 billion
Refrigeration and health	Medicine	Magnetic Resonance Imaging machines	50.000
Refrigeration in Industry	Liquefied Natural Gas (LNG)	LNG receiving terminals	126
		LNG tanker fleet (vessels)	525
Heat Pumps		Heat Pumps	220 million
Leisure and sports		Ice rinks	17.000

Based on the data above, the total number of cold systems in operation worldwide corresponds roughly to 5 billion units, of which around 2 billion are domestic refrigerators. This translates to roughly an amount of 500 billion USD, representing roughly three quarters of global supermarket sales. [5]

1.2.2 Refrigeration and energy

Most refrigeration installations are electrically driven, and the consumption is increasing over time, with more and more AC units being installed every year due to 1) increasing refrigeration demands and 2) global warming. This translates to a total consumption of about 20% the overall energy usage worldwide, which means energy usage efficiency is a major concern and huge energy savings potential comes from an increase in efficiency. The growth of electricity demand for cooling by 2050 is estimated to be double of the demand of 2019. [5]

1.2.3 Refrigeration and environment

Sustainable development is a keyword in today's industries and refrigeration has a big role in this development, providing new technologies that are being implemented as a means to capture CO_2 from large industrial facilities and power producing plants, and not to mention that refrigeration machines and heat pumps are among the most environmentally friendly technologies that may use renewable energy. [5]

However, the adverse effects of refrigeration, more specifically refrigerants, for the environment must also be addressed. As much as 37% of the global-warming impact of refrigeration systems are due to direct emissions (by leakage) of fluorocarbons (CFCs, HCFCs and HFCs), with the remaining 63% coming from indirect emissions from the production of electricity by means of burning fossil fuels. The objectives for refrigeration for the upcoming years in order to fight global warming are as follows: [5]

- Reduction of fluorocarbons emissions to the atmosphere through better built components that minimize leakage and reduce refrigerant charge and/or development of alternative refrigerants with negligible or no climate impact;
- Reduction in primary energy usage by increasing energy efficiency of refrigeration systems; [5]

The use of CO_2 as a refrigerant may lead to a significant decrease in emissions while maintaining or even decreasing energy consumption. The importance of this refrigerant will be explored in the next sub-chapter.

1.3 Importance of CO_2 as a refrigerant

1.3.1 Environmental advantages

Since the beginning of the artificial refrigeration era, choosing the right refrigerant has always been a challenge. The usage of CO_2 as a refrigerant (R744), a natural fluid, dates back to mid-19th century, however it was quickly replaced during the 1930's with the big expansion of CFC refrigerants (Chlorofluorocarbons) and later HCFC (Chlorofluorocarbons), especially in the air conditioning sector. CFC were chosen as they are excellent refrigerants, very stable and safe for the human body, so much so that they were used as inhalers, directly in contact with the human organism. [6] [7]

In 1974 however, scientists *Rowland* and *Molina* published a study [8] demonstrating that CFC usage was related to the depletion of the ozone layer in the stratosphere, recommending a complete ban on the future release of CFC's to the environment. Following this study, in 1987, an international agreement called Montreal Protocol was signed in order to phase out ozone depletion substances (ODS). However, HCFC gases were initially not included, because they have a very low Ozone Depletion Potential (ODP). ODP can be defined as a given refrigerant's effect on atmospheric ozone, with a reference point usually adopted as ODP=1 for CFC R11. The higher the ODP, the higher the effects on the ozone layer. Global warming potential (GWP) was also later defined for gases as an index comparing the climate impact of its emission to that of emitting the same amount of carbon dioxide. HCFC, although have a low ODP, have a substantial GWP, which fuelled their phase-out. Following amendments have been made in order to gradually phase out more and more harmful refrigerants and can be seen in Table 2. [9] [7]

TABLE 2: CHRONOLOGY OF IMPOSED MEASURES BY THE MONTREAL PROTOCOL AND FOLLOWING AMENDMENTS [6]

Year	Event	Measures
1987	Montreal Protocol	Regulation of the production and consumption of ODS, focused specially on CFC gases with high ODP and global warming potential.
1990	London Amendment	Definition of the phase-out of all CFC refrigeration gases, halon and Carbon tetrachloride in developed and developing countries.
1992	Copenhagen Amendment	Inclusion of HCFC gases on the ODS phase-out list, just for developed countries. Limiting the usage of common fluids such as R22 and R123.
1997	Montreal Amendment	Phase-out of HCFC extended to all countries and a deadline for the phase-out of Bromomethanes was set to 2005 and 2015 for developed and developing countries, respectively.
1999	Beijing Amendment	A higher restriction was defined for the production and commercialization of HCFC gases
2016	Kigali Amendment	Definition of the phase-down of HFC due to their high GWP value.

With tighter and tighter restrictions made by the Montreal Protocol, namely the higher pressure to reduce GWP, the usage of chlorine-free HFC refrigerants became more popular, as a better alternative to CFC refrigerants, and had the advantage of being almost totally compatible with existing systems. With retrofit procedure many existing CFC systems were converted in HFC systems. Therefore, the majority of industries made the conversion to HFCs without altering their manufacturing processes, workflows, or employee skill sets. This was expected from an economic and technological standpoint as fluorinated gases (referred to from now on as F-gases) were not subject to any restrictions at the time. Consequently, we may say that the Montreal Protocol is what caused the HFCs to enter the market. In fact, the Montreal Protocol gave rise to the HFCs. [6]

In 2006, with a revision in 2014, the EU proposed a new regulation regarding F-gas usage, in order to limit the amount of the most important F-gases sold in EU territory and slowly phase them down, with the objective of moving towards more climate-friendly technologies. The regulation also bans the use of F-gases in many new types of equipment where less harmful alternatives are available, such as household items like fridges, AC, foams and sprays. The prevention of emissions is also mentioned, with the incentive of proper maintenance and servicing and end of life gas recovery. [10]

With these new regulations and with new developments in the usage of ozone friendly refrigerants, such as the work of scientist and engineer Gustav Lorentzen in 1990, and with the development of low ODP and GWP refrigerants, namely HFO's (Hydrofluro-Olefins), a new era of refrigeration was born, where environmental conscience is key. CO_2 became a competitive solution from environmental standpoint, as it has a GWP of 1, by definition, and an ODP of 0. In fact, pressure to use low GWP fluids was the main reason why R744 became, once more, a viable option for refrigerant. [7]

1.3.2 Practical advantages

Besides environmental advantages such as low GWP, no ODP and the fact that no impending legislations phasing down or phasing out exist, making R744 a long-term refrigerant, the usage of this refrigerant can bring serious advantages when compared to traditional HFCs. For once, it has a high refrigeration capacity due to high volumetric cooling capacity (22545 kJ/m^3, almost 5 times higher than that of R404A), reducing compressor displacement and sizing of heat exchangers and pipe work. The pressure-drops in pipe works and heat exchangers are also lower than traditional fluids, reducing the impact of long suction and liquid lines. High-pressures and density translates in high heat transfers in evaporators and condensers/gas coolers, improving heat exchange efficiency and, therefore, the usage of smaller evaporators and lower quantity of refrigerant needed. However, these higher pressures will require more robust materials to withstand them, potentially increasing costs. The comparison of saturation pressures of R744A with R744 and R134a can be seen in Figure 1.2. [11]

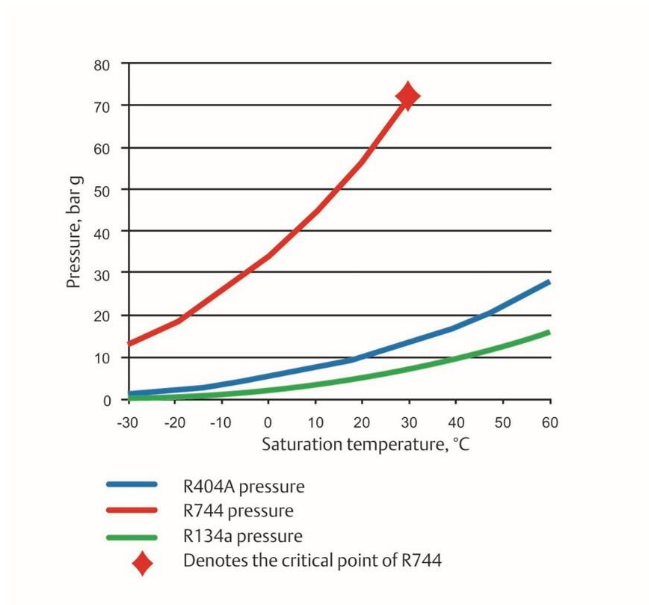

FIGURE 1.2: P-T DIAGRAM COMPARING CO_2 WITH R404A AND R134A [11]

Apart from these main practical advantages, R744 is much less expensive to produce and is widely available, even though purity for CO_2 usage in refrigeration must be higher than 99.99%. It is also non-flammable, non-toxic, stable and has a good miscibility with compressor lubricants for oil return. [11]

1.4 Presentation of the company

This project was developed with *RACE S.A. – Refrigeration & Air- Conditioning Engineering*, a company focused on developing, implementing, and managing competitive and integrated refrigeration solutions for commercial and industrial use. Besides that, the company also develops climatization and building efficiency projects, with a team of over 300 people working from Portugal, Brazil and Romania.

Race S.A. originated from the fusion of two former companies, *Selfrio S.A.* and *Sistavac S.A.*, the first one being founded in 1985 and the second one in 1992, with the introduction of an HVAC department. In 2011 both companies became one, with the designation *of Sistavac S.A.*, and in 2017 a rebranding was made, changing the official name to *RACE S.A.*, whose logo can be seen in Figure 1.3.

RACE

Refrigeration & Air Conditioning Engineering

FIGURE 1.3: RACE S.A. LOGO [12]

1.5 Project Goals

With the development of this project, the main goal set to achieve was the maximization of energy efficiency across the company's working and future installations, resorting only to parameterization and optimization of the systems' control units, with no further intervention. The main equation in play during the development of this work is defined in equation 1.1, with the definition of COP – Coefficient of Performance or EER – Energy Efficient Ratio, a more correct name for usage in refrigeration. For the sake of simplicity and conformity with the company's work nomenclature, only EER will be used from now on.

$$EER = \frac{\dot{Q}_l}{\dot{W}_{net}} \quad \textbf{1.1}$$

where:

- $\dot{Q}_l$ is the refrigeration power of a given system;
- $\dot{W}_{net}$ is the total net electrical energy power consumed by the system.

Given that the refrigeration power is usually defined in the project and not as an input variable, EER maximization will be made focusing on the reduction of electrical energy reduction, i.e., the reduction of compressor power usage, the main player in energy spendings on a refrigeration unit.

1.6 Structure of the dissertation

This dissertation is divided in 5 main topics. After this introductory chapter, an extensive state of the art chapter focused on refrigeration cycles will be made, from a baseline Carnot Cycle to the most developed real R744 systems today. This can be found on chapter 2.

Chapter 3 focuses on the presentation of the problem, fully characterizes the studied refrigeration system, and presents the methodology used in order to choose the changing parameters, how the theoretical study was done, how data was gathered from the system and how it calculates EER. In chapter 4, the results from both the *software* simulations and the real study are presented and analysed, as well as an economic analysis which aims to predict savings in the system from the increase in EER.

Chapter 5 concludes the work done summarizing the most important conclusions obtained in chapter 4 and suggests some future work that could complement the developed work.

2 Refrigeration cycles overview

In this chapter, an overview of relevant refrigeration cycles, as well as all its components will be made, starting with the reversed Carnot cycle, ideal and real vapor compression refrigeration cycles, and then focusing in detail on CO_2 cycles and the particular components these types of installations have. The methods of controlling these installations and the principles for real-world applications are also presented.

2.1 Reversed Carnot Cycle

Latent heat provides a higher quantity of energy to be manipulated and extracted from a fluid. In theory, a certain quantity of fluid can be isentropically compressed and expanded between two temperature (and pressure) values, defined between the fluid's freezing point and critical temperature. This enables the theoretical extraction of energy in a fully reversible way and is referred to as *reversed Carnot cycle*. The cycle can be schematically seen in Figure 2.1 a) which shows the four essential components needed for this cycle to work: a compressor, a turbine and a condensation and evaporation unit. [7] [13]

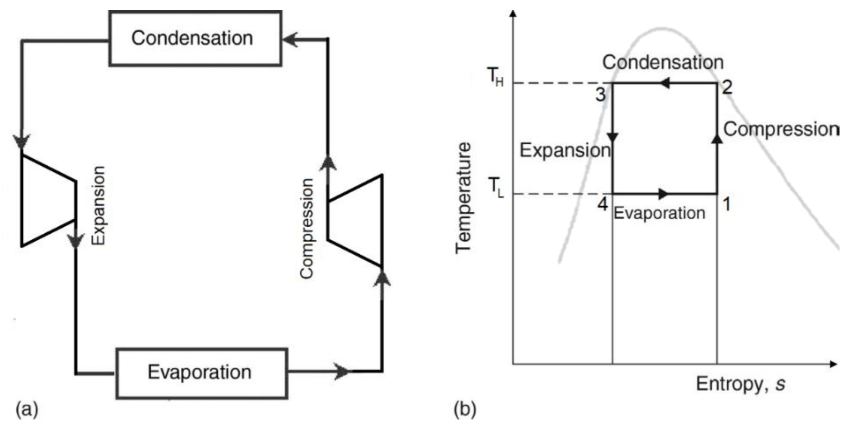

FIGURE 2.1: THE REVERSED CARNOT CYCLE: (A) CIRCUIT SCHEMATIC AND (B) TEMPERATURE–ENTROPY DIAGRAM (ADAPTED FROM [7])

In Figure 2.1 b), on the T-s diagram, the four fundamental processes of the cycle can be seen with T_h and T_l being the temperatures at which the hot and cold source are at. [13] [14]

The energy transfers in the cycle are given by the following equations:

$$Q_h = T_h(S_3 - S_2) \quad \textbf{2.1}$$

Where Q_h is the heat rejected between the fluid and the cold source.

Given that the cycle is fully reversible, that $S_1 = S_2$ and $S_3 = S_4$:

$$Q_l = T_l(S_1 - S_4) = T_l(S_2 - S_3) \qquad \textbf{2.2}$$

$$W_{net} = Q_h - Q_l \qquad \textbf{2.3}$$

Substituting equation 2.2 and 2.3 into equation 1.1:

$$COP_{Carnot} = \frac{T_l}{T_h - T_l} \qquad \textbf{2.4}$$

These reversible cycles have a great importance in the study of refrigeration cycles because, although they are technically impossible to implement, have two important properties: a) between the same temperature points, no real cycle can have higher EER than the ideal cycle and b) between the same temperature limits, all ideal cycles will have the same EER, as this property only depends on the temperatures, as seen previously in equation 2.4. The ideal cycles provide therefore a good comparison base to the real cycles. [9]

2.1.1 Cycle infeasibility

Although useful as a comparison, the ideal cycle has many practical limitations, making it impossible to implement:

- The usage of a turbine to do the fluid expansion poses serious structural limitations due to the phase change inside this element. Besides, the work produced from expansion is low compared to the work necessary for the compression, which makes the turbine economically unviable. The solution is to replace the turbine to an isenthalpic expansion valve;
- Similarly, in the compressor, the same physical constraints occur when dealing with a phase change, and it’s difficult to start the compression process strictly in point 1. Consequently, although there are some additional constraints, it is easier to do a dry compression, thus avoiding the formation of bubbles of liquid inside the element;
- Even ignoring the two reasons stated above, the heat transfer is physically impossible to do isothermally. As such, a finite temperature difference must be present, making the heat transfer processes irreversible. [13]

2.2 Ideal vapor compression refrigeration cycle

Considering what was mentioned in 2.1.1, an ideal cycle was developed, taking into consideration the compression in gaseous state and the replacement of the turbine with an expansion valve. This cycle can be seen in Figure 2.2 , with Figure 2.2 a) showing the circuit schematic. [13]

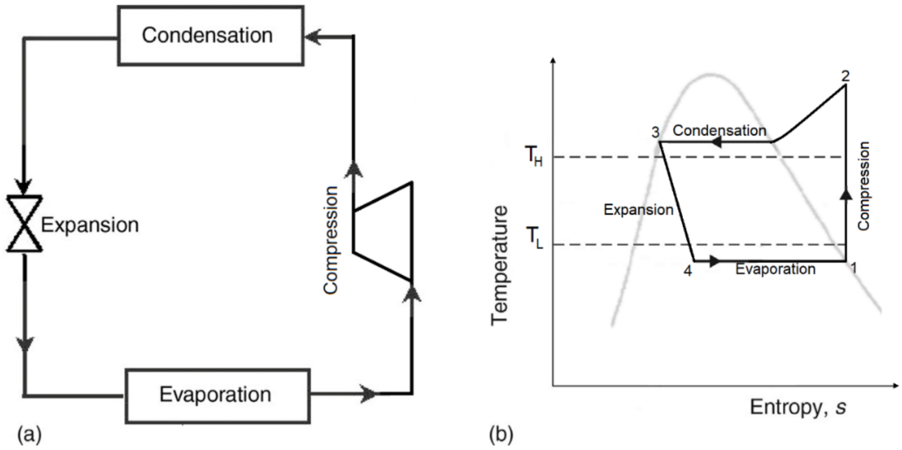

FIGURE 2.2: THE IDEAL VAPOR-COMPRESSION CYCLE: (A) CIRCUIT SCHEMATIC AND (B) TEMPERATURE- ENTROPY DIAGRAM (ADAPTED FROM [7])

The represented processes are analogous to the Carnot cycle and can be seen in Figure 2.2 b) with, once again, T_H and T_L being the temperatures at which the hot and cold source are at. [2]

The energy balance can be done assuming that, at steady state, there are no significant variations of kinetic and potential energy in the components of the system and the mass flow through these are constant and equal for every component. On the evaporator:

$$q_L = h_1 - h_4 \qquad \textbf{2.5}$$

With similar simplifications, and considering the reversibility of the compressor:

$$w_c = h_2 - h_1 \qquad \textbf{2.6}$$

Using 2.5 and 2.6, the coefficient of performance of the cycle can now be calculated:

$$COP = \frac{q_l}{w_c} = \frac{h_1 - h_4}{h_2 - h_1} \qquad \textbf{2.7}$$

As seen, EER depends on the given refrigeration fluid's enthalpy. As such, it is generally easier to represent refrigeration cycles in Mollier diagrams, rather than T-s diagrams. These relate pressure and enthalpy and make the representation of the vapor compression cycle simpler to read. Since heat exchanges in this cycle are isobaric, the evolutions on the evaporator and condenser are represented by horizontal lines, and the expansion represented by a vertical line, as the enthalpy is constant. The ideal vapor compression refrigeration cycle is represented in a p-h diagram in Figure 2.3. [2]

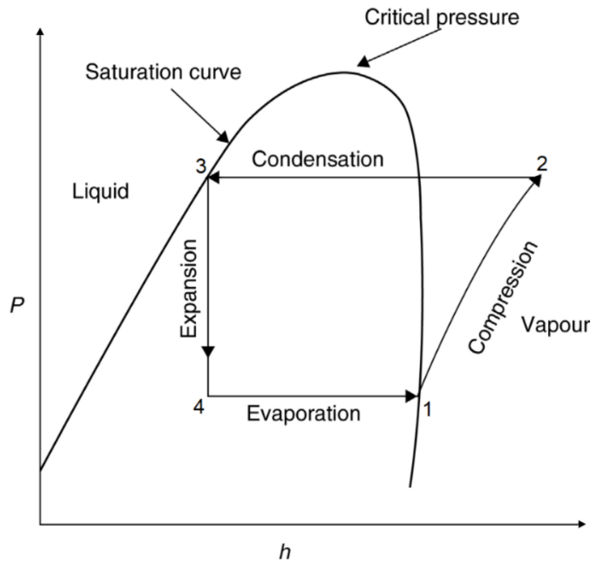

FIGURE 2.3: GENERAL P-H DIAGRAM OF AN IDEAL VAPOR COMPRESSION REFRIGERATION CYCLE (ADAPTED FROM [7])

2.2.1 Superheat and Subcooling

It is difficult to control with precision the state the fluid is at in the end of the heat exchanges in the cycle. For example, when entering the compressor, the fluid isn't necessarily in the state of saturated vapor and can be a superheated gas. In the same way, when leaving the condenser, the liquid might not be saturated but instead a compressed liquid. When this happens, the fluid is said to be superheated and subcooled, respectively. The superheat and subcooling can be quantified:

- $Superheat = T_{entrance\ of\ compressor} - T_{sat.@evaporation\ pressure}$
- $Subcooling = T_{sat.@condensation\ pressure} - T_{condensor\ exit}$

Superheat and subcooling can be obtained independently from one another. A cycle with both superheat and subcooling can be seen in Figure 2.4. [2]

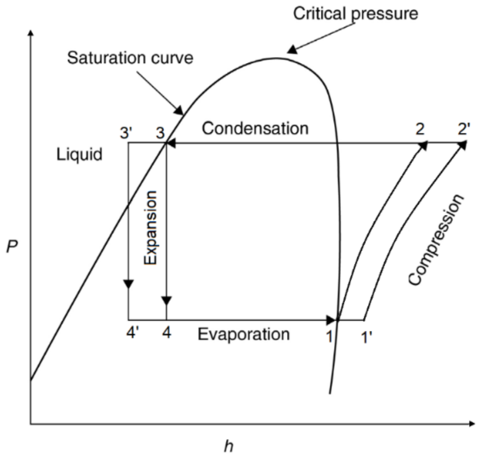

FIGURE 2.4: GENERAL P-H DIAGRAM OF AN IDEAL VAPOR COMPRESSION REFRIGERATION CYCLE WITH SUPERHEAT AND SUBCOOLING (ADAPTED FROM [7])

When comparing with a cycle without subcooling, a subcooled cycle will always produce a higher refrigeration effect because of a lower enthalpy of the fluid when entering the evaporator. This can be seen in Figure 2.4 where the point 4 changes to 4'. This effect does not alter the compressor work, which means the EER always increases with subcooling. [2]

Regarding superheat, it can be useful, useless or a mixture of both. If it is considered useful, the additional heat the fluid absorbs comes directly from the cold source, in the evaporator, increasing the refrigeration effect which corresponds in Figure 2.4 from the point 1 to 1'. Despite this increase, the compression work also increases due to the increase in entropy (the evolution 1' – 2' it's energetically more expensive than 1 – 2, in Figure 2.4). This means it is impossible to assure an increase in EER. If the superheat is useless, it means that, although the fluid entered the compressor as a superheated gas, it left the evaporator as a saturated gas, meaning the increase in temperature occurred somewhere between the evaporator and the compressor and the additional heat was not removed from the cold source. The refrigeration effect is not altered but the compression energy increases, decreasing the EER. [2]

The EER of the different cases are presented below, following the numbering presented in Figure 2.4:

$$COP_{superheat} = \frac{h_{1'} - h_4}{h_{2'} - h_{1'}} \qquad \textbf{2.8}$$

$$COP_{subcooling} = \frac{h_1 - h_{4'}}{h_2 - h_1} \quad \mathbf{2.9}$$

$$COP_{superheat+subcooling} = \frac{h_{1'} - h_{4'}}{h_{2'} - h_{1'}} \quad \mathbf{2.10}$$

As mentioned in 2.1, the reversed Carnot cycle is useful as a comparison because no cycle can have higher EER than the Carnot cycle, for the same extreme temperatures. The refrigeration efficiency of the cycle can be defined as:

$$\eta_R = \frac{COP_{Cycle}}{COP_{Carnot}} \quad \mathbf{2.11}$$

Where COP_{Carnot} is calculated using equation 2.4 for the maximum and minimum temperature of the cycle in study. [2]

2.2.2 Multi-Stage compression

It is a common practice to separate the compression into two or more stages. This means that instead of compressing the fluid from evaporation pressure to condensation pressure all at once, the cycle is fractioned with one or more intermediate pressures, using multiple compressors or multi-stage compressors. The comparison between a single stage and a two-stage compression can be seen in the cycle of Figure 2.5. [2]

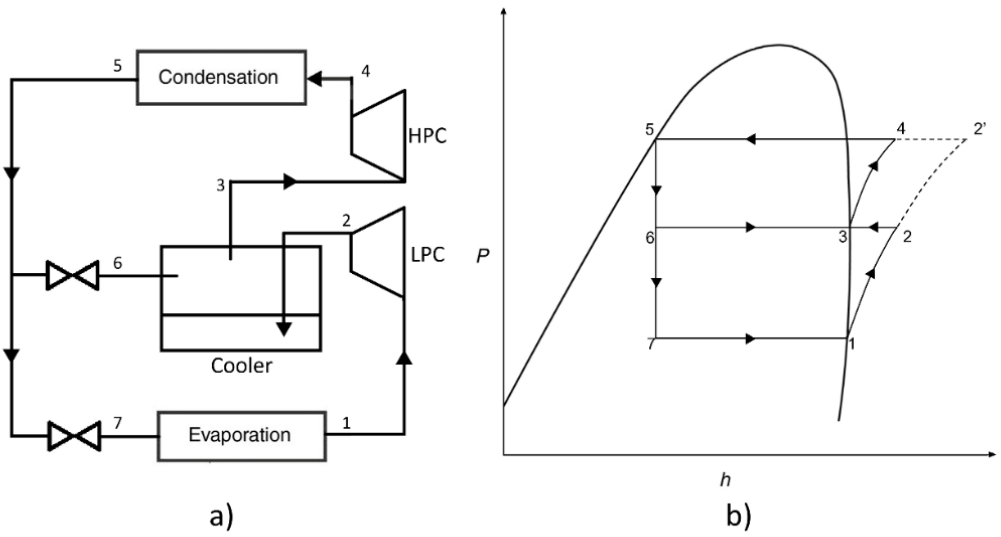

FIGURE 2.5: MULTI COMPRESSION CYCLE WITH INTERMEDIATE COOLER: (A) CIRCUIT SCHEMATIC AND (B) P-H DIAGRAM (ADAPTED FROM [2])

Following Figure 2.5 b), the process 1 – 2' is replaced with the process 1 – 2 – 3 – 4, with two compressors (a Low-Pressure Compressor, LPC and a High-Pressure Compressor, HPC) and an intermediate cooler working at a constant intermediate pressure. With a single stage compression, the compression work is given by $h_{2'} - h_1$ or $[(h_2 - h_1) + (h_{2'} - h_2)]$ and with a two-stage process it is given by $[(h_2 - h_1) + (h_4 - h_3)]$. It is possible to observe that using two compressors will reduce the overall work necessary because $(h_4 - h_3) < (h_{2'} - h_2)$ (the isentropic lines diverge). In the end of the compression process the temperature will also be reduced, $T_4 < T_{2'}$. Other ways of implementing multi-stage compression are also available. [2]

The EER of the cycle given in Figure 2.5 is given by:

$$COP = \frac{\dot{m}_1(h_1 - h_7)}{\dot{m}_1(h_2 - h_1) + \dot{m}_3(h_4 - h_3)} \quad \textbf{2.12}$$

Where:

- $\dot{m}_1$ is the mass flow rate of refrigerant going through the evaporator and the low-pressure compressor;
- $\dot{m}_3$ is the mass flow rate of refrigerant going through the high pressure compressor.

2.2.3 Multi-Stage expansion

Identically, the expansion process can also be divided in two or more stages in order to maximize refrigeration work. One example of this installation can be seen in Figure 2.6.

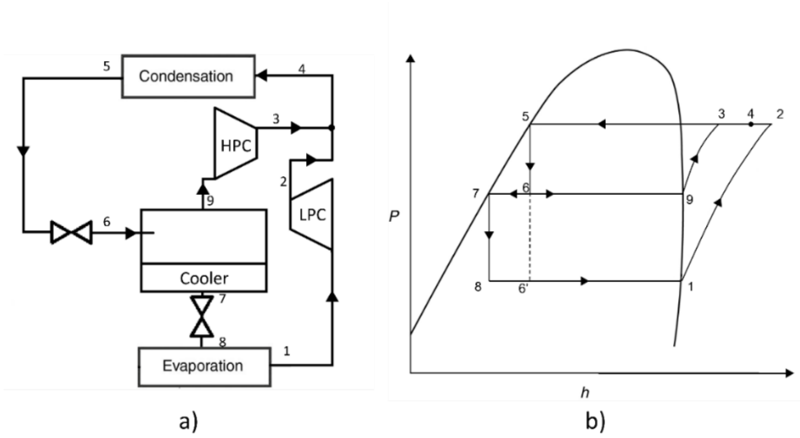

FIGURE 2.6: MULTI EXPANSION CYCLE WITH INTERMEDIATE COOLER: (A) CIRCUIT SCHEMATIC AND (B) P-H DIAGRAM (ADAPTED FROM [2])

In Figure 2.6 b), if the expansion was done directly from the condensing pressure to the evaporation pressure, evolution 5 – 6', the refrigeration effect (6' – 1) would have a very low value, reducing EER. Admitting now that the liquid from the exit of the condenser is expanded to an intermediate pressure, to point 6. The humid vapor would then enter an expansion tank and separate into compressed liquid (7) and saturated vapor (9). Compressed liquid can then be expanded to the evaporator pressure, increasing the overall refrigeration effect and saturated vapor is compressed to the condensing pressure. The EER of the cycle is given by: [2]

$$COP = \frac{\dot{m}_1(h_1 - h_8)}{\dot{m}_1(h_2 - h_1) + \dot{m}_3(h_3 - h_9)} \quad \textbf{2.13}$$

Where:

- $\dot{m}_1$ is the mass flow rate of refrigerant going through the evaporator and the low-pressure compressor;
- $\dot{m}_3$ is the mass flow rate of refrigerant going through the high pressure compressor.

2.3 Real vapor compression refrigeration cycle

In reality, when implementing cycles studied in 2.2, some irreversibilities appear that cannot be ignored and can be seen in Figure 2.7. Namely:

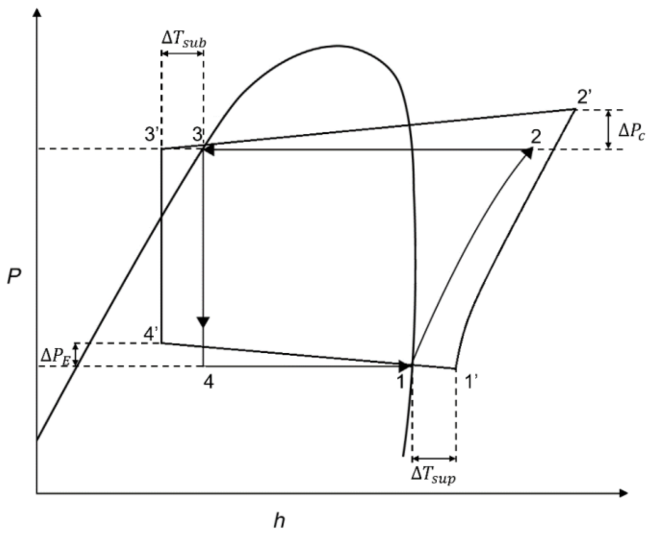

FIGURE 2.7: GENERAL P-H DIAGRAM OF A REAL VAPOR COMPRESSION REFRIGERATION CYCLE (ADAPTED FROM [2])

- In the condenser and evaporator, pressure drops occur, ΔP_C and ΔP_E , respectively, which increase the compression work;
- Some superheat and subcooling take place non-intentionally (ΔT_{Sup} and ΔT_{Sub}) which can, however, be beneficial to the overall system performance;
- Compression isn't isentropic, meaning that $s_{2'} > s_{1'}$;
- Some residual pressure drops along the system occur.

Ultimately, these irreversibilities will most likely reduce the efficiency of the system but are impossible to eliminate and should, therefore, be accounted for. [2]

2.4 CO_2 refrigeration cycle

As seen in 1.3 CO_2 cycles are becoming increasingly popular thanks to the fluid's low environmental impact, its negligible contribution to greenhouse effect and no ozone depletion potential, being non-toxic and non-flammable. Before continuing, however, it is important to note that using CO_2 as a refrigerant also brings some disadvantages, such as:

- The refrigerant's triple point is high, taking special attention so that there is no formation of solid CO2;
- Its high thermal expansion coefficient means a rapid pressure increase can occur when confined to a space;
- The cycle's pressures are higher than traditional refrigerant's cycles, requiring the usage of better built components;
- Systems working above the critical point, so called trans-critical, are more complex and its operation is different from traditional systems;

- Although it has low environmental impact, higher concentrations CO_2 exposure can constitute a health hazard, being necessary the installation of leak detectors. [15]

In this sub-chapter, an overview of the different CO2 cycles is made, and its main modifications in order to increase EER. Being a low critical temperature fluid (31.1ºC), CO_2 systems offer low EER for given applications, and some changes to the general cycle need to be made in order to make them competitive. [16]

2.4.1 Subcritical and trans-critical systems

Fundamentally, CO_2 refrigeration cycles, due to the refrigerant's properties, can be subdivided in two categories, as seen in Figure 2.8:

- Subcritical CO_2 cycles (Figure 2.8(a)): the high-pressure part of the cycle is below the critical point. In this case the carbon dioxide condenses when exchanging energy with the hot source. The highest pressures can be in the order of 30 bar (-5ºC). This cycle is essentially the same seen in 2.2;
- Trans-critical CO_2 cycles (Figure 2.8(b)): the high-pressure part of the cycle is above the critical point. The carbon dioxide doesn't condensate, it simply cools down. The pressure values are around 80 to 100 bar. [2]

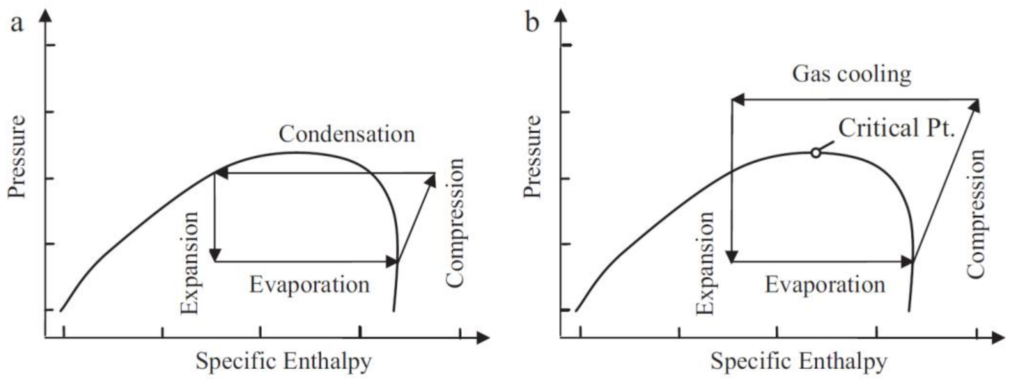

FIGURE 2.8: P-H DIAGRAM OF (A) A SUBCRITICAL CO_2 CYCLE AND (B) A TRANS-CRITICAL CO_2 CYCLE (FROM [17])

In both cycles, the compressor, evaporator, and expansion valve have the same function. In the trans-critical cycle, however, the condenser is replaced with a so-called *gas cooler* where the fluid only lowers its temperature, not changing phase. The heat exchange, however, occurs in a similar way in both cases, the only difference being on the trans-critical cycle the CO_2 temperature is always above the critical temperature of 31.1ºC. Usually, CO_2 systems can change from subcritical to critical automatically, depending on the outside ambient temperature, although trans-critical systems require stronger components in order to account for the higher pressures. The EER of the transcritical cycle also varies substantially with the change in hot-source temperature, which can constitute a big drawback in places where the ambient temperature varies considerably. This is due to the fact that the isothermal lines on the left of the critical point are almost vertical and successive increases in cooling pressure leads to higher increases in the compression work than those verified in the refrigeration effect. The effect can be seen in Figure 2.9. [2]

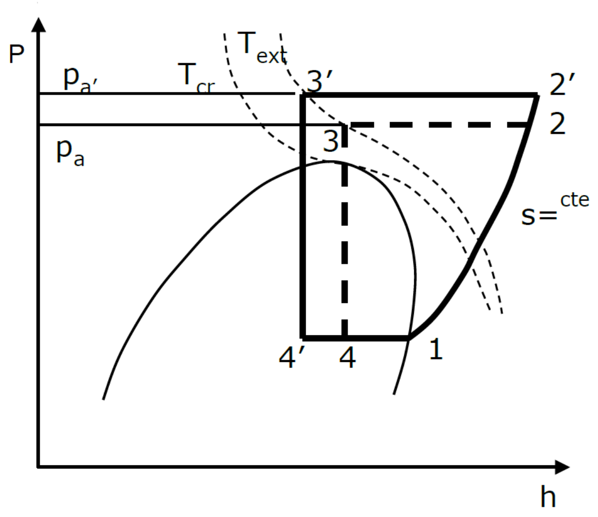

FIGURE 2.9: P-H DIAGRAM OF A TRANS-CRITICAL CO_2 CYCLE FOR TWO DIFFERENT COOLING PRESSURES (ADAPTED FROM [2])

Following the figure's numbering, an increase in pressure from p_a to $p_{a'}$ will increase the compression work from 1-2 to 1-2' and the refrigeration effect from 4-1 to 4'-1. However, the increase in refrigeration effect is lower than the increase in compression work. [2]

2.4.2 CO_2 cycle with vapour injection

A modification to the simple Co2 expansion cycle can be made in order to increase EER. This consists of adding a liquid tank at an intermediate pressure between the expansion valve and the evaporator and extracting vapour from thus liquid, maintaining the tank's pressure and the enthalpy of the remaining saturated liquid, making sure only liquid goes to the evaporator line. The extracted vapour is then expanded in a so-called *flash gas valve* and injected in the suction line which reduces the total superheating degree and discharge temperature of the compressor. A representation of this cycle can be seen in Figure 2.10. [18]

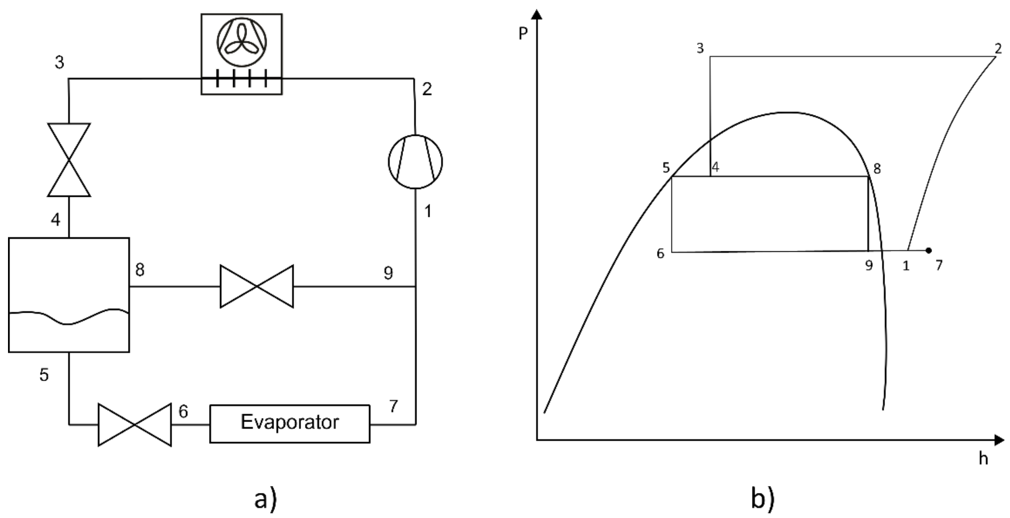

FIGURE 2.10: CO_2 TRANS-CRITICAL CYCLE WITH VAPOUR INJECTION: (A) CIRCUIT SCHEMATIC AND (B) P-H DIAGRAM (ADAPTED FROM [18])

Following the p-h diagram from Figure 2.10 b), the extracted vapour from the liquid tank (point 8) goes through the flash gas valve and is expanded (point 9) and injected in the suction line (point 7), lowering its temperature, and reducing the compression temperature (from point 7 to point 1) ,the tank's pressure and lowering the fluid's enthalpy (from h_4 to h_5). This, however, is counterbalanced by a reduction in the mass flow going through the evaporator, reducing the overall refrigeration effect. The interaction between these opposite effects can increase or decrease the overall EER, depending on the balance between the two. When balanced to maximize EER, it can lead to an increase of up to 10%, when comparing to a general CO_2 expansion cycle. [18]

The EER of the cycle can be given, following Figure 2.10's numbering scheme by:

$$COP = \frac{\dot{m}_6(h_7 - h_6)}{\dot{m}_1(h_2 - h_1)} \quad \mathbf{2.14}$$

Where:

- $\dot{m}_6$ is the mass flow rate of refrigerant going through the evaporator;
- $\dot{m}_1$ is the mass flow rate of refrigerant going through the compressor.

2.4.3 Booster CO_2 cycles

In many cold production applications, the need for two distinctive temperatures is present, which is the case for supermarket refrigeration: typically, there are medium temperature circuits (referred to MT from now on) for the chilled food display cabinets and cold rooms, and low temperature circuits (LT) for the frozen food fixtures. Having this need in mind, an additional lower pressure stage can be added to the cycle seen in 2.4.2. The cycle can be seen in Figure 2.11. This is what is called a booster system. [19]

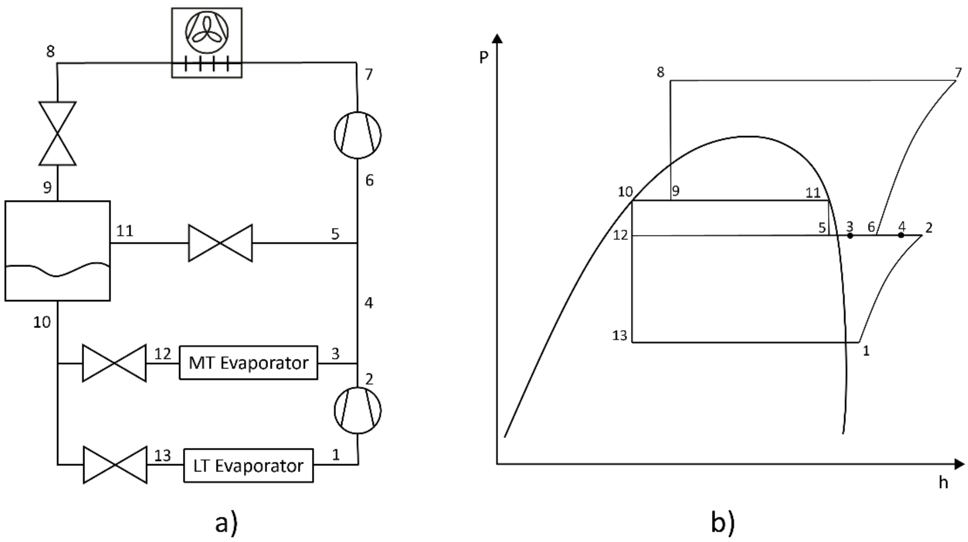

FIGURE 2.11: BOOSTER CO_2 CYCLE: (A) CIRCUIT SCHEMATIC AND (B) P-H DIAGRAM [20]

It is possible to observe in Figure 2.11 a) that the addition of a lower pressure evaporator requires a new compressor (or compressor group) in order to return the fluid's pressure to the MT pressure and complete the cycle. The low-pressure compressor operates in a subcritical regime, while the high pressure operates in transcritical. Following the figure's numbering, the EER is given by:

$$COP = \frac{\dot{m}_3(h_3 - h_{12}) + \dot{m}_1(h_1 - h_{13})}{\dot{m}_1(h_2 - h_1) + \dot{m}_6(h_7 - h_6)} \qquad \mathbf{2.15}$$

Where:

- $\dot{m}_3(h_3 - h_{12})$ is the refrigeration effect from the MT evaporator;
- $\dot{m}_1(h_1 - h_{13})$ is the refrigeration effect from the LT evaporator;
- $\dot{m}_1(h_2 - h_1)$ is the compression work from the low-pressure compressor;
- $\dot{m}_6(h_7 - h_6)$ is the compression work from the high-pressure compressor.

It is important to define the load ratio, the ratio between cooling capacities at medium and low temperature levels:

$$LR = \frac{Q_{MT}}{Q_{LT}} \qquad \mathbf{2.16}$$

A typical European supermarket has a load ratio of around 3, meaning cooling loads on the high stage are approximately 3 times higher than those on the low stage. [21]

2.4.4 Booster CO_2 with parallel compression

In the cycle seen in 2.4.2, although the better liquid quality and the vapour injection can increase the overall EER of the system, the bypass flow rate can be up to 50% the total compressed fluid. This means that there is a waste of compressor work since this bypass is expanded and no refrigeration effect results from it. Instead of fully expanding the gas coming from the tank, a fraction of it can be compressed again to the highest cycle pressure, reducing the compression ratio and energy consumption. The cycle schematics can be seen in Figure 2.12. [18]

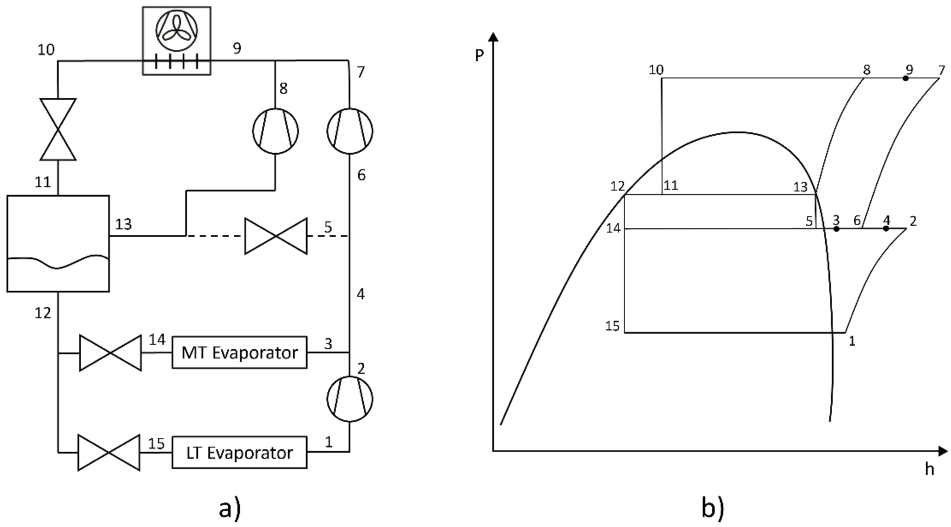

FIGURE 2.12: BOOSTER CO_2 CYCLE WITH PARALLEL COMPRESSION: (A) CIRCUIT SCHEMATIC AND (B) P-H DIAGRAM ([20] [22])

Following the figure's numbering, the fluid coming from 13 is split and part of it is expanded and mixed the gas coming from the evaporators, lowering the overheating from 4 to 6, as seen in 2.4.2, and part of it is expanded again (13 to 8), meaning a reduced compression work, as the tank's pressure is higher than the MT pressure. The EER of the cycle is given by:

$$COP = \frac{\dot{m}_3(h_3 - h_{14}) + \dot{m}_1(h_1 - h_{15})}{\dot{m}_1(h_2 - h_1) + \dot{m}_6(h_7 - h_6) + \dot{m}_8(h_8 - h_{13})} \qquad \textbf{2.17}$$

Where:

- $\dot{m}_3(h_3 - h_{14})$ is the refrigeration effect from the MT evaporator;
- $\dot{m}_1(h_1 - h_{15})$ is the refrigeration effect from the LT evaporator;
- $\dot{m}_1(h_2 - h_1)$ is the compression work from the low-pressure compressor(s);
- $\dot{m}_6(h_7 - h_6)$ is the compression work from the high-pressure compressor(s);
- $\dot{m}_8(h_8 - h_{13})$ is the compression work from the parallel compressor(s).

The refrigeration effect is the same with or without parallel compression. However, the total work done by the compressors is lower due to the lower compression ratio of the parallel compressor(s), which leads to an overall increase in EER. This solution is particularly attractive in warmer climates, as gas cooler temperatures increase when the ambient temperature increases, increasing compression work. The use of parallel compression, when compared with the base CO_2 refrigeration cycle, can increase the theorical EER by up to 40%. [18] [23]

2.5 Main Components of a CO_2 Booster refrigeration system with parallel compression

This sub-chapter will focus on the main components of a CO_2 booster refrigeration system with parallel compression.

2.5.1 Compressor

Compressors may be considered the main component of a refrigeration installation and are responsible for compressing the fluid, raising its pressure and temperature in the most isentropically efficient way. Although many different types of compressors are available such as alternative, scroll and screw, due to compressor efficiency, technology maturity and the high pressures in CO_2 applications, alternative compressors are used in the majority of systems, with commercially offered solutions available from manufacturers such as *Bitzer, Emerson, GEA, Frascold, Mycon* and *Dorin.* The alternative compressor is analogous to internal combustion engines, compressing a given fluid through the movement of pistons inside a cylinder connected to a crank and connecting rod mechanism. Also, similarly to the combustion engine, phases of the cycle can be identified: admission, compression and exhaust. Admission and exhaust valves guarantee a one-way movement of the fluid. A representation of the internals of such compressor can be seen in Figure 2.13. [2]

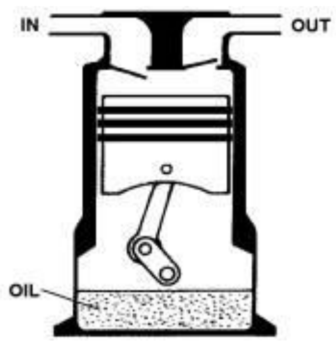

FIGURE 2.13: GENERIC REPRESENTATION OF AN ALTERNATIVE COMPRESSOR [2]

Alternative compressors may be divided into three groups, according to their drive type: open, semi-hermetic and hermetic. These three types can be seen, respectively, in Figure 2.28. [2]

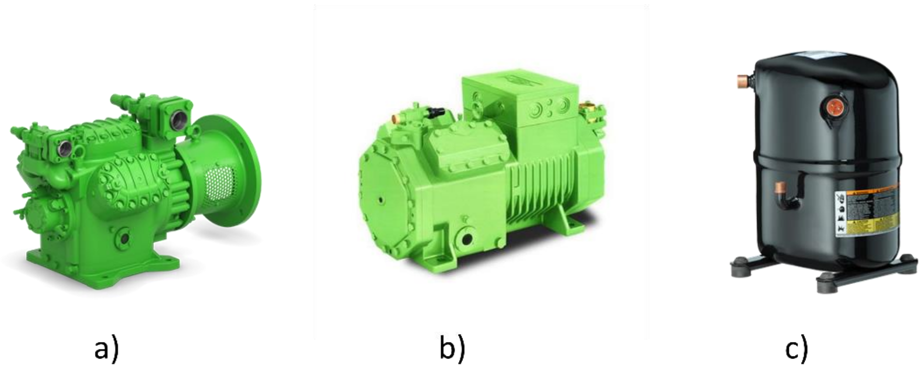

FIGURE 2.14: COMPRESSOR DRIVE TYPES: (A) OPEN, FROM BITZER, (B) SEMI-HERMETIC, FROM BITZER AND (C) HERMETIC, FROM COPELAND ([22] [24] [25])

Open type compressors (A) completely separate the source of rotation from the compressor part which means easier disassembly and maintenance but higher risk of oil and/or refrigerant leakage through the crankshaft seals. Hermetic compressors (B) are the opposite, where both the motor and compressor are encapsulated in a sealed structure. In these types of compressors, only the refrigerant lines and the electric cables are accessible, meaning almost zero risk of leaks but without the option of servicing, indicating that, in case of breakdown, the unit has to be replaced. Semi-hermetic solutions (C) offer compromises between the two types referred, with a motor rotor attached to the crankshaft to eliminate leaks but with a non-permanent unit assembly, meaning that a rebuild for maintenance is possible. [2]

Compressors, being real physical components, are always constrained by physical phenomena such as friction and pressure loss and aren't completely efficient. From a thermodynamical point of view, we can define compressor isentropic efficiency as:

$$\eta_i = \frac{Isentropic\ compressor\ work}{Real\ compressor\ work} = \frac{W_{isentropic}}{W_{real}} = \frac{h_{2s} - h_1}{h_2 - h_1} \quad \mathbf{2.18}$$

Where:

- h_{2s} is the specific enthalpy for the gas at the exit of the compressor in an isentropic compression;
- h_2 is the specific enthalpy for the gas at the exit of the compressor in a real compression;
- h_1 is the specific enthalpy for the gas at the entrance of the compressor.

Assuming that the state 2s and 2 have the same pressure, the difference in enthalpy comes from a higher temperature in 2 than 2s. This difference in temperature should be accounted for when maximizing efficiency. A high isentropic efficiency doesn't necessarily guarantee, however, a high EER. [7] [2]

Due to the nature of design of reciprocating compressors, not all the volume of the cylinder is available to actually displace gas. An efficiency that quantifies this ratio can be defined:

$$\eta_v = \frac{Displaced\ volume\ of\ gas}{Swept\ volume\ of\ the\ piston} = \frac{\dot{V}_{Dis}}{\dot{V}_v} \qquad \textbf{2.19}$$

This efficiency is related to the fraction of dead volume in the compressor, which is the volume of unused space between the head of the cylinder and the piston, as they can’t “touch”. For the same compression ratio, the bigger the dead volume, the worse the volumetric efficiency is and, as a consequence, the worse the EER is. [2]

Compressing capacity requirement isn’t always constant in an installation and running a compressor all the time can significantly increase overall energy consumption and, as such, worsen the EER. It is, therefore, necessary to have a way of regulating compressing capacity and some examples are presented:

- **All or nothing**. For simpler and smaller installations like domestic refrigerating units, a simple thermostat is able to control the compressor work: when above a given set temperature the compressor is working at full power and when a certain temperature is reached it shuts off. The lower the difference between the cut in and cut off temperature, the less temperature variations the unit will have but the more cycles the compressor will do, which can hurt its longevity;
- **Rotational speed variation.** Compressor capacity is, to an extent, directly proportional to the rotational speed of said compressor. The usage of multiple velocity motors can be a way of controlling the capacity. This control is not, however, continuous, being that multiple velocity motors usually have two to four distinct velocities;
- **Step control.** Instead of using one compressor to fulfil the required compressing needs, distributing the work to multiple machines will reduce the energy consumption during low-load times, when not all compressors need to be working;
- **Continuous regulation with frequency variation.** While having discrete steps in speed or capacity is a more efficient way of using compressor work, compared to on/off cycles, ideally the supplied power would match the required power at all times. Alternative compressors are usually powered by single or triple phase electric motors, whose velocity can be continuously changed using a frequency regulator, achieving this effect and, effectively, saving energy and increasing efficiency;

- **Other**, such as controlling the opening of admission valves, varying dead space or having partial service windows. [2]

Bigger refrigeration systems such as those present in supermarkets and the industry often have multiple compressors in each stage, with one or two compressors equipped with a frequency regulator. Mixing frequency variation with step control, these units can practically achieve optimal energy efficiency on the whole capacity range. An example of the capacity regulation for a compressor group with 3 identical compressors with one equipped with a frequency regulator can be seen in Figure 2.15. [20]

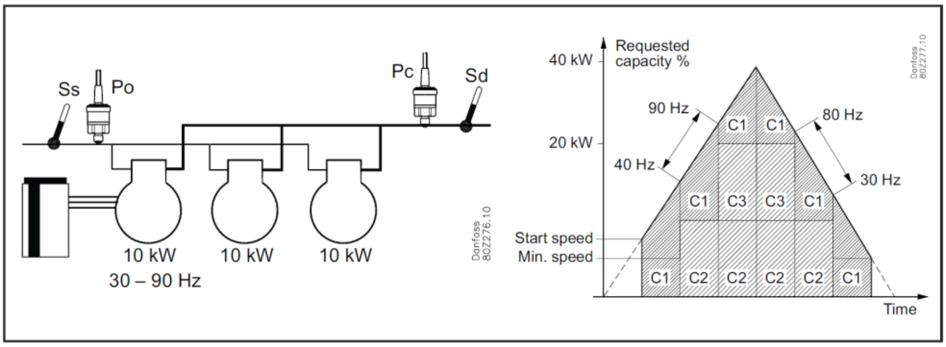

FIGURE 2.15: CAPACITY REGULATION WITH TWO SINGLE STAGE COMPRESSORS AND ONE EQUIPPED WITH A FREQUENCY VARIATOR [26]

2.5.2 Expansion devices: Electronic expansion valve

Expansion devices have an opposite role to the compressors, meaning that their main goal is to reduce the fluid's pressure while maintaining its enthalpy. At their core, expansion valves are nothing more than an orifice or some other sort of restriction in the system that has two functions:

- Reducing the fluid's pressure so that the phase change in the evaporator occurs at low temperature;
- Regulating the mass flow of refrigerant in the evaporator so that it satisfies the thermal load required and that it matches the suction flow on the compressor.

Although manual expansion valves exist and are readily available and still used today on simpler devices, when working with bigger refrigeration systems other solutions are preferred that provide a more precise control of the installation. Electronic expansion valves (EEV) provide a more precise degree of control and system protection. Their main benefits are as follows:

- Precise flow control over a wide range of capacities;
- Fast load response;
- Less evaporator surface required for superheat due to better control at low superheats;
- Electrical connection only, meaning a great flexibility in system layout, potentially reducing system dimensions;

- When the system is turned off, the valve can fully close, eliminating the need for a separate shut-off solenoid valve.

These advantages, however, come with an increase in initial cost due to the need for additional pressure and temperature sensors and the greater cost of the valves and actuators themselves. Two main types of electronic valves are available: continuous flow and pulse width modulated (PWM). In a continuous flow valves, the orifice size is varied by a stepper motor continuously. PWM valves vary the flow by opening and closing the valve in pulses with a very specific frequency. In each case a controller is used in conjunction with the valve and it's pre-configured for the refrigerant and valve type, receiving signals sent by the temperature and pressure sensors, allowing for the superheat in the exit of the evaporator to be exactly determined. A scheme of an installation can be seen in Figure 2.16. [2] [7]

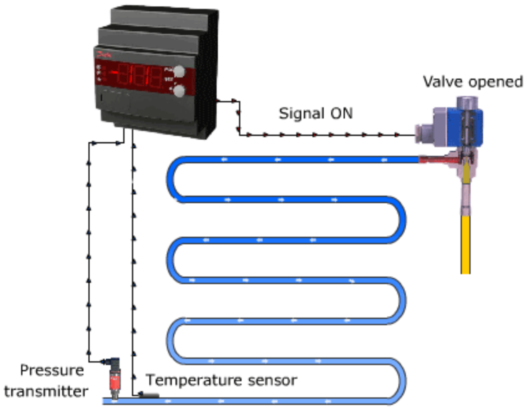

FIGURE 2.16: ELECTRONIC EXPANSION VALVE SCHEME WITH A CONTROLLER, PRESSURE AND TEMPERATURE SENSOR [27]

2.5.3 Liquid tank

As seen in 2.4.2, the addition of a liquid tank can significantly improve the quality of liquid, thus increasing refrigeration effect, as well as working as a buffer, temporarily storing refrigerant within the system or accommodating excess liquid. A receiver tank generally has two liquid levels, the minimum and maximum, working at an intermediate operation level. An example from a manufacturer can be seen in Figure 2.17. [7]

FIGURE 2.17: CO_2 VERTICAL LIQUID RECIEVER FROM TECNAC [28]

A liquid tank must include a relief safety valve in order to avoid reaching dangerous levels of pressure and the total refrigerant in a given system should not be higher than 90% the volume of the tank for a temperature not higher than 40ºC. For higher temperatures this value is reduced to 80%. [2]

2.5.4 Condenser/Gas cooler

In a vapour compression cycle, the condenser receives the hot, high-pressure gas from the compressor and cools it to remove superheat and subsequently latent heat, allowing the refrigerant to condense back to a liquid. Furthermore, the fluid is frequently somewhat chilled. The cooling medium will almost always be air or water. Because R744 does not condense under these conditions, the term *Gas Cooler* is used for transcritical CO_2 heat rejection systems. Broadly speaking, there are three different types of condensers:

- **Air-cooled condensers**. The most basic air-cooled condenser consists of a refrigerant-filled tube that is placed in still air and relies on natural air circulation. Forced convection, by means of fans, will be used to move air over the condenser surface above this size, increasing heat exchange. This second type's efficiency is highly dependent on the ventilator position and configuration. An example of such unit can be seen in Figure 2.18;
- **Water-cooled condenser**. The higher heat capacity and density of water make it a better heat transfer medium than air, meaning a more efficient condenser. Three main types of water-cooled condensers are available: double-pipe condenser, where water is circulated in counterflow from the refrigerant to get the most sub-cooling; immersion condensers, composed of a tank in which water circulates inside in a serpentine; and shell-and-tube condenser, which are similar to immersion, composed of a cylindrical tank with pipes inside circulating cooling water and condensing the refrigerant on the outside of the tubes;

- **Evaporative condensers**. In these types of condensers, the fluid circulates in a pipe which is humidified by pulverized water while a forced flow of air surrounds it, promoting water evaporation and removing heat from the refrigerant. These units' performance is affected by the psychometric parameters of the forced air, being more efficient in drier climates. [2] [7]

Mixed condensers are also available, where the refrigerant passes through an air-cooled unit and then through a water-cooled one. [2]

FIGURE 2.18: FORCED CONVECTION AIR COOLED CONDENSER/GAS-COOLER IN A REFRIGERATION INSTALLATION FROM CENTAURO

2.5.5 Evaporators

A typical refrigeration system will have many evaporators suited to the application of the units that need cooling, which means that classifying the different evaporators used can be complex. That being said, evaporator can generally be divided into three different groups: dry, shell-and-tube and flooded:

- **Dry evaporators**, that work directly with the expanded refrigerant (humid vapour), which is evaporated along its length. Their relatively simple construction mean they are widely available and are most common in simpler consumer applications. However, because of their simplicity, they are vulnerable to refrigerant or air flow misdistribution, resulting in reduced heat transfer effectiveness and consequently lower system efficiency;
- **Shell-and-tube evaporators**, usually used for the cooling of liquids by direct expansion, are most used in AC installation or in the beverage industry. They work, in principle, in a similar way of shell-and-tube condensers: refrigerant circulates inside a cylinder with the soon-to-be cooled liquid flowing inside tubes in said cylinder, or vice-versa;
- **Flooded evaporators** circulate more refrigerant than it's possible to evaporate. The expanded fluid is separated in two phases in a reservoir and,

while the vapour flows to the compressor, the liquid goes to the evaporator, obtaining humid vapour at the end, which is again separated in the reservoir, with a recirculation ratio. Having all surfaces of the evaporator wet mean a higher heat transfer coefficient which leads to a better performance. The recirculation ratio has an ideal value that leads to the best evaporation performance; increasing the liquid flow rate further reduces the heat transfer coefficient and increases the pressure drop. [2] [29]

A general scheme of the presented evaporator types can be seen in Figure 2.19.

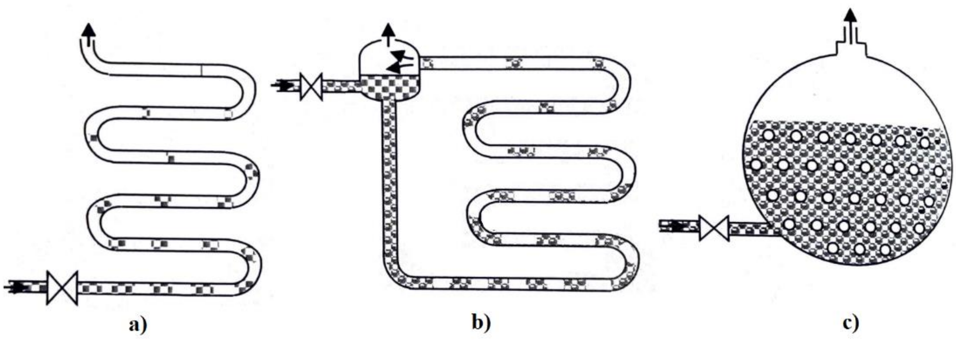

FIGURE 2.19: TYPES OF EVAPORATORS SCHEME: (A) DRY EVAPORATOR, (B) FLOODED EVAPORATOR AND (C) SHELL AND TUBE EVAPORATOR (FROM [2])

2.6 Real CO_2 Booster system with parallel compression - installation considerations

Although R744 systems as described as in section 2.4.4 will, in theory, work and be capable of producing cold, many optimization principles can and should be applied in order to make a system that works in the real world with no issues and with competitive EER . First of all, under no circumstances liquid can enter inside a compressor, as liquids are not very compressible and will certainly damage it. Although evaporators will generally work with superheat and lines will further increase this superheat, almost all R744 installations are equipped with internal heat exchangers to guarantee a minimum superheat of the compressors. Their usage is usually in two configurations, seen in Figure 2.20 and Figure 2.21. [20]

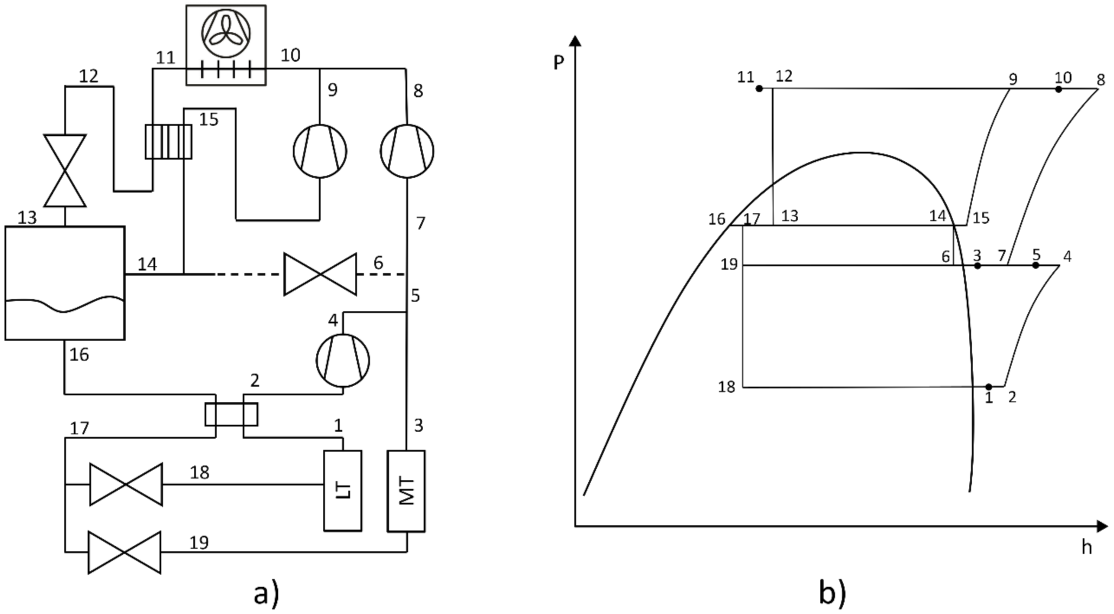

FIGURE 2.20: BOOSTER CO_2 CYCLE WITH PARALLEL COMPRESSION AND TWO EXTERNAL IHE: (A) CIRCUIT SCHEMATIC AND (B) P-H DIAGRAM [20]

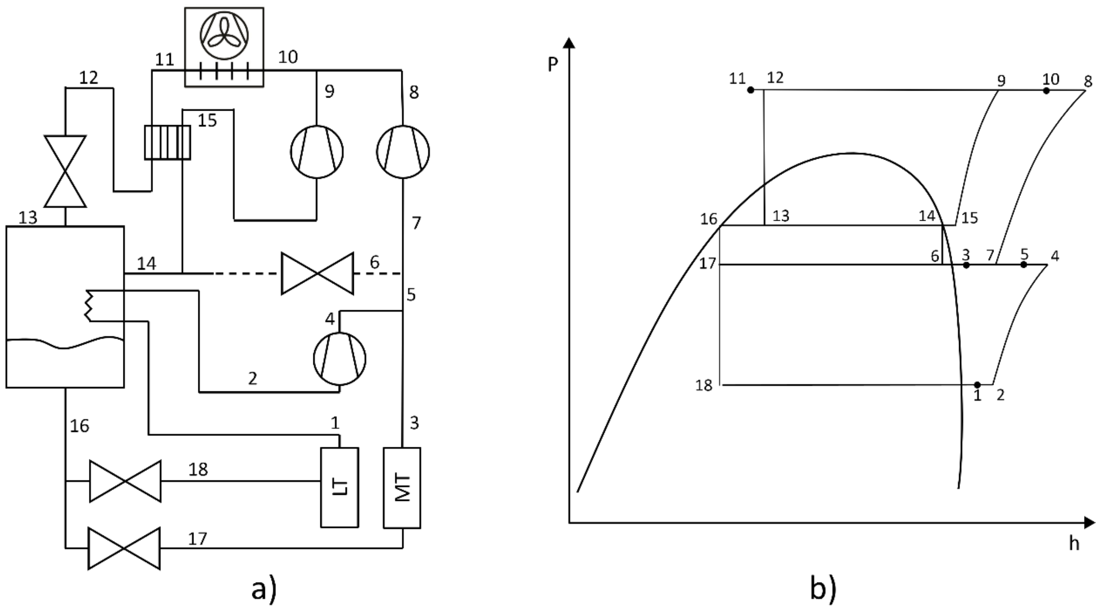

FIGURE 2.21: BOOSTER CO_2 CYCLE WITH PARALLEL COMPRESSION, ONE EXTERNAL IHX AND A IHX INSIDE THE RECEIVER: (A) CIRCUIT SCHEMATIC AND (B) P-H DIAGRAM (ADAPTED FROM [20])

Both configurations provide minimum superheat for both the LT and IT compressors, with MT superheat being automatically provided by the mixture of flash gas, LT compressor exit vapour and suction from MT evaporator. At that expense, in the configuration of Figure 2.20, an enthalpy lost occurs before the fluid expands in the evaporator valves, meaning potential cooling effect is lost, which needs to be compensated with an increase in mass flow, for the same refrigeration capacity. [20]

It is also relevant to understand how the relationship flash gas valve – parallel compressor works. In real installations, compressors have a minimum admissible flow that needs to be fulfilled in order for it to work, meaning that there must be a minimum flow of flash gas in order for the IT compressors to work. The coordination between the flash gas valve and the IT compressor can be seen in Figure 2.22.

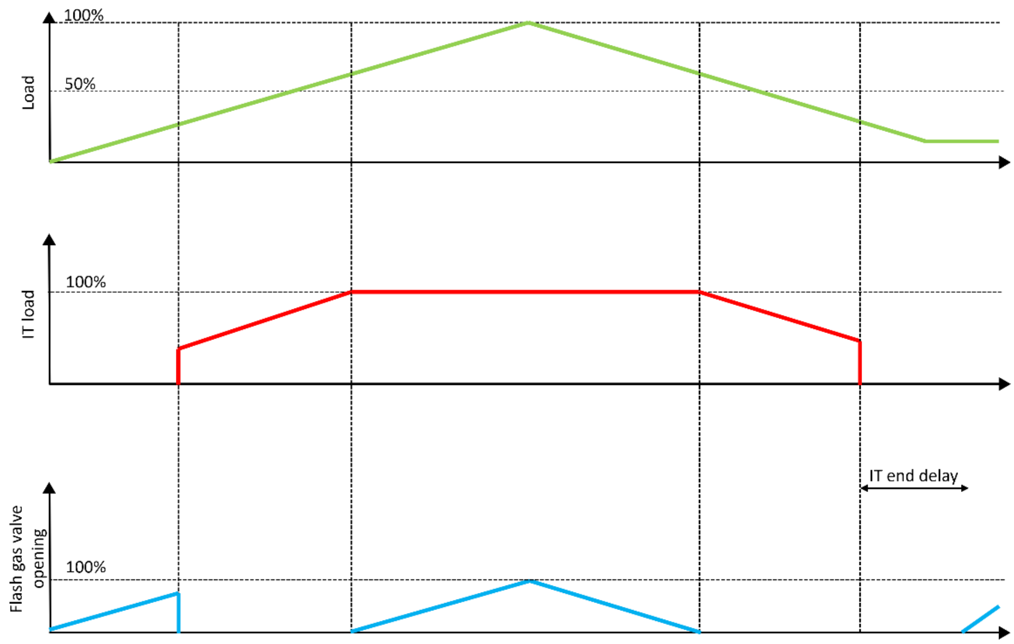

FIGURE 2.22: VARIATION OF IT COMPRESSOR LOAD ANS FLASH GAS VALVE OPENING WITH SYSTEM LOAD (ADAPTED FROM [26])

As system load increases, the flash gas valve opens progressively in order to maintain receiver pressure. When enough mass flow is passing through the system that fulfils the IT compressor minimum flow, the valve closes, and the compressor increases frequency until it reaches its maximum. When that happens and if system load is still rising, the valve opens again until its fully opened. As system load decreases, the valve progressively closes, until fully closed, followed by a ramp down of the parallel compressor. When it reaches below minimum flow, the compressor closes. However, a defined time period called IT end delay occurs between compressor shutdown and valve opening, in order to increase operating hours of IT stage. [26]

A R744 system can also use the excess expelled heat to heat water for Domestic Water Heating, or DWH for short. This is a quite common application because it only requires the installation of an additional heat exchanger before the fluid enters the condenser/gas cooler and can significantly improve the energy usage of the system. The hot fluid exchanges heat with the water, heating it and loosing energy in the process. From the refrigeration point of view, this usage does not affect the system's performance, the only difference is that instead of releasing energy in the gas cooler, the fluid releases part of its energy in the heat exchanger and the rest in the gas cooler. A heat exchanger for DWH can be seen in Figure 2.23. [20]

FIGURE 2.23: DWH HEAT RECOVERY EXCHANGER FROM SWEP ([30])

The placement of such unit in an installation schematic can be seen in Figure 2.24, an adaptation from the system scheme of Figure 2.21. In fact, this figure represents a theoretical scheme of the real installation that was studied.

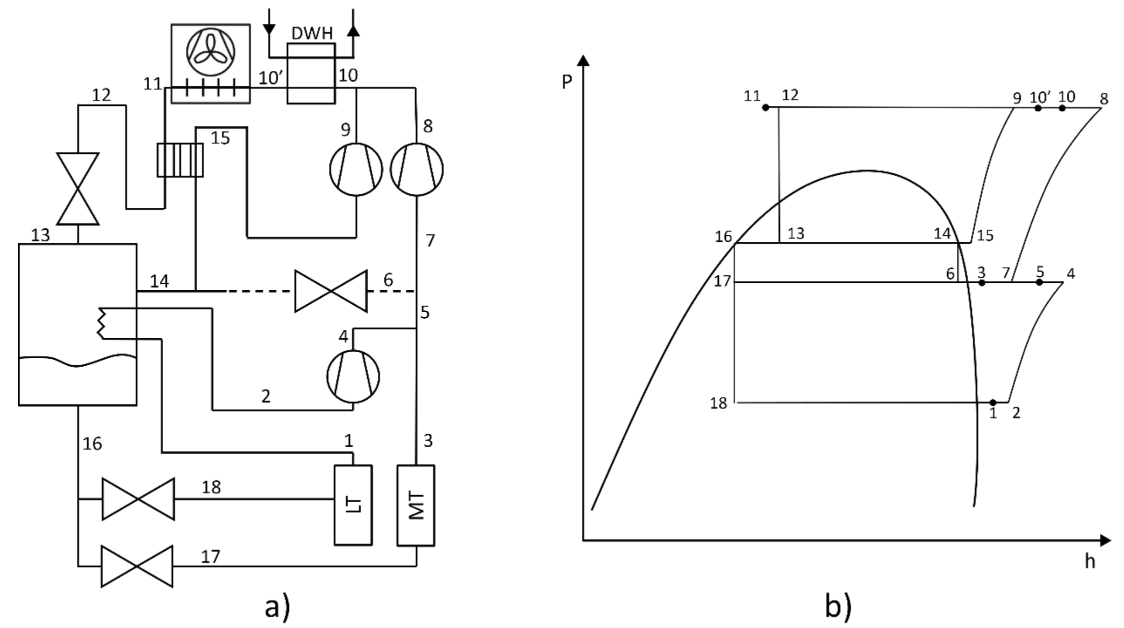

FIGURE 2.24: BOOSTER CO_2 CYCLE WITH PARALLEL COMPRESSION, ONE EXTERNAL IHX, A IHX INSIDE THE RECEIVER AND A DHW HEAT EXCHANGER: (A) CIRCUIT SCHEMATIC AND (B) P-H DIAGRAM

2.7 Control of an installation

Control systems are essential in any installation as they provide system protection and maximum efficiency by constantly reading data and applying changes. This subchapter will focus on the main components used in order to control, maintain and optimize CO_2 booster systems with parallel compression and their main functions. Specific components used in these types of applications will be studied from the three main manufacturers:

Danfoss, *Carel* and *Dixell*, with proprietary control *software* and algorithms, and many expansion modules that control the installation. [7]

2.7.1 Main system control

A given refrigeration system must be capable of adapting operation conditions all the time in order to maximize efficiency and, at the same time, provide real-time information about its operation while maintaining safety. This management is provided by system controllers that ensure all data is collected and algorithms are implemented to maximize EER. Data can generally be accessed remotely, facilitating operation. The main functions of these controllers are:

- **Capacity control of compressor groups.** System load is not constant over time and the controllers provide signals to ramp up or down compressing work, making smart usage of variable compressors and, at the same time, ensuring equalization of different compressors active time, usually applying a principle of "First In First Out" (FIFO) if all compressors are similar, while minimizing as much as possible start-up processes;
- **Condenser/Gas cooler control.** Sub-cooling is regulated by the high-pressure valve, rather than by the condenser itself, as in an HFC system. The controller is able to regulate the gas cooler temperature discharge so that it has the lowest possible value and the fans' energy consumption is minimized. A minimum receiver pressure has to be assured, however. The control is done by cutting in and out condenser steps and/or by regulating fan speeds;
- **Oil management**. While not directly affecting efficiency, a well-managed and maintained oil system ensures optimum system performance, specially from the compressor side. The controller is able to control the pressure in an oil receiver and ensure the evacuation of oil separators;
- **CO_2 transcritical system and heat recovery**. The high pressures and temperatures in CO_2 systems makes it possible to recover heat for tap water and heating. The controller will control the gas cooler/condensing pressure, maximizing EER when the recovered heat is taken into account. The recovery, however, is secondary and the cooling system will always be prioritized;
- **Setpoint management**. With increasingly complex systems, a corresponding increase in the number of setpoints makes it difficult to handle them. Controllers have the capacity to automatically define setpoints or assist user-defined points, ensuring correct control;
- **Safety control**, such as automatic valve shutoffs, alarm control, sensors check and control, guaranteeing soft starts and stops, and more. [26]

Examples of control units from the three different referred manufacturers can be seen in Figure 2.25.

a) b) c)

Figure 2.25: System controllers: (a) Carel pRack pR300T (b) Danfoss AK-PC 782A (c) Dixell XM679K

2.7.2 Evaporator control

Maintaining a good and efficient operation of the evaporators is a fundamental operation in order to maximize a given installation's EER, especially in supermarket applications where user interaction with the refrigerating units can alter significantly the required cooling needs. Having this in mind, the need of a control unit for each evaporator unit or group is necessary and can significantly reduce energy consumption, avoiding unnecessary usage of fluid's flow. The main functions of these types of devices are:

- Valve control: Adapting the amount of fluid circulating in each evaporator according to cooling needs. This can be done via on/off cycles, PWM or stepper motors;
- Valve shutoff in case of power loss to the system, preventing fluid movement;
- Superheating control;
- Defrosting cycle management. Frosting in evaporators reduces heat exchange and can damage equipment;
- Defining cycles, such as day/night cycle, usually present in supermarket applications;
- Fan-speed control;
- Alarm control, such as measuring temperature, humidity, leaks of fluid and high concentrations of CO_2;
- Other functions such as managing the illumination of a given unit, anti-haze measures and other. [31]

Some examples of units of evaporator controls can be seen in Figure 2.26 from the three different manufacturers stated above.

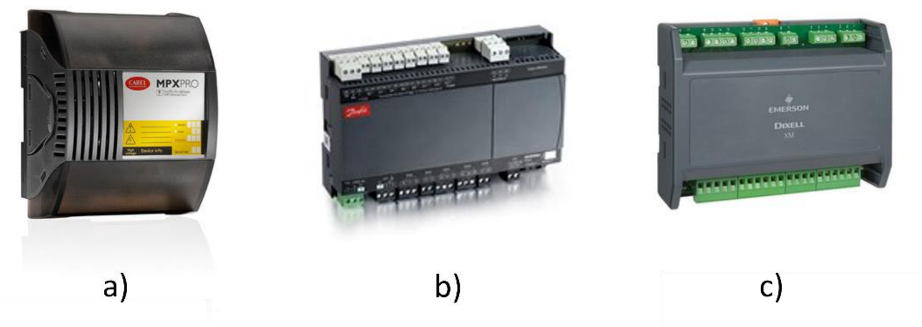

FIGURE 2.26: EVAPORATOR CONTROLLERS: (A) CAREL MPXPRO (B) DANFOSS AK-CC55 (C) DIXELL XM679K

These units rely on temperature and pressure sensors without which the controllers could not operate. A typical array of used sensors can be seen in Figure 2.27. Following the figure's nomenclature, the temperature in the appliance is measured by one or more temperature sensors located in the airflow before the evaporator (S3) and after (S4). These influence the defined values for the thermostat, alarm thermostat and display readings. Additionally, an optimally placed sensor (S6) provides a more accurate environment reading, defining the expansion valve's opening. Defrosting control is assured by S5. S2 and P control the return liquid's temperature and pressure, respectively, which is crucial in order to define certain evaporator parameters, such as superheat. [31]

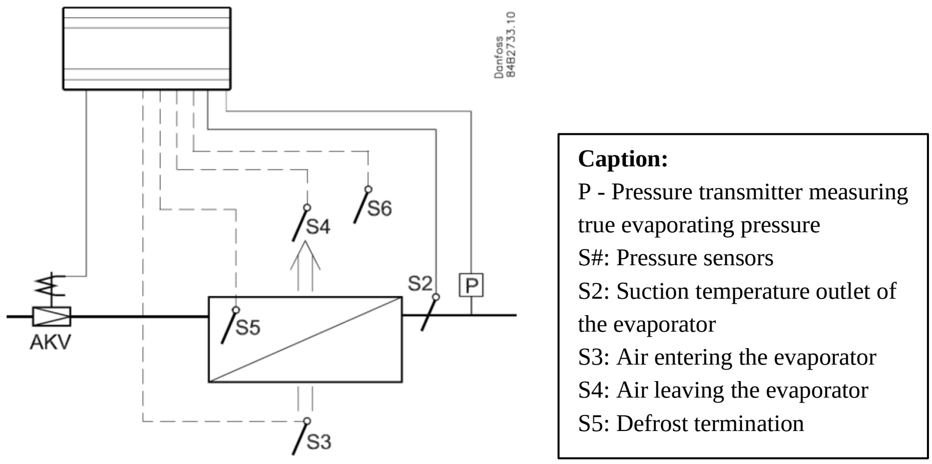

FIGURE 2.27: EVAPORATOR UNIT SENSORS NECESSARY TO PERFORM THE CONTROL (ADAPTED FROM [31])

2.7.3 Supervisioning systems

Having a central system capable of coordinating data to and from individual refrigeration controllers, including data for logging and alarms is essential. For that purpose, supervisioning units exist and contain processing capacity and *software* interfaces, usually user-friendly. Some of these systems capabilities are:

- Refrigeration control, providing centralized or de-centralized options for controlling and managing the system, scheduling, EER optimization, load shed and other;
- Live installation status, providing real-time information on specific temperatures, pressures and cooling capacity;
- Data logging;
- Remote managing options via web or local networks;
- Real-time alarm notification. [32] [33]

Examples of interfaces these devices have can be seen in Figure 2.28. These devices usually have options for customizing their interfaces, making it easier to control, even for non-specialized users. [33]

FIGURE 2.28: SUPERVISIONING SYSTEMS INTERFACES: (A) CAREL BOSS (B) DANFOSS AK-SM800 (C) DIXELL XWEB EVO

3 Problem Presentation & Methodology

This chapter will be dedicated to the presentation of the problem, the refrigeration system that will be object of study and its characterization and the methodology used in order to gather and analyse data and change setpoint values in the system. It is important, firstly, to define the constraints of the project: the object of study will be fully characterized bellow, but it is important to note that during the development of this work, the plant had to be fully functional 100% of the time, meaning that the practical study could not be taken to extreme values, due to the risk of a sudden stop, malfunctioning or even breakage of components.

3.1 Object of study characterization

For the development of this project, a supermarket refrigeration system was chosen, a typical area of business of the company the work was developed at. Regarding capacity, supermarket systems can be divided in three categories, with three series of systems:

- Small supermarkets: MT capacity from 12 to 60kW and LT capacity from 7 to 20kW;
- Medium supermarkets: MT capacity from 80 to 140kW and LT capacity from 15 to 40kW;
- Hypermarkets: MT capacity from 120 to 185kW and LT capacity from 15 to 80kW;

For the project, a medium-sized supermarket refrigeration plant was chosen in Felgueiras, a city in the north of Portugal with a warm and temperate climate, and the tests were conducted during the months of August and September. These months were chosen particularly for being generally the hottest of the year, when heat rejection to the ambient is toughest, resulting in lower EER's. The plant can be divided in three main systems: the refrigeration system, comprising of all the cold-producing components such as compressors, valves, and receiver tank; the cooling loads, meaning all the evaporator units in the supermarket and the condensers, located outside the building. These components will be detailed bellow.

3.1.1 Refrigeration system

The refrigeration system that will be object of study is made by *Advansor* model *CuBig 3+1x3 Cu-1R*, of which a similar model can be seen in Figure 3.1: Advansor CuBig 3+1x3 Cu-1R refrigeration rack. It comprises of a transcritical R744 flash-gas booster system with parallel compression, with internal heat exchangers in both stages, with the particularity of having the LT heat-exchanger embedded in the liquid receiver. A heat exchanger for DHW is also installed but was offline at the time of study and will not be considered.

FIGURE 3.1: ADVANSOR CUBIG 3+1X3 CU-1R REFRIGERATION RACK

The system has a total of 7 semi-hermetic reciprocating compressors, with three compressor groups:

- For the high-pressure stage: 3 compressors in parallel, one of which equipped with a frequency inverter;
- For the low-pressure stage: 3 compressors in parallel, one of which equipped with a frequency inverter;
- For the parallel stage: 1 compressor equipped with a frequency inverter.

A receiver tank is incorporated, with a capacity of 130l with a design pressure of 80bar. Allowable temperature limits of the whole system are -50 to 150ºC, with a charge of refrigerant of 150kg.

The control of the installation is done with the usage of 6 *Carel* controllers, whose features were already discussed in section 2.7.1 with two allocated for each compressor group, a main controller, and a backup controller. Remote access to the controllers is available through *Carel Boss,* as previously discussed.

A simplified installation theoretical scheme, as well as the p-h diagram can be seen in. A more detailed scheme of the refrigeration system can be seen in Annex A, in figure A-1.

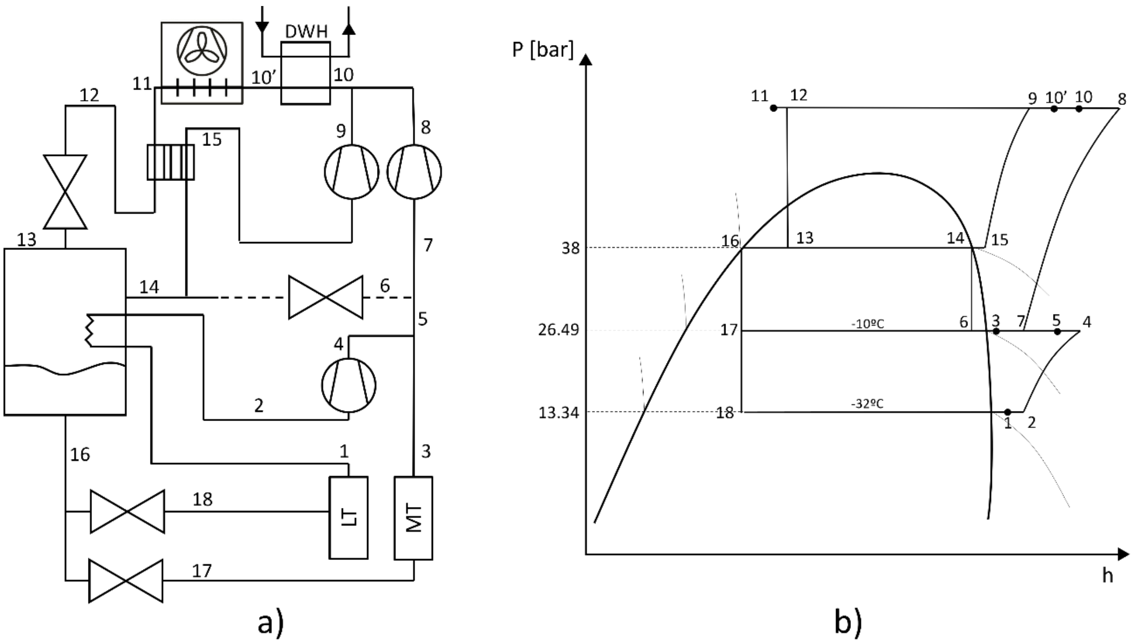

FIGURE 3.2: SIMPLIFIED INSTALLATION: (A) SCHEME AND (B) THEORETICAL P-H DIAGRAM

3.1.2 Cooling loads

Being a medium-sized supermarket, the system has an extensive amount of evaporator units, with many applications. In this case, a total of 51 cooling loads are connected to the main system, 10 of which are low-temperature and 41 medium-temperature. The total cooling capacities per group is shown in Figure 3.3. The given names (in Portuguese), references and power of each individual unit can be seen in Table A-1 in Annex A.

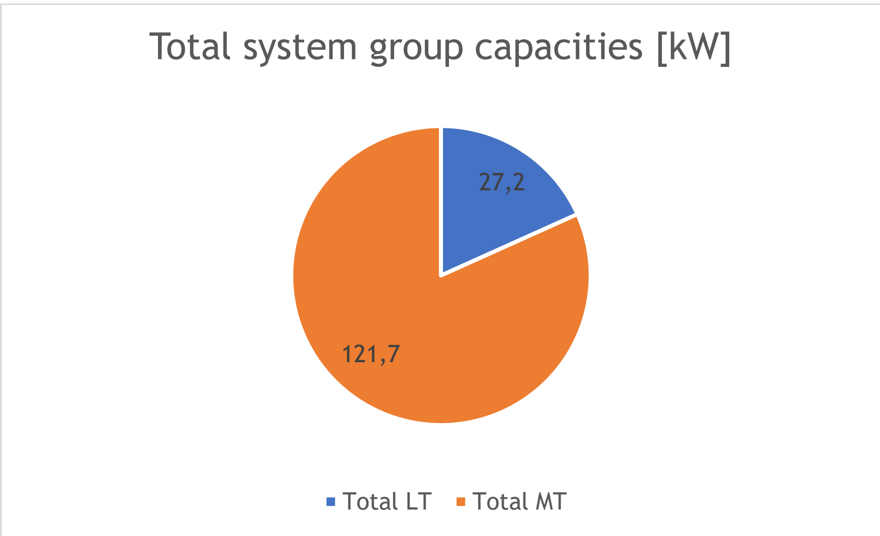

FIGURE 3.3: TOTAL SYSTEM GROUP CAPACITIES BY TYPE

The load ratio LR of the system is $LR = \frac{121.7}{27.2} = 4.47$.

3.1.3 Condenser/Gas Cooler

For the type of analysis being made, a full definition of the condensers/gas coolers used may not be necessary. However, their behaviour is absolutely necessary to be understood in order to do a complete analysis of the system. In this case, the *Carel pRack pr300T* controllers control the units by setting a gas-cooler setpoint temperature and a so-called gas-cooler temperature differential. The controller aims for the gas cooler temperature to be between gas-cooler setpoint temperature +/- the gas-cooler temperature differential, turning on or off ventilators as needed. Of course, when outside temperatures are above the set temperature + offset, it is thermodynamically impossible to maintain a certain set temperature, meaning that a certain $\Delta Temperature$ between ambient and gas cooler outlet temperature will be maintained. In order to evaluate how much this delta would be, the data from the month of August 2022 was retrieved and was plotted and can be seen in Figure 3.4. Hourly values for the whole month were used, from the 1st to the 31st of August.

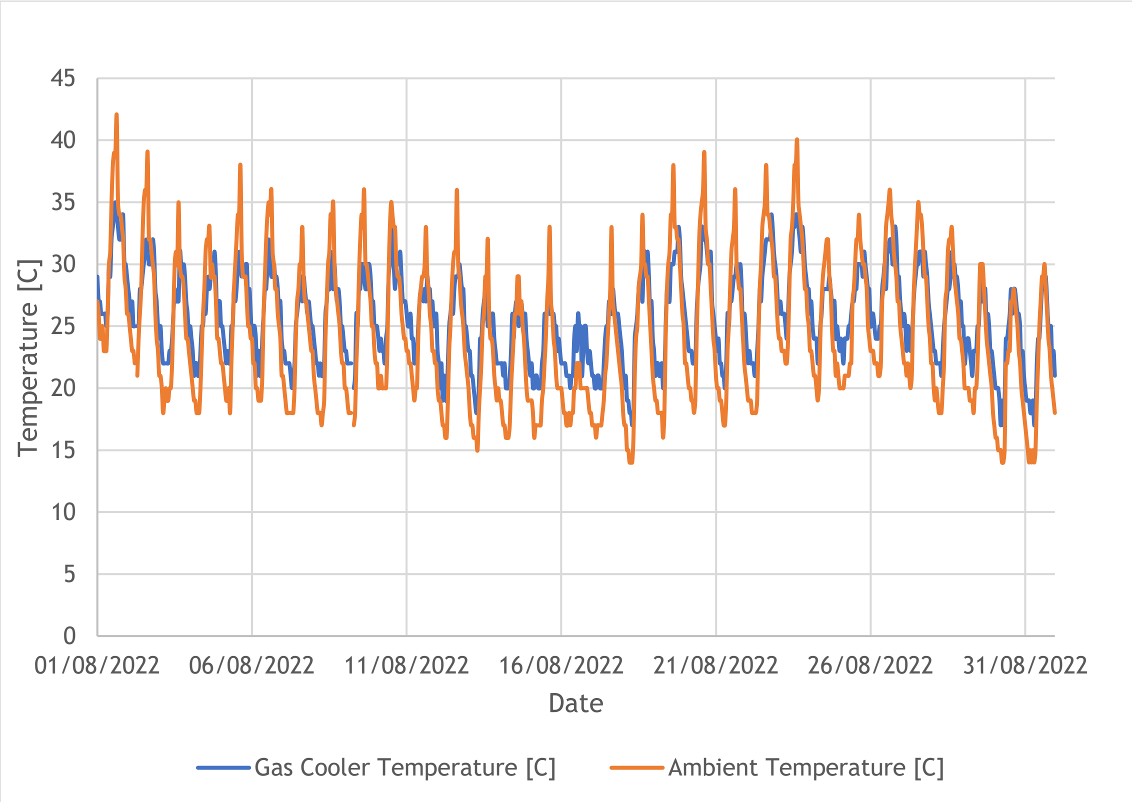

FIGURE 3.4: HOURLY GAS COOLER AND AMBIENT TEMPERATURE VARIATION DURING AUGUST 2022

From these data, the $\Delta Temperature$ was calculated and averaged for the whole month. The averaged result was $\Delta Temperature = 1.24$, which will be rounded to $\Delta Temperature = 2.0$ and used when necessary. This means that, on average, during the month of August 2022, the refrigerant temperature at the gas-cooler outlet was 1.24ºC hotter than the ambient temperature, for a given moment. These results lead to a possible error either in the measurement of the temperatures by a defective, uncalibrated or badly placed temperature probe or an error in the data gather. A delta of, at least, 5ºC was to be expected and the discussion and conclusions will be influenced by these results.

3.1.4 Initial conditions

Before making any changes in parameters, the system's initial conditions were saved for reference and to aid the theoretical study and are presented on Table 3. The cooling load's initial conditions, namely superheat and setpoints are also presented in table A-1 in Annex A.

TABLE 3: INITIAL CONDITIONS FOR SYSTEM'S PARAMETERS AND SETPOINTS

Parameter	Description	Value
P_{tank}	Reciever tank's set pressure	38 [bar]
Gas cooler setpoint	Gas cooler outlet temperature setpoint	25 [ºC]
Gas cooler offset	Allowable offset for gas cooler temperature setpoint before the controller acts (positive or negative)	±5 [ºC]
MT suction	Suction temperature for MT line setpoint	-10 [ºC]
LT Suction	Suction temperature for LT line setpoint	-32 [ºC]
LT suction line superheat[1]	Temperature delta between LT evaporator temperature and LT compressor intake	27 [ºC]
MT suction line superheat[1]	Temperature delta between MT evaporator temperature and MT compressor intake	15 [ºC]
IT suction line superheat[1]	Temperature delta between the receiver tank's temperature and the IT compressor intake	12 [ºC]
RPRV band	Band for P+I RPRV valve regulation	3
RPRV Integral time	Integral time for P+I flash-gas valve regulation	60 [s]

[1] These values are not setpoints and are dependent on IHX efficiency and useless superheat, and were the result of a monthly average of August 2022 values

3.2 Methodology

The project will be divided into two main parts: on a first approach, a theoretical study will be made not only to understand not only the magnitude of EER values and evolution, but to serve as a validation to the results obtained; on a second approach, using a real CO_2 booster system with parallel compression, parameters will be altered and their influence in EER will be studied

3.2.1 Theoretical study

Associated with real working installations there are always uncertainties and having a way of validating results is vital. For that, a theoretical study will be developed alongside the practical study, using software provided by the manufacturer of the installation's compressors, *Bitzer*. Although more complex programs exist and algorithms could be developed in differential equation solver *software*, the datasheet of the used compressors is very limited and does not fully characterize their efficiencies, which is crucial information. By contrast, *Bitzer*'s software has a built-in database of its compressors, enabling the production of more accurate results and saving time. The software's interface can be seen in Figure 3.5.

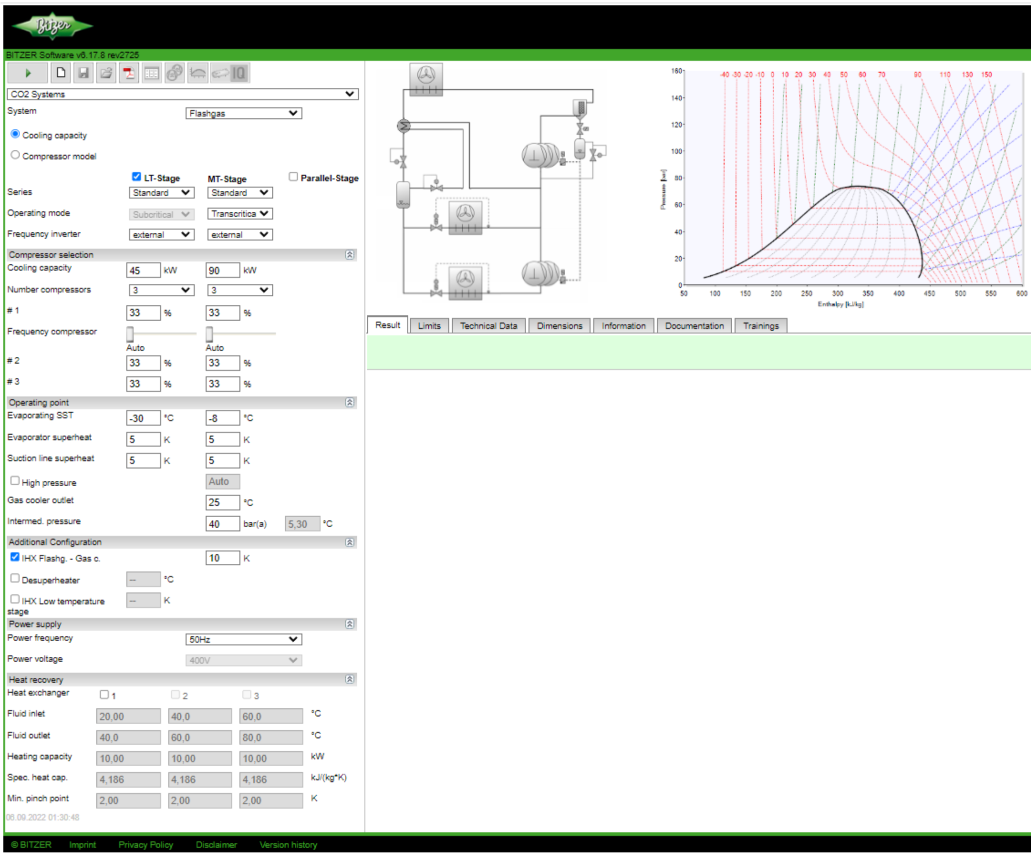

FIGURE 3.5: BITZER SOFTWARE'S INTERFACE

The program allows for an almost complete definition of the real system, namely:

- Definition of a R744 transcritical flashgas system with a parallel-stage;
- Selection of all three compressor groups and definition of variable-frequency compressors;
- Evaporation temperature, superheat, gas cooler temperature and receiver tank pressure setpoints;
- Addition of IHX for flashgas - gas cooler and low temperature configurations.

With these parameters, an almost complete definition of the system working in project capacities is defined, and the output is a full report of compressor performance, namely frequency, evaporator capacity, power, current, mass flow, total superheat and discharge gas temperature. Additionally, and most importantly, a EER estimation is also provided, which will be then used as comparison, for the different configurations. The referred parameters will be obtained from real data from the system which will be specified in later sub- sections.

It is worth noting that EER calculation will always be done for determined ambient temperatures, but the *software* works as a function of gas cooler outlet temperature. As seen in subsection 3.1.3, it is possible to relate gas cooler outlet temperature and ambient temperature, eliminating this potential problem.

One software limitation that is important to discuss is its incapability of combining parallel compression with flash gas bypass. As seen, in a real installation, from a determined flash gas mass flow the parallel compressor group turns on and as long as this minimum mass flow exists the compressor group will be working. When flash gas mass flow is higher than what the parallel stage can handle, the mass flow difference will go through the flash gas valve, meaning both valve is opened, and compressors are fully working. *Bitzer* software does not have this capability, meaning that when the maximum allowable compressor mass flow is exceeded the program returns an error and stops the calculation. To get around this, different calculations for fully parallel situations and for fully flash gas situations were made, in order to study the effects of the parameter changes in both conditions. Whenever the parallel compression mass flow was higher than the parallel compressor capacity, a similar higher capacity compressor was used. Similarly, when parallel compression mass flow was lower than the minimum compressor admissible flow, a similar smaller capacity was chosen.

3.2.2 Data Gathering & parameter change

As seen in section 2.7, the control of an installation is as important as the installation itself and, in this case, will allow for easy parameter change remotely and instantly. The controllers used in the object of study will be detailed bellow, but it is important at this point to explain how the data will be gathered and the parameters changed. The refrigeration system uses a *Carel boss* supervision system alongside with a *LOYTEC LINX*, an automation server capable of logging and running automation and calculation programs, which come useful in certain analysis. The gathered data will be accessed remotely, directly from *boss*'s IP address, with an interface shown below, on Figure 3.6.

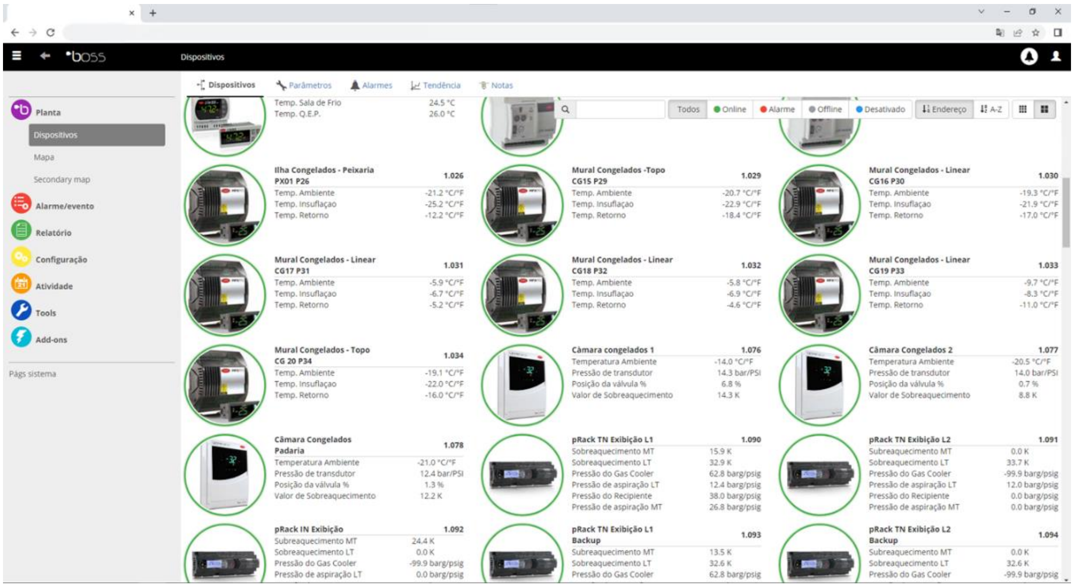

FIGURE 3.6: CAREL BOSS CONTROL PAGE INTERFACE

In this page it is also possible to access the main system's controllers and individual evaporators to change parameters and data can be downloaded for any given time period, for any given interval, being exported in .csv files. This is done via the creation of a report: from any device, parameters can be chosen and included in the report which will then be exported every set time value. To avoid excessive data and disparate values, the time-step of the data collection was defined to be 5 minutes, meaning that a given variable will produce 288 entries every day. It was considered to be enough precision for the study.

3.2.3 EER calculation

Although EER calculation is a simple task in theory, in practice obtaining values such as enthalpies and mass flows is not a direct task and some calculations need to be made in order to obtain them from pressure values, temperature readings and fluid properties. How a controller calculates EER is through an algorithm that will be explained in simplified terms in this sub-section.

First of all, there are two main EER parameters that are taken into consideration:

- The consideration or not of DWH for the EER: $COP_{DWH}\ VS\ COP_{w/o\ DWH}$
- The consideration or not of all the systems components for the total energy spend: $COP_{real}\ VS\ COP_{thermodynamic}$

The difference between the consideration or not of DHW is self-explanatory, if it is considered, then DHW capacity needs to be accounted for in the numerator of the equation, otherwise it doesn't. This capacity won't be accounted for in the calculations of this project.

The difference between real and thermodynamic EER is as follows:

$$COP_{real} = \frac{Q_{MT} + Q_{LT}}{P_{total}} \quad \mathbf{3.1}$$

Where:

- Q_{MT} is the total MT cooling capacity;
- Q_{LT} is the total LT cooling capacity;
- P_{total} is the total energy consumed by the whole refrigeration system and gas cooler ventilators.

Thermodynamic EER can be defined as:

$$COP_{thermodynamic} = \frac{Q_{MT} + Q_{LT}}{\sum_i x_i \times P_{comp,i}} \quad \mathbf{3.2}$$

Where:

- x_i is the active percentage of total power of compressor i;
- $P_{comp,i}$ is the nominal power of compressor i;
- i is the total number of compressors.

For the scope of this work, real EER will be used. The question now is how the controller is able to calculate the three necessary values for the calculation. The total power is the easiest one as its directly measured by an electrical power meter connected to the whole system, that feeds information to the controller.

Starting with MT cooling capacity, it is given by:

$$Q_{MT} = \dot{m}_{evap,MT} \times (h_{exit,evap,MT} - h_{receiver}) \quad \mathbf{3.3}$$

Where:

- $\dot{m}_{evap,MT}$ is the total mass flow passing through the MT evaporators;
- $h_{exit,evap,MT}$ is the enthalpy at the exit of the MT evaporator;
- $h_{receiver}$ is the enthalpy in of the liquid in the receiver.

MT evaporator mass flow is calculated by analysing the mass flow that enters the MT compressor group. It is known that all the flow that enters this compressor group ($\dot{m}_{comp,MT}$) comes from either flash gas valve ($\dot{m}_{flashgas}$), MT evaporators or from the low stage compressors ($\dot{m}_{comp-LT}$), meaning:

$$\dot{m}_{evap,MT} = \dot{m}_{comp,MT} - \dot{m}_{flashgas} - \dot{m}_{comp,LT} \quad \mathbf{3.4}$$

All three compressors mass flows, $\dot{m}_{comp,MT}$, $\dot{m}_{comp,LT}$ and $\dot{m}_{comp,IT}$ are calculated via the algorithm, given the following inputs:

- Compressor frequency;
- Superheat of the fluid;
- Evaporating temperature of the fluid;
- Discharge pressure;
- Temperature of the fluid at discharge pressure.

Flash gas mass flow is also calculated given the parameters:

- Pressure at the MT evaporators;
- Receiver pressure;
- Opening of the flashgas valve (0 to 100);

With these mass flows, the evaporator mass flow is calculated.

$h_{exit,evap,MT}$ is given by doing an energy balance at the MT pressure line:

$$\begin{aligned}\dot{m}_{comp,MT} \times h_{suction,MT} \\ &= \dot{m}_{comp,LT} \times h_{discharge,LT} + \dot{m}_{flashgas} \times h_{flashgas} \\ &+ \dot{m}_{evap,MT} \times h_{exit,evap,MT}\end{aligned} \tag{3.5}$$

Rearranging:

$$h_{exit,evap,MT} \frac{\dot{m}_{comp,MT} \times h_{suction,MT} - \dot{m}_{comp,LT} \times h_{discharge,LT} - \dot{m}_{flashgas} \times h_{flashgas}}{\dot{m}_{evap,MT}}$$

The referred enthalpies are easily calculated given pressure and temperature from the sensors. Same happens with receiver enthalpy. Q_{MT} is now fully defined.

For Q_{LT}:

$$Q_{LT} = \dot{m}_{evap,LT} \times (h_{exit,evap,LT} - h_{receiver}) \tag{3.6}$$

This parameter is easier to calculate because the enthalpies are directly calculated from temperature and pressure values and $\dot{m}_{evap,LT} = \dot{m}_{comp,LT}$. The EER calculation is now fully defined.

3.2.4 Parameter choice

As mentioned in section 1.5, EER optimization had to be made with minimal work done in the installation. The parameters had to be chosen as to not structurally affect the cooling installation, being easily parameterized, and can be fully and rapidly reversed, when the study ends and/or in case of emergency.

As mentioned, the main focus of this EER improvement was to minimize compressor work, because cooling capacity is fixed. This can be done either by decreasing mass flow going through compressors or by decreasing compressing ratio. MT and LT stages are fixed, and gas-cooler pressure is dependent on ambient temperature. The only pressure stage that can be chosen is receiver pressure. As such, it was chosen as a parameter, in order to study the influence of its increase.

On the evaporator side, while maintaining capacity and unit set temperature, two parameters can be chosen to study their influence: evaporating pressure and superheat. It is nothing new that a higher evaporator pressure, mentioned from now on as evaporator suction pressure to follow the company nomenclature, will reduce compressing ratio and, as such, reduce compressor energy usage. However, being directly connected to evaporating temperature, it's difficult to evaluate just how much performance increase can be obtained without compromising evaporator unit's set temperature, making it an interesting parameter to study. Superheat change, as seen in 2.2.1, does not clearly lead to an increase or decrease in EER, making this parameter a suitable object for the study. The bulk of energy consumption in a system of the studied type comes from the high-stage phase and it's this phase that is mostly affected by flash-gas and tank pressure. For that reason, a focus only on the MT phase was chosen to be analysed, namely MT suction pressure and MT evaporators superheat. The LT stage influence in the whole system was not considered because its capacity is more then 4 times lower than the MT's.

The parameter change was done in order not to change too much the initial values, to maintain system stability, but, at the same time, with significant impact to EER, which could then be extrapolated. The choice of setpoint interval can be seen in Table 4.

TABLE 4: PARAMETER SETPOINT INTERVAL CHANGE

Parameter	Setpoint interval
Receiver tank pressure	38 to 40 [bar]
MT suction pressure	-10 to -9 [bar]
MT evaporators Superheat	10 to 9 [K]

4 Results, analysis & discussion

In this chapter, the results of the theorical and practical tests will be presented and analysed in detail, from an efficient to economic standpoint. Starting with a software analysis that will serve as validation to the then analysed practical results.

4.1 Software results and analysis

The software was loaded with Table 3's parameters and was run for gas cooler outlet temperatures from 25ºC to 40ºC. As presented in 3.1.3, and considering gas cooler outlet setpoint temperature in the real installation is 25ºC and the measured $\Delta Temperature = 2.0℃$, this means that, in theory, the results from 25ºC represent every ambient temperature up to 23ºC, with the following gas cooler temperatures representing $T_{amb} - 2.0℃$. A gas cooler outlet temperature of 40ºC represents an ambient temperature of 38ºC, for example. However, and due to the more than 10ºC offset between set and allowable temperatures, it will just be considered that:

$$T_{amb} = T_{gas\ cooler\ outlet} - 2.0 \qquad \textbf{4.1}$$

As discussed, the software limitation meant that separate flash gas and parallel compression calculations were made, and whenever the parallel compressor had to be changed for a higher capacity one the results will explicit that.

A baseline simulation was conducted with initial parameters and a gas-cooler temperature of 25ºC and the scheme and p-h diagram can be seen in Figure 4.1.

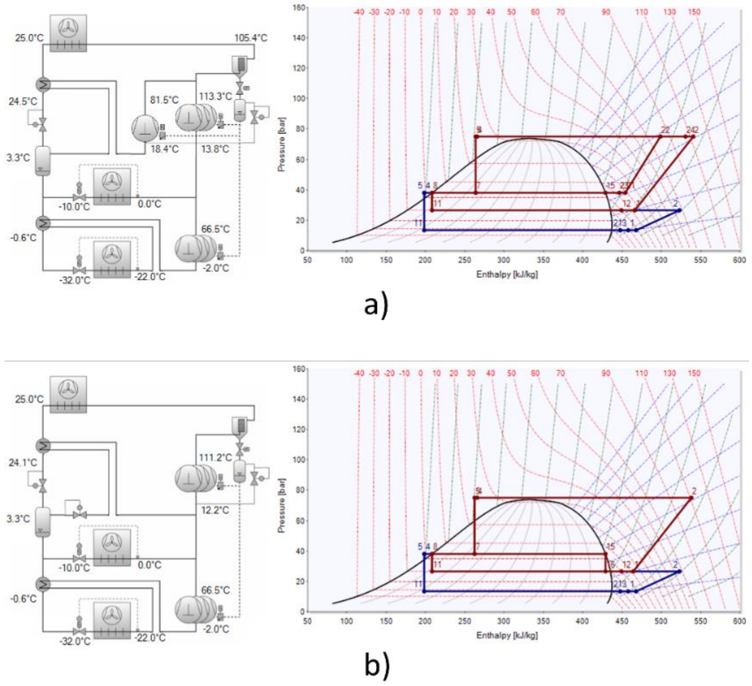

FIGURE 4.1: SIMULATION SCHEMES FROM BASELINE CONDITIONS: (A) PARALLEL COMPRESSION AND (B) FLASH GAS ONLY

As it is possible to see, specially concerning superheat temperatures, the chosen values were matched as close as possible to the initial values. Just as a reference, the parallel compression only and flash gas only EER results were, respectively, **2.38** and **2.13**.

4.1.1 Receiver tank pressure

The program was run for gas cooler temperatures between 25 and 40ºC, and receiver tank's pressure from 34 to 42 bar. Since the initial receiver's pressure was 38 bar, it made sense to test lower and higher pressures, taking into account the implications of too low and too high pressures, which will be discussed. For the parallel system, the results are shown in Annex B, in Table B-1.

The data was plotted in in order to understand EER evolution and can be seen in Figure 4.2. It is possible to observe that in any pressure case, a steep variation of EER occurs with the increase in gas cooler (and, as a consequence, ambient) temperature, as expected. The various results start to deviate from each other at higher temperatures, which may give a hint on the usefulness of higher receiver pressures.

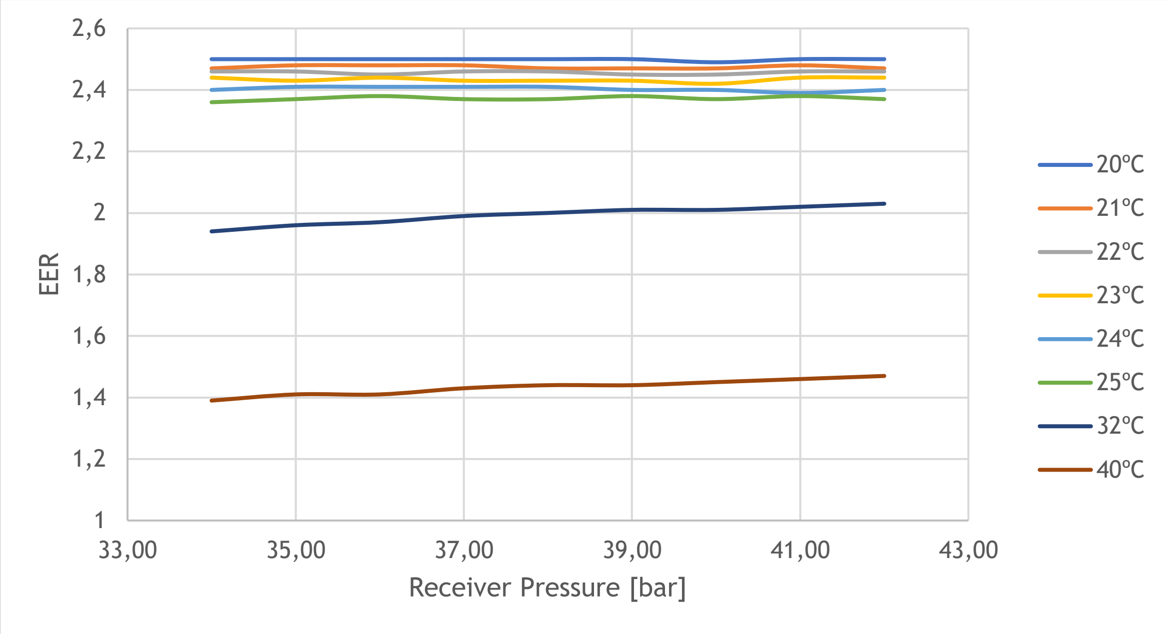

FIGURE 4.2: THEORETICAL EER VARIATION WITH RECEIVER PRESSURE, FOR VARIOUS GAS COOLER TEMPERATURE VALUES, FOR A PARALLEL COMPRESSION SYSTEM

To evaluate just how much the increase in EER was, the average percentual increase per bar was plotted, for each set gas cooler temperature. This graph can be seen in Figure 4.3.

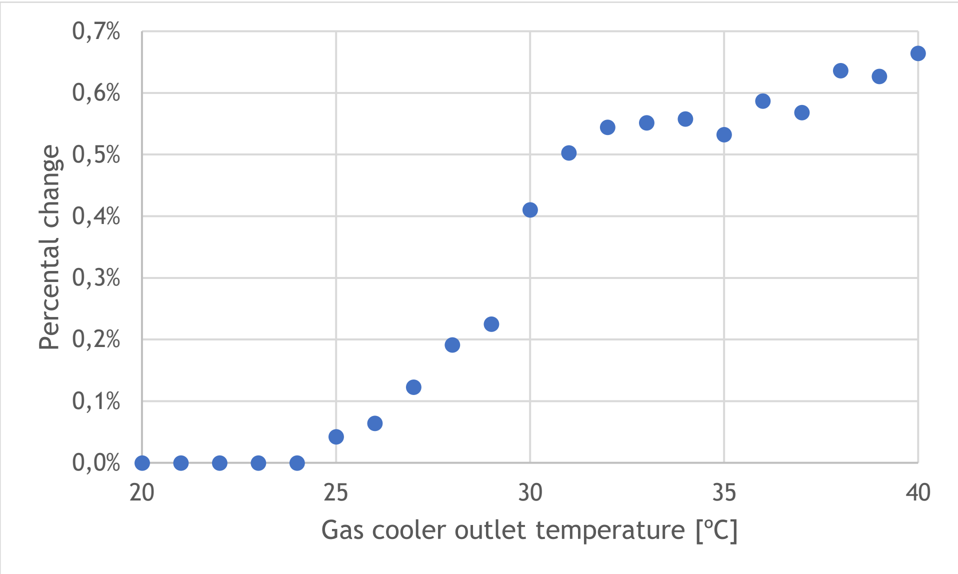

FIGURE 4.3: AVERAGE PERCENTUAL PER BAR INCREASE OF RECEIVER PRESSURE, WITH GAS COOLER TEMPERATURE, FOR A PARALLEL SYSTEM

An analysis of the behaviour is easier to understand with the evolution represented in a p-h diagram. This can be seen in Figure 4.4.

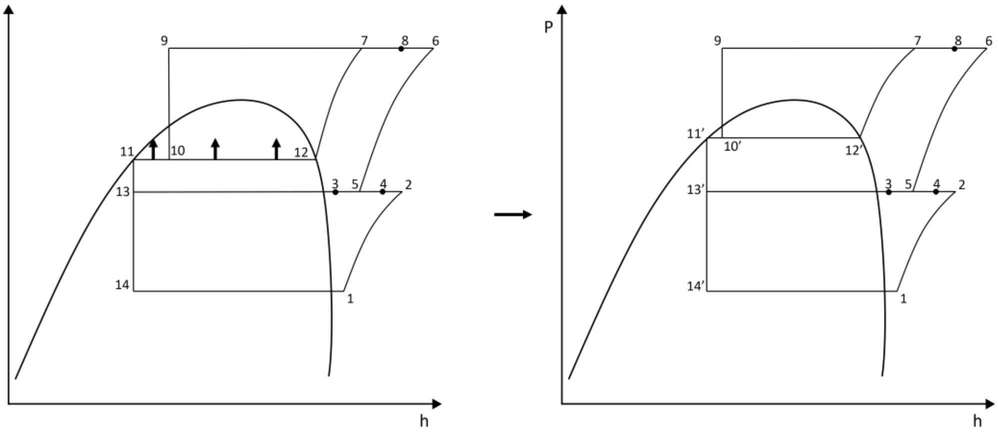

FIGURE 4.4: P-H DIAGRAM EVOLUTION OF AN INCREASE IN RECEIVER PRESSURE, FOR A PARALLEL COMPRESSION-ONLY SYSTEM

It is observable that, in order to maintain the same cooling load, when the receiver pressure increases the mass flow going through the MT and LT compressors needs to also increase, because $(h_3 - h_{13'}) < (h_3 - h_{13})$ and $(h_1 - h_{14'}) < (h_1 - h_{14})$, potentially increasing the MT and LT compressor work. However, the compression ratio of the IT compressor decreases, decreasing its work. This balance will define the EER evolution and explains why at higher temperatures the EER increase in higher: more mass flow exits the receiver and goes through the parallel compressor, increasing the effect of the decrease in compression ratio.

The simulation was then run for the same conditions but for a flash-gas only system. The results can be seen in Table B-2, in Annex B. The results were plotted and can be seen in Figure 4.5.

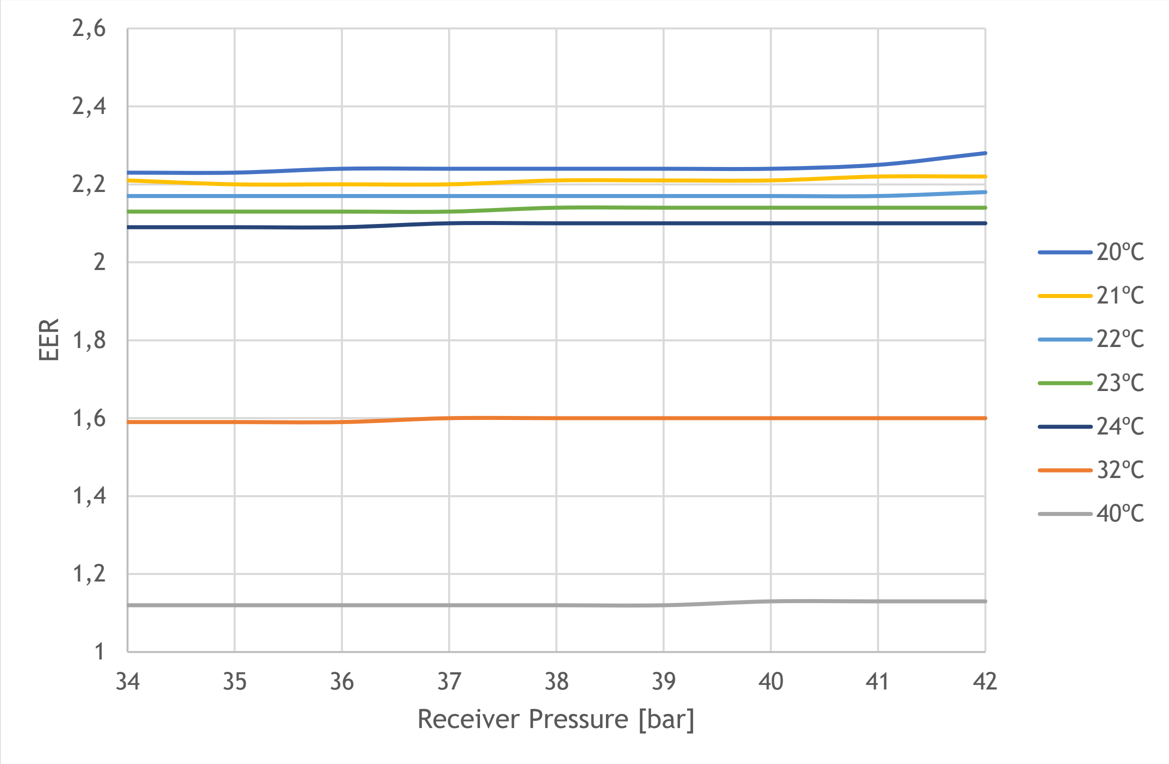

FIGURE 4.5: THEORETICAL EER VARIATION WITH RECEIVER PRESSURE, FOR VARIOUS GAS COOLER TEMPERATURE VALUES, FOR A FLASH GAS ONLY SYSTEM

The average percentual changes were calculated and plotted, and can be seen in Figure 4.6.

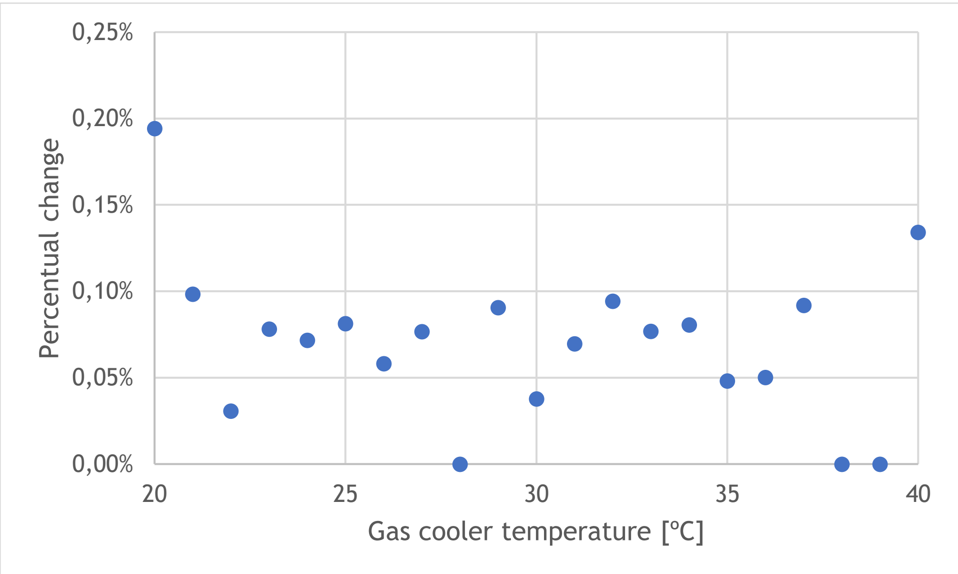

FIGURE 4.6: AVERAGE PERCENTUAL PER BAR INCREASE OF RECEIVER PRESSURE, WITH GAS COOLER TEMPERATURE, FOR A FLASH-GAS ONLY SYSTEM

Observing Figure 4.6, it is clear that no trend appears in the EER evolution, contrasting with the clear trend of Figure 4.3. This lack of pattern can lead to questioning the validity of this particular simulation, which will be discussed.

To better analyse the results, once again, the evolution was drawn in a p-h diagram and can be seen in Figure 4.7.

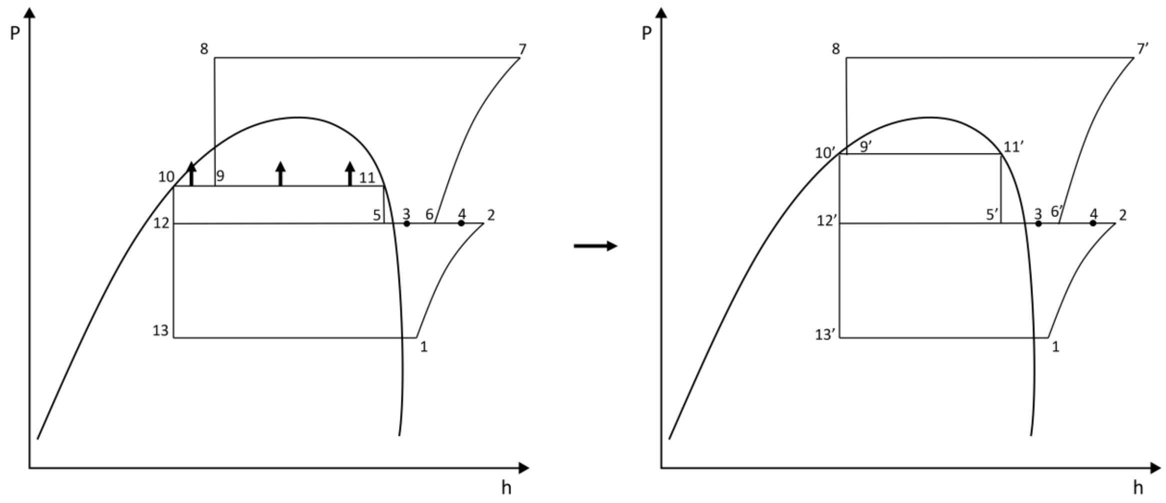

FIGURE 4.7: P-H DIAGRAM EVOLUTION OF AN INCREASE IN RECEIVER PRESSURE, FOR A FLASH GAS-ONLY SYSTEM

The same behaviour occurs where the increase in enthalpy at the entrance of the evaporators leads to an increase in mass flow, for the same cooling effect. However, the flash gas properties change with the increase in pressure and when mixed at the entrance of the MT compressor, change the conditions of the fluid in admission which affects the conditions of the fluid at the discharge. It is unclear what is the relationship between $(h_{7'} - h_{6'})$ and $(h_7 - h_6)$, which may explain the lack of a particular trend in Figure 4.6. A general conclusion is that most likely the increase in receiver pressure may increase EER, which will be validated upon the real test.

It is also worth noting that, although both parallel compression and flash-gas only simulations were presented, in the real world only flash-gas situations will be considered. The reason why will be discussed.

4.1.2 MT suction pressure

MT suction pressure variation was set to run an increase from 24.3 bar to 28.03 bar, which corresponds to a suction temperature increase from -13ºC and -8ºC. The software only inputs temperatures and not pressures. The results running only with parallel compression can be seen in Table B-3, in Annex B, which also shows the percentual increase from -13ºC to -8ºC. The results were then plotted, for various temperature values and can be seen in Figure 4.8. The percentual increase was also plotted and can be seen in Figure 4.9.

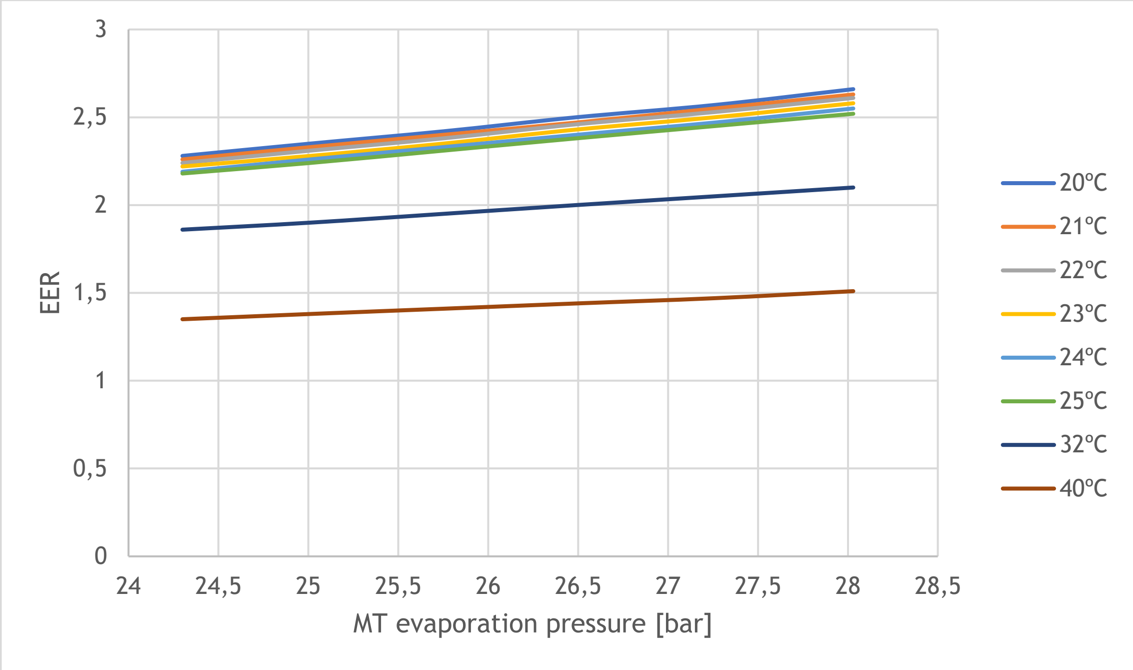

FIGURE 4.8: THEORETICAL EER VARIATION WITH MT EVAPORATION PRESSURE, FOR VARIOUS GAS COOLER TEMPERATURE VALUES, FOR A PARALLEL COMPRESSION SYSTEM

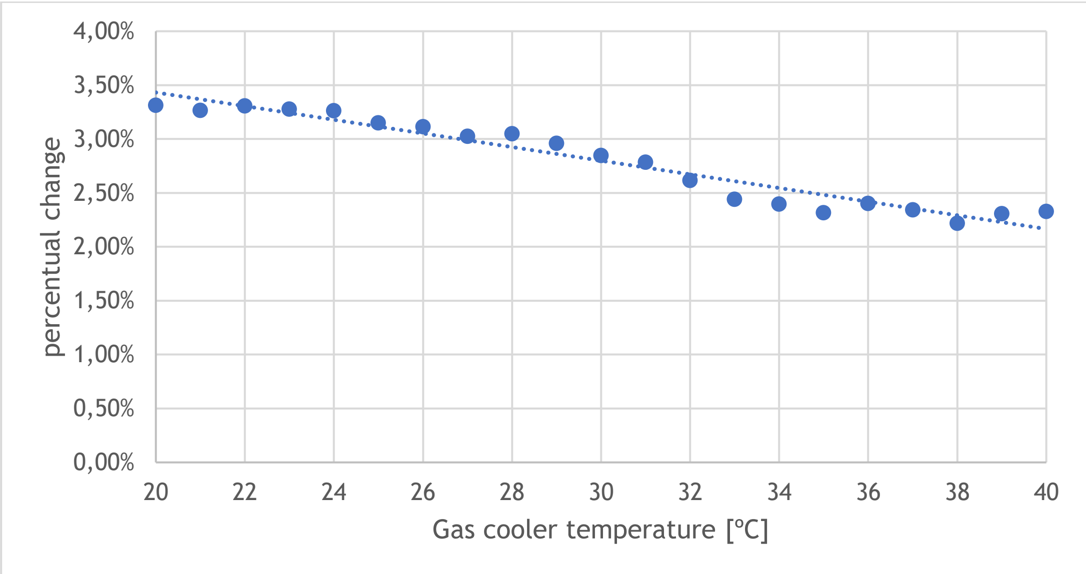

FIGURE 4.9: AVERAGE PERCENTUAL PER °C INCREASE OF MT EVAPORATION TEMPERATURE/PRESSURE, WITH GAS COOLER TEMPERATURE, FOR A PARALLEL COMPRESSION SYSTEM

A first simple analysis may help to understand the EER increase. Maintaining every other pressure and load in the system the same, an increase in MT pressure will "push" the line in a p-h diagram, as shown in Figure 4.10.

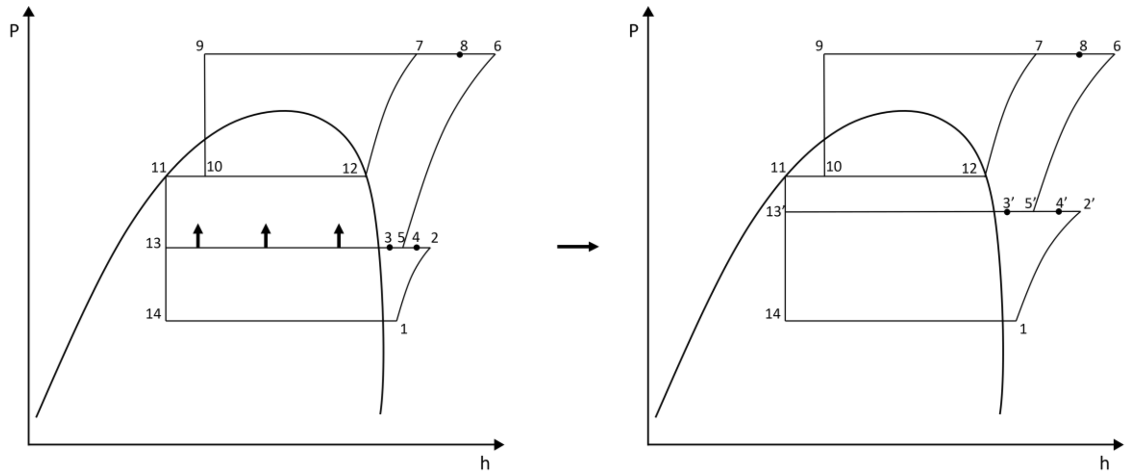

FIGURE 4.10: P-H DIAGRAM EVOLUTION OF AN INCREASE IN MT PRESSURE, FOR A PARALLEL COMPRESSION ONLY SYSTEM

With overheat maintaining the same value and ($h_{13} = h_{13'}$) it is not apparently clear what is the relationship between ($h_3 - h_{13}$) and ($h_{3'} - h_{13'}$). It's possible to do a quick calculation to understand relationship, assuming receiver pressure @38 bar, an increase in MT pressure from 25 to 28 bar (-12ºC to -8ºC) and a superheat of 10ºC. The enthalpy values come from R744 enthalpy tables:

- $h_{13} = h_{13'} = h_{11} = h_{f@38\,bar} = 208.1\ [kJ/kg]$
- $h_3 = h_{\,P=25bar\ and\ T=-12+10=-2ºC} = 450.6\ [kJ/kg]$
- $h_3 = h_{\,P=28bar\ and\ T=-8+10=2ºC} = 448.4\ [kJ/kg]$

It is possible to observe that, around the studied pressure and temperature values, the change in enthalpy difference is negligible, meaning that the evaporator and compressor mass flow will be approximately the same in both cases, not leading to a significant work increase

However, low-stage compressors will have to do additional work due to the higher MT pressure. This additional work is offset by the significant decrease in work in intermediate stages compressors due to the lower pressure gradient between stages, meaning a decrease in total work is achieved. Because work from MT stages is much higher than LT stages, mainly because of the almost 4-time higher MT capacity than LT, seen in Figure 3.3, EER will increase. This increase is clearly seen in Figure 4.8. In summary:

$$Aditional\ work\ from\ higher\ LT\ compression\ ratio$$

$$<$$

$$Saved\ work\ by\ decreasing\ MT\ compression\ ratio$$

From this equation, it becomes clearer why the percentual increase in EER decreases with ambient temperature: for the same difference in pressure the additional work from higher LT compression ratio stay the same. However, as ambient temperature increases, gas cooler temperature also increases, meaning that the pressure ratio for the MT compressors increases, which in turn reduces the saved work by decreasing MT compression ratio.

The simulation was run with the same parameters for a system with flash-gas only. The results can be seen in Annex B. in Table B-4. Once again, the results were plotted for various temperatures, as well as the percentual change. These can be seen in Figure 4.11 and Figure 4.12, respectively.

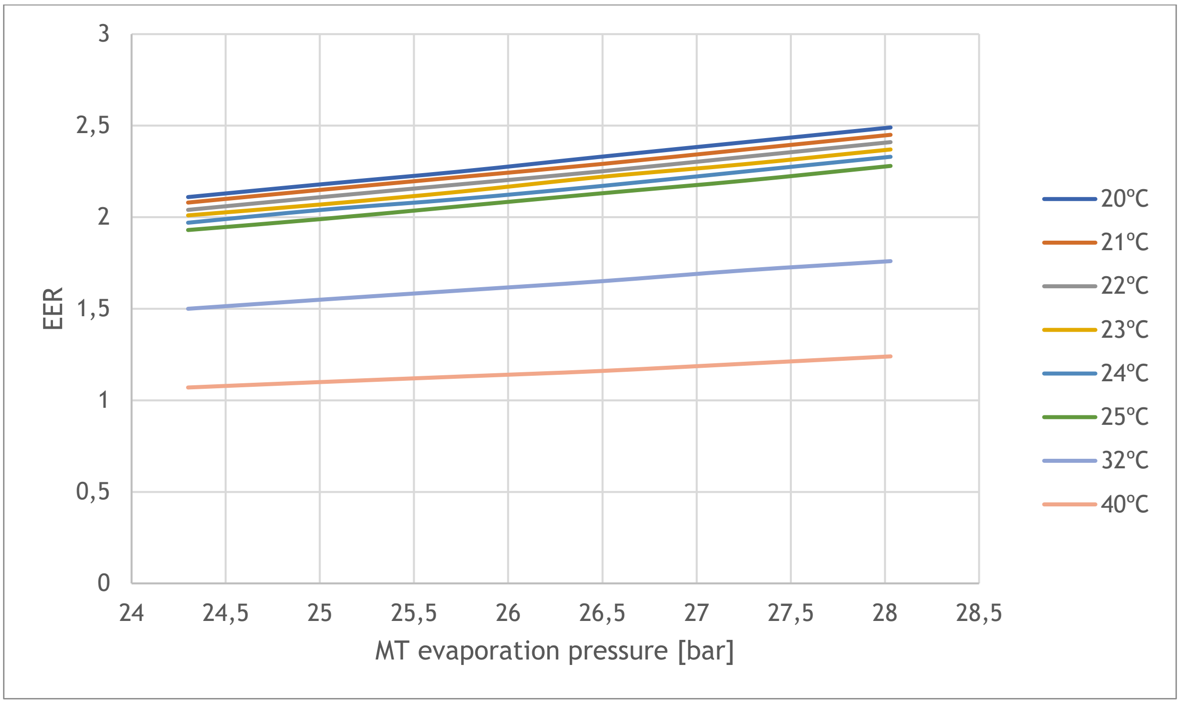

FIGURE 4.11: THEORETICAL EER VARIATION WITH MT EVAPORATION PRESSURE, FOR VARIOUS GAS COOLER TEMPERATURE VALUES, FOR A FLASH GAS ONLY SYSTEM

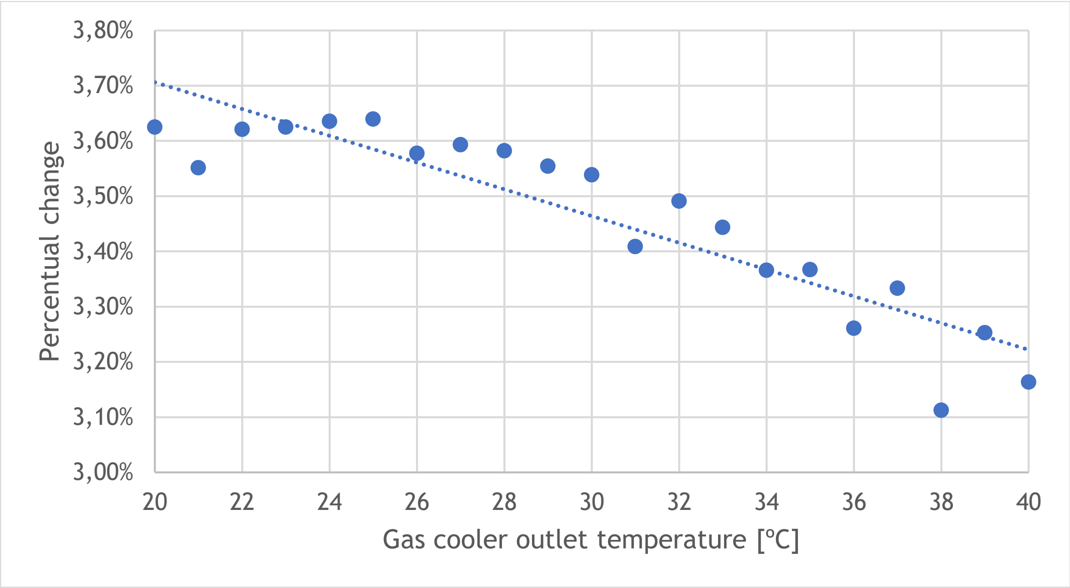

FIGURE 4.12: AVERAGE PERCENTUAL PER °C INCREASE OF MT EVAPORATION TEMPERATURE/PRESSURE, WITH GAS COOLER TEMPERATURE, FOR A FLASH GAS ONLY SYSTEM

The behaviour in this case is similar to the previous system, apart from the slightly lower EER values, which is to be expected. Studying the p-h diagram evolution, seen in Figure 4.13, can help understand the results.

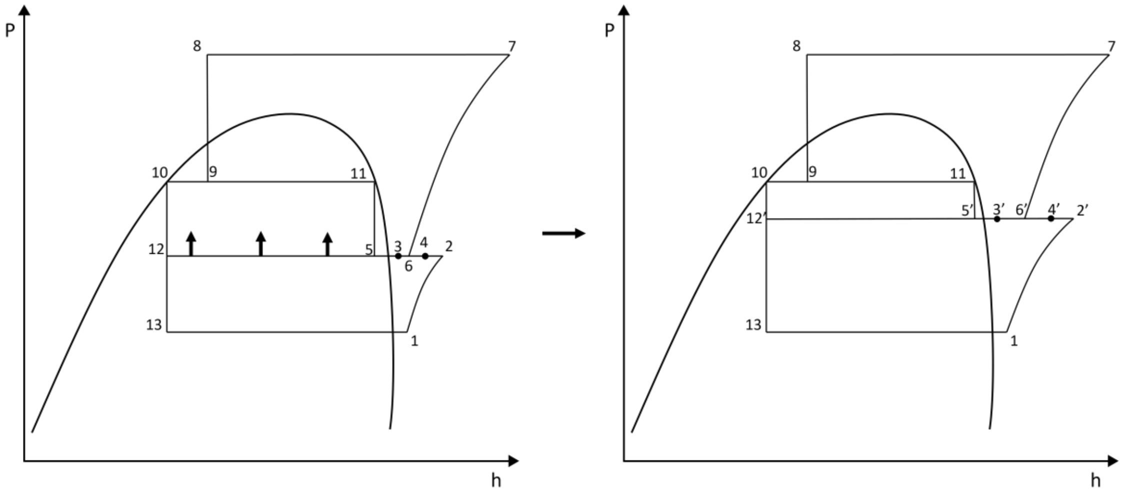

FIGURE 4.13: P-H DIAGRAM EVOLUTION OF AN INCREASE IN MT PRESSURE, FOR A FLASH-GAS ONLY SYSTEM

Similarly, the increase in MT pressure will, undoubtably, increase low stage compressors compression ratio and decrease high stage compression ratio, with a negligible potential increase in MT compressor mass flow. Due to the higher MT capacity, the savings in intermediate compression will be higher than the increase in low-stage compression ratio. This saving will decrease with ambient temperature increase, due to the gas-cooler pressure increase.

One of the downsides of increasing MT evaporation pressure is the existing possibility of not being able to reach setpoint temperatures in the cooling units. This will be analysed in the real system study.

4.1.3 MT evaporator superheat

Superheat was changed in the *software* from 4 K to 16K, for the MT evaporator, in 2 K increases and 1 K increase around the real superheat initial value of 10 K. For the parallel system, the EER results and percentual change from 4 to 16K, from gas cooler temperatures of 20 to 40 ºC. The results are summarized in Table B-5, in Annex 5. In the presented results, it was also assumed that the whole system had, on average, a 5K higher total superheat than the evaporator's. This value comes from Table 3, where for a an average evaporator superheat value of 10K, the whole system's was 15K, a 5K difference.

Once again, the results along with the percentual change were plotted and can be seen in Figure 4.14 and Figure 4.15.

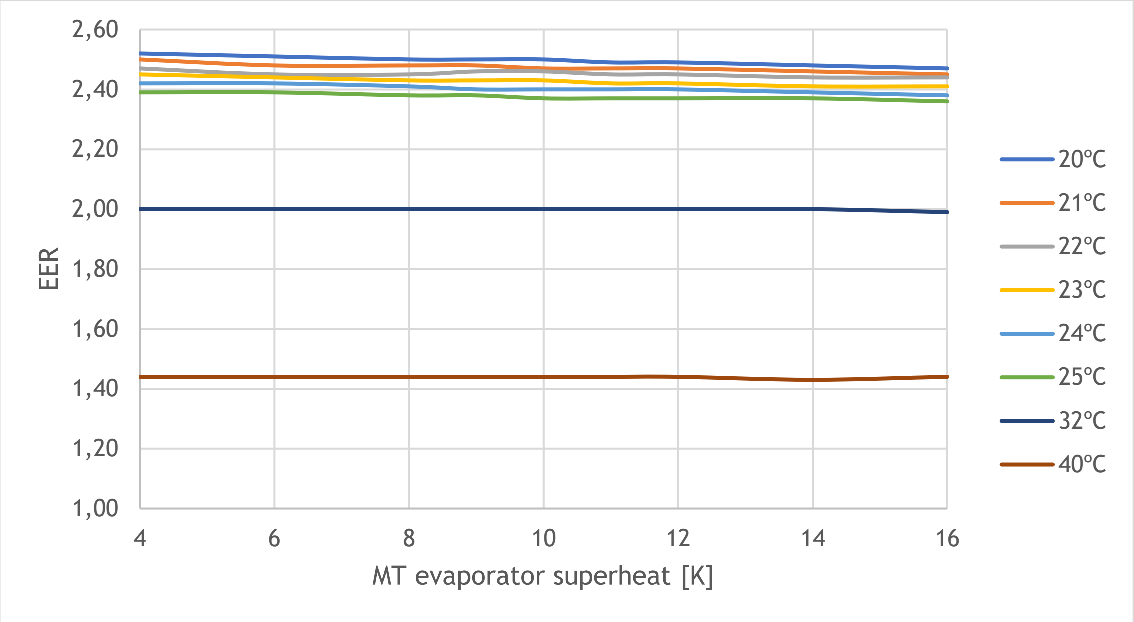

FIGURE 4.14: THEORETICAL EER VARIATION WITH MT EVAPORATION PRESSURE, FOR VARIOUS GAS COOLER TEMPERATURE VALUES, FOR A PARALLEL COMPRESSION SYSTEM

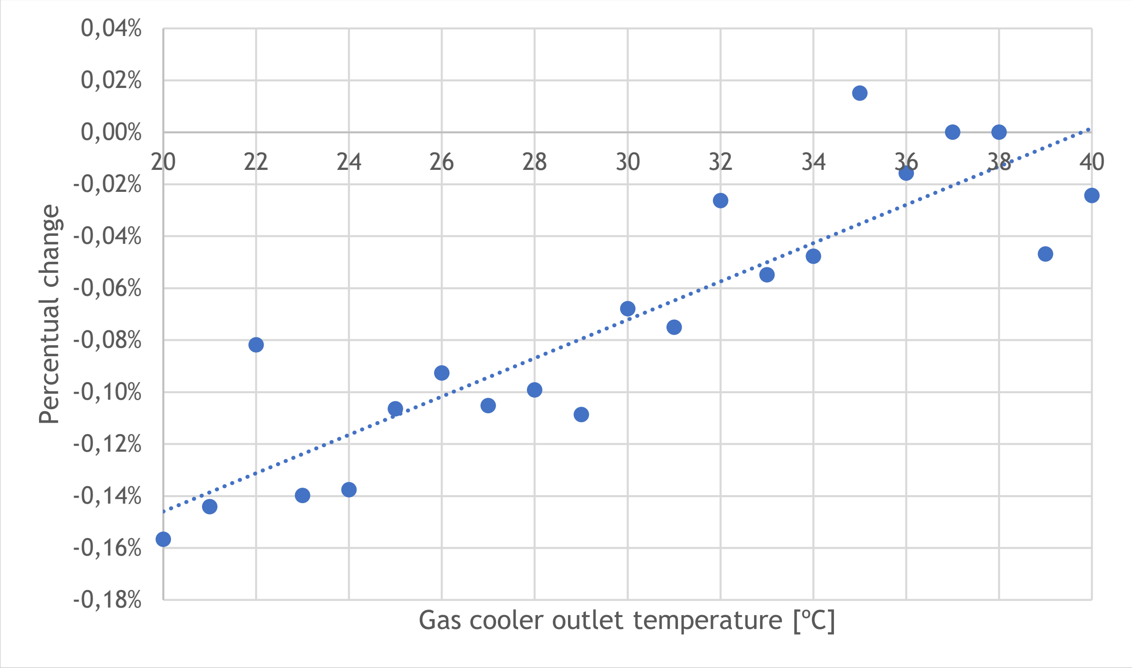

FIGURE 4.15: AVERAGE PERCENTUAL PER K INCREASE OF MT SUPERHEAT TEMPERATURE/PRESSURE, WITH GAS COOLER TEMPERATURE, FOR A PARALLEL COMPRESSION SYSTEM

The analysis can be done, once again, with the help of a p-h diagram of the parameter change evolution, which can be seen in Figure 4.16.

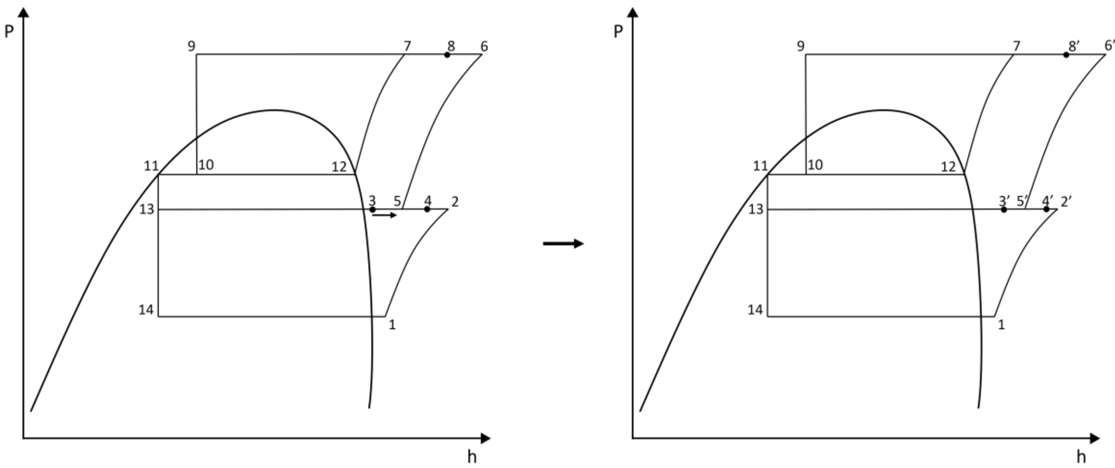

FIGURE 4.16: P-H DIAGRAM EVOLUTION OF AN INCREASE IN MT EVAPORATOR SUPERHEAT

A mentioned in section 2.2.1, superheat change will not necessarily lead to and increase or decrease in EER, meaning that the analysis needs to be done for every specific case. Following Figure 4.16's numbering, for the same refrigeration load, and given that $(h_{3'} - h_{13}) > (h_3 - h_{13})$, when superheat is higher the refrigerant's mass flow passing through the MT evaporator must decrease in order to maintain the same cooling effect. This will lead to a decrease in mass flow passing through the high stage compressors. However, the refrigerant will enter said compressors with a higher temperature and, in consequence, higher enthalpy. This means that $(h_{6'} - h_{5'}) \neq (h_6 - h_5)$. In this specific case, with the increase in superheat, the decrease in compressor mass flow is lower than the potential increase in enthalpy difference, specially at lower ambient temperatures, which lead to an overall increase in compressor work, decreasing EER. With the increase in ambient temperature, the percentual increase in compressor work is less and less which evens the EER variation.

The simulation for a flash-gas system only was run and the results can be seen in Table B-6, in Annex B.

Right away, a different trend to the previous study was observed, which is further demonstrated with the plots of Figure 4.17 and Figure 4.18.

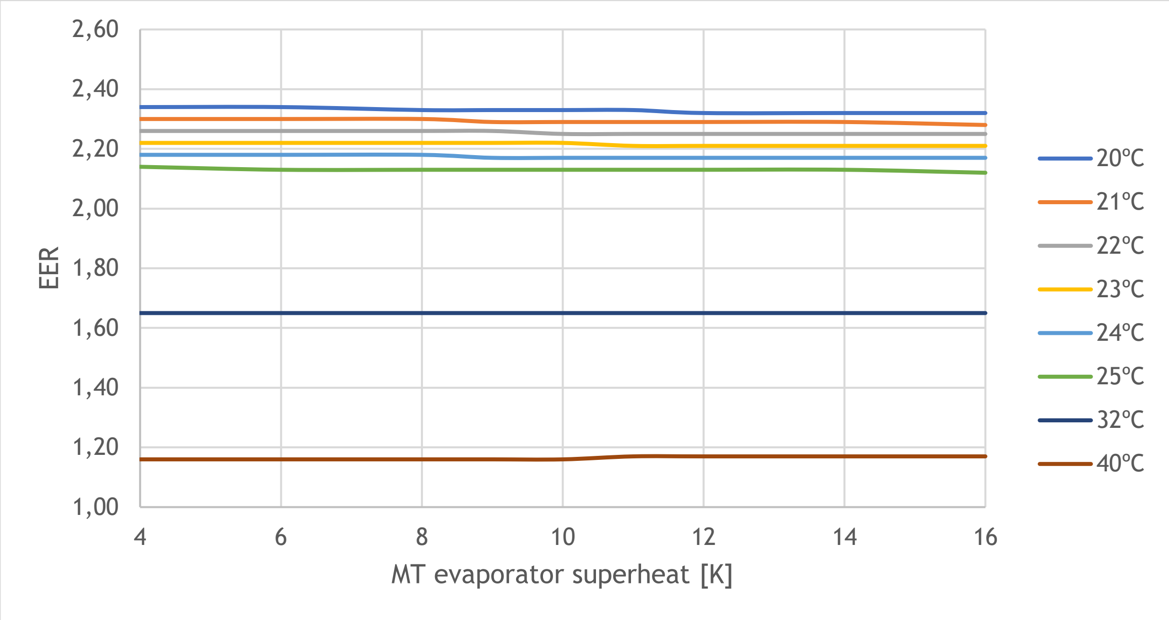

FIGURE 4.17: THEORETICAL EER VARIATION WITH MT EVAPORATION PRESSURE, FOR VARIOUS GAS COOLER TEMPERATURE VALUES, FOR A FLASH GAS ONLY SYSTEM

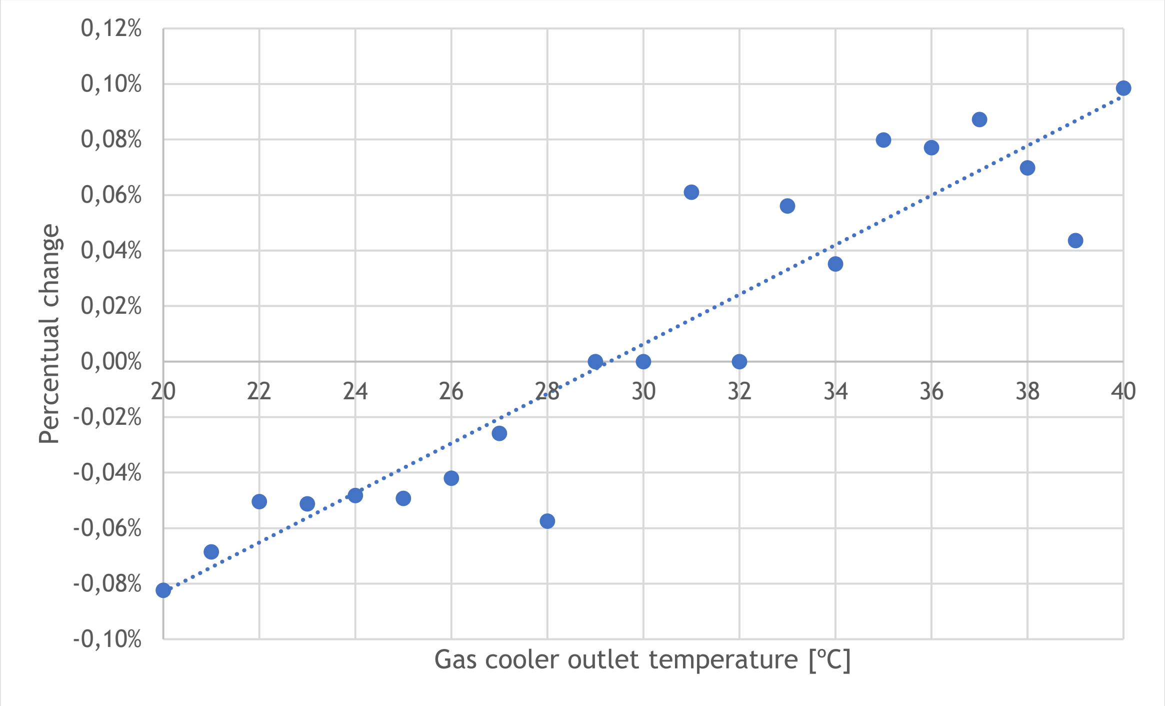

FIGURE 4.18: AVERAGE PERCENTUAL PER K INCREASE OF MT SUPERHEAT TEMPERATURE/PRESSURE, WITH GAS COOLER TEMPERATURE, FOR A FLASH GAS ONLY SYSTEM

In this case, from approximately 32ºC onwards, the decrease in mass flow passing through the high stage compressor has a bigger impact than the potential increase in enthalpy difference at the entrance and exit of said compressors, meaning a slight increase in EER can be observed. These results are inconclusive and the pattern in the real world, given that the system is dynamic, will have to be analysed separately.

4.2 Real installation results and analysis

The real installation analysis was done sequentially, with changes made from the baseline conditions. After each change, the system was allowed to return to initial conditions, in order not to affect further changes results. Dealing with a real working installation, as mentioned, has a risk associated, namely stoppage and risk of damaging something that turned the system non-operational, which was out of question, even for shorts amount of time. With this in mind, small changes were made, in small intervals with a time between changes of, at least, 1 day, and every change was logged with type and hour of alteration. It is also worth noting that weekend alterations were not possible, due to the remote chance that a problem would appear, and no maintenance team was available. This subchapter will analyse every change made.

The results were exported and uploaded to *MS Excel* to be filtered and analyzed. Right away, a trend appeared, where, unlike expected, there were certain moments of the day when the EER increased and decreased in a similar fashion for every studied day. From a random day, a T-EER relationship was plotted and the times where the trend changed were analyzed and can be seen in Figure 4.19.

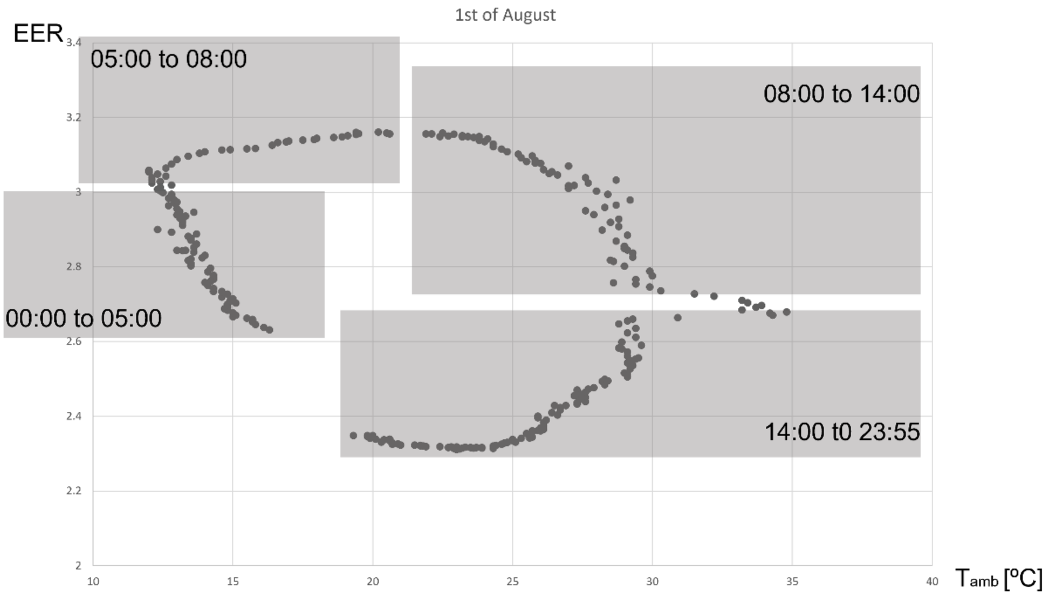

FIGURE 4.19: T-EER PLOT FOR THE 1ST OF AUGUST 2022 WITH 4 DISTINCT EVOLUTION PATTERNS DURING THE DAY

As they were, the produced data would not be usable for comparison because there was clearly a trend associated with the system programming and store schedules. It was decided to use only the interval between 00:00 and 05:00 because, during this period:

- No product replacement in the store, meaning no interaction with cooling units and chambers;
- No door openings, meaning no warmer air entering units;
- No HVAC system working;
- No energy efficiency measures in place, such as dynamic loads;
- No indirect heating loads (solar radiation, people, lighting, computers, etc.).

In turn, these result in constant cooling loads during homologous periods in different days, providing more accurate comparisons. As a negative consequence, however, significant values will tend to have lower temperatures because the chosen period is typically the colder of a day.

4.2.1 Receiver tank pressure

As briefly mentioned, in this section of the study, only flash-gas situations will be used. This is because of the method the controller uses for regulation. Direct pressure regulation in *Carel Boss* is not possible, meaning that the variations are obtained by regulating the flash-gas valve or, as the software calls it, Receiver Pressure Release Valve, or RPRV for short. This only affects MT suction, and IT compression setpoints are independent of RPRV regulation, meaning no direct EER variation could be explained in a parallel compression environment. Changes to IT stages need to be made in the IT controller, independently.

The receiver tank pressure was varied, as seen in previous sections, between 38 and 40 bar. The regulation was done from the 4th to the 11th of August 2022, in 0.5 bar steps, with the following change log:

- 04/08/22 12:23 : RPRV setpoint **38.0** → **38.5** [bar]
- 05/08/22 12:10 : RPRV setpoint **38.5** → **39.0** [bar]
- 08/08/22 12:50 : RPRV setpoint **39.0** → **39.5** [bar]
- 09/08/22 14:56 : RPRV setpoint **39.5** → **40.0** [bar]
- 10/08/22 14:42 : RPRV setpoint **40.0** → **39.5** [bar]
- 11/08/22 12:52 : RPRV setpoint **39.5** → **40.0** [bar]

It is worth noting that the 6th and 7th of August were weekend days, resulting in no alteration. Additionally data was used from the day before the first change and the day after the last change, i.e., results will be presented with data from the 3rd to the 12th of August. On the software, a Report was created with the following data:

- Date and time;
- Measured EER;
- Exterior Temperature;
- Receiver Pressure;
- RPRV valve opening (percentage);
- Parallel compressor ON/OFF status (ON=1 and OFF=1).

The selected interval was then filtered from the dataset, as well as the periods when the parallel compressor was working (when the variable "Parallel compressor ON/OFF status" was equal to 0) and the daily results of the average EER, for every significant temperature can be seen in Table 5. The daily average pressure of the reservoir and ambient temperatures were also retrieved and will be used to choose representative days of certain pressure values, and to validate comparisons.

TABLE 5: EER RESULTS FOR 3/08 TO 12/08, FROM TEMPERATURES FROM 18 TO 22ºC

Day	Temperature					AVG P_{tank} [bar]	AVG T_{amb} [ºC]
	18	19	20	21	22		
3/08	2.31	2.33	2.23	2.18	2.27	37.97	19.9
4/08	2.40	2.35	2.31	2.29	2.32	37.59	19.9
5/08	2.44	2.41	2.37	2.32	2.23	38.50	20.4
6/08	-	2.32	2.30	2.25	-	38.93	21.1

7/08	2.44	2.32	2.29	2.28	-	38.91	18.9
8/08	2.47	2.39	2.36	2.35	-	38.95	19.0
9/08	2.48	2.37	2.35	-	-	39.38	18.8
10/08	-	2.41	2.39	2.32	2.31	39.80	20.8
11/08	-	-	2.34	2.30	2.27	38.82	21.9
12/08	2.45	2.39	2.36	-	-	38.46	18.3

Directly from the table, it's possible to access that the setpoints alteration resulted in consequences in the next day. From Table 5, representative days for average reservoir pressures can be chosen, which will be used in the economic analysis:

- 4^{th} of August: 38.0 bar;
- 5^{th} of August: 38.5 bar;
- 8^{th} of August: 39.0 bar;
- 9^{th} of August: 39.5 bar;
- 10^{th} of August: 40.0 bar.

However, organizing data by date could result in erroneous results since, although the studied days were similar in weather, average ambient temperatures were not, with a maximum variation of average temperature of 3.1 ºC, which can be significant. With this in mind, the results were organized by ambient temperature, maintaining the used filters, and the EER variation with receiver tank pressure, for every studied temperature was plotted, along with the linear trendlines and can be seen in Figure 4.20. Although the setpoints are between 38 and 40 bar, the system has slight variations during the day, and the obtained results had values of receiver pressure from 34 to 42 bar. However, these values may be sporadic and may only appear once or twice during a given period, leading to non-accurate results. For this reason, only pressures around the defined setpoints were considered.

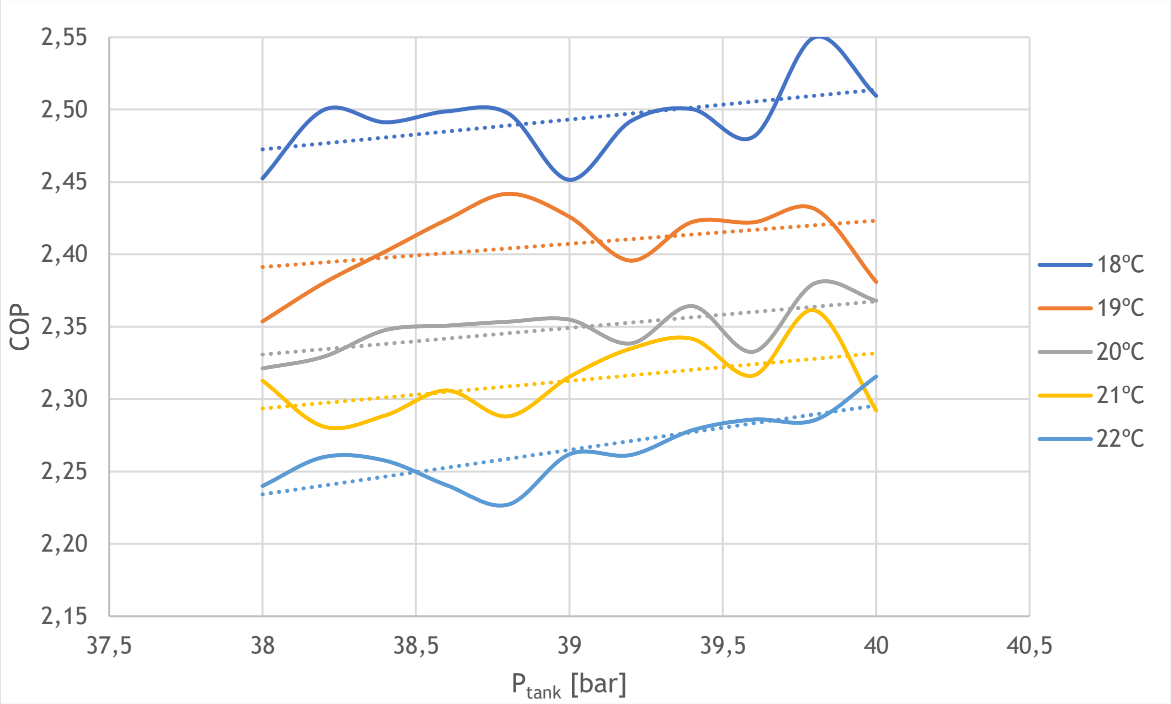

FIGURE 4.20: EER VARIATION WITH RECEIVER PRESSURE FOR DIFFERENT AMBIENT TEMPERATURES, ALONG WITH TRENDLINE

The trendlines were obtained by linear regression and were then used to calculate more standardized EER values for comparisons, which can be seen in table Table 6.

TABLE 6: EER VARIATION WITH TANK PRESSURE AND AMBIENT TEMPERATURE, FROM LINEAR REGRESSION, ALONG WITH PERCENTUAL CHANGE

P_{tank} [bar]	Ambient Temperature [°C]				
	18	19	20	21	22
38	2.47	2.39	2.33	2.29	2.23
38.5	2.48	2.4	2.34	2.30	2.25
39	2.49	2.41	2.35	2.31	2.26
39.5	2.50	2.42	2.36	2.32	2.28
40	2.51	2.42	2.37	2.33	2.30
% change / bar	**0.8%**	**0.7%**	**0.8%**	**0.8%**	**1.4%**
Average % change	**0.9%**				

4.2.2 MT suction pressure

The MT suction pressure (and, as a consequence, evaporator temperature) change is perhaps the most delicate parameter of study. That is because this parameter is the most likely to directly affect the final temperature of the cooling units. Given that the object of study is a supermarket, temperature control is highly important because perishable products' quality is dependent on it. As such, in this analysis, not only EER variation was analysed, but also the variation in product temperature.

The study was done from 17th of August to 23rd of August, and the parameter changed was evaporation temperature, from -10ºC to -9ºC. The parallel compressor worked for 35 minutes during the analysed timeframe, which corresponds to 1.2% of the total studied time. As studied, evaporator temperature is directly associated with a pressure value, for a sub-critical condition. As such, both temperature and pressure will be used in this analysis. The parameter change was as follows:

- 17/08/22 11:43 : Evaporation setpoint MT **-10.0→ -9.5** [ºC] or **26.5 → 26.9** [bar]
- 18/08/22 11:46 : Evaporation setpoint MT **-9.5→ -9.0** [ºC] or **26.9 → 27.5** [bar]
- 23/08/22 12:22 : Evaporation setpoint MT **-9.0→ -9.5** [ºC] or **27.5 → 26.9** [bar]
- 23/08/22 14:09 : Evaporation setpoint MT **-9.5→ -10.0** [ºC] or **26.9 → 26.5** [bar]

For the temperature check, for every station, an average of the real temperature value will be calculated from 12th of August to the 16th of August, to serve as a reference value before the change, and an average between the 18th and the 22nd to serve as a comparison value, after the change.

The results will be presented in pressure because that was the way the software exported data and for the sake of simplicity the same units were conserved. The results can be seen in Figure 4.21.

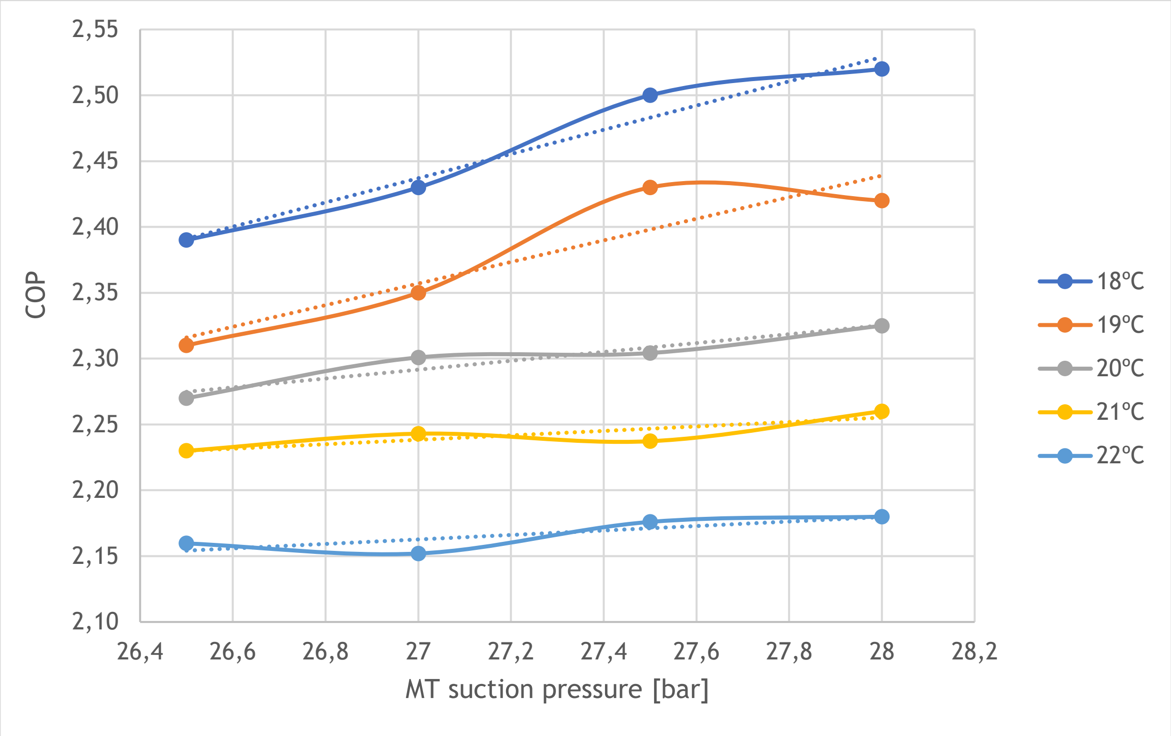

FIGURE 4.21: EER VARIATION WITH MT SUCTION PRESSURE, FOR DIFFERENT AMBIENT TEMPERATURES, ALONG WITH TRENDLINE

The trendline was calculated for each ambient temperature value and the values, along with percentual change per bar increased and average percentual change are observable in Table 7.

TABLE 7: EER VARIATION WITH MT SUCTION PRESSURE AND AMBIENT TEMPERATURE, FROM LINEAR REGRESSION, ALONG WITH PERCENTUAL CHANGE

MT suction pressure [bar]	Ambient temperature [ºC]				
	18	19	20	21	22
26.5	2.39	2.32	2.27	2.23	2.15
27	2.44	2.36	2.29	2.24	2.16
27.5	2.48	2.40	2.31	2.25	2.17
29	2.53	2.45	2.36	2.27	2.20
%change / bar	3.8%	3.9%	2.9%	1.5%	1.6%
Average % change	**2.8%**				

The temperature change analysis was then conducted, between the previously mentioned periods. For every cooling unit, the average temperature before and after the change was calculated, as well as the difference between both. This information can be seen in Annex C, in table C-1.

As a general rule, a difference of ±2°C is an acceptable average difference, as this value corresponds to the temperature offset for the thermostat. In this case, it can be concluded that an increase of 1 bar of MT suction pressure did not significantly affect the temperature in the cooling units.

4.2.3 MT evaporator superheat

Evaporator superheat is controlled by each evaporator unit's controller, as previously explored in section 2.7.2. In order to change the overall MT evaporator superheat of the system, each unit's setpoint had to be changed. Apart from 3 evaporator units (CL,CB and CP), the remaining 38 MT evaporators all had their initial superheat setpoint at 10K, which were chosen for the analysis. It was not clear at the time why the other 3 units had different values and was decided not to work with them. Still, 110.64kw out of 121.7kw, roughly 91% of the MT load was studied, which was considered to be enough to have representative values. The setpoint were changed from 10 to 9K, in the following sequence:

- 05/09/22 14:50 : evaporator superheat **10.0** → **9.0** [K] for 46% of MT units;
- 07/09/22 14:51 : evaporator superheat **10.0** → **9.0** [K] for 47% of MT units;
- 12/09/22 15:10 : evaporator superheat **9.0** → **10.0** [K] for 93% of MT units;

Although the superheat was changed in evaporators, from the whole system perspective it makes sense that the EER analysis is done in relationship to the unit's whole superheat, i.e., the measured superheat just before the admission of the high-pressure compressors. This superheat is the result of evaporator superheat + IHX superheat + useless line superheat. It was not clear before the study if the relationship evaporator superheat – system superheat was linear, which was an important piece of information. In order to obtain it, data from one week before the beginning of the study and during the week of the study was gathered. In the week before, the evaporators setpoints were all at 10K and the average of the total MT superheat values from the 29th of August to the 4th of September was **14.7** K. During the week of the study, from the 7th to the 12th of September, when 96% of the evaporator units had their MT superheat setpoints at 9 K, the average of the total system's MT superheat was **13.8** K. These results not only prove that, at least for low superheat variations, the relationship can be assumed as linear, and also that the estimation of 5K difference between system's and evaporator's superheat is correct. The selected superheat interval of study was between 13.5K and 15K, between the 29th of August and the 12th of September. During the study period, the parallel compressors were ON during a total time of 20 minutes, meaning the analysis can be compared with a flash gas only system. The data was plotted and can be seen, along with trendlines, on Figure 4.22.

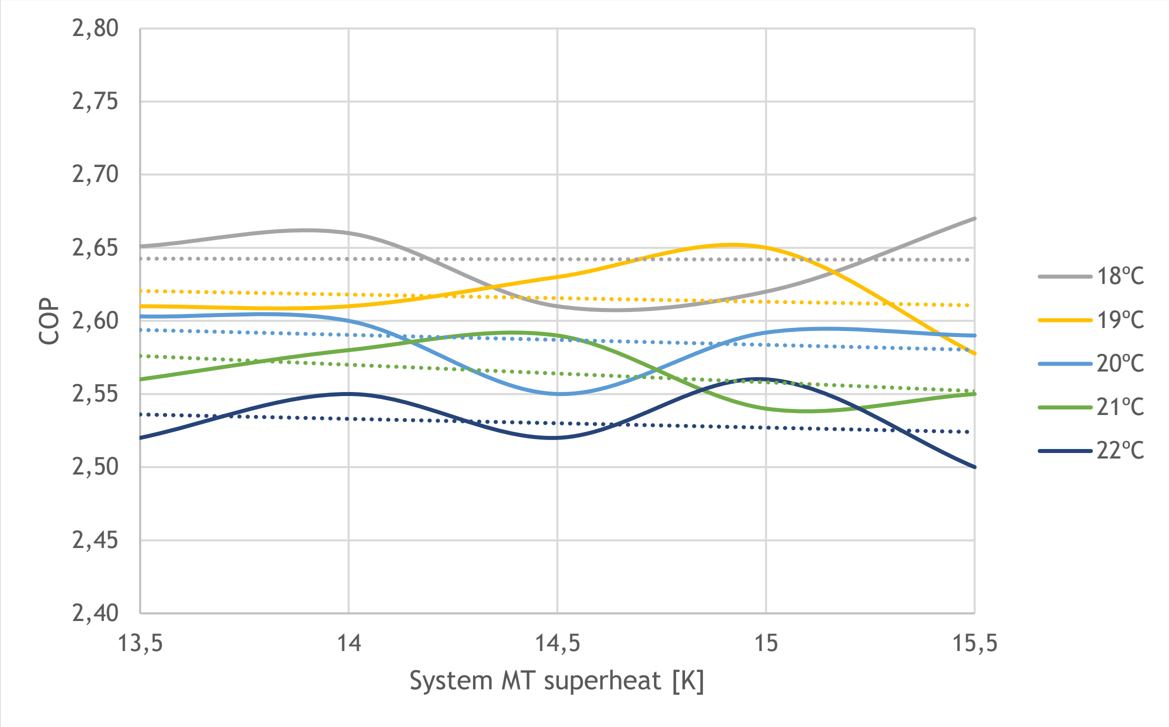

FIGURE 4.22: EER VARIATION WITH WHOLE SYSTEM MT SUPERHEAT, FOR DIFFERENT AMBIENT TEMPERATURES, ALONG WITH TRENDLINE

Linear regressions were once again calculated in order to obtain the percentual change per superheat degree. These results can be seen in Table 8.

TABLE 8: EER VARIATION WITH SYSTEM SUPERHEAT AND AMBIENT TEMPERATURE, FROM LINEAR REGRESSION, ALONG WITH PERCENTUAL CHANGE

System Superheat [K]	**Ambient temperature [ºC]**				
	18	**19**	**20**	**21**	**22**
13.5	2.64	2.62	2.59	2.58	2.54
14	2.64	2.62	2.59	2.57	2.53
14.5	2.64	2.62	2.59	2.56	2.53
15	2.64	2.61	2.58	2.56	2.53
15.5	2.64	2.61	2.58	2.55	2.52
% change / K	0.0%	-0.2%	-0.3%	-0.5%	-0.2%
Average change	**-0.2%**				

A temperature analysis similar to the one done in section 4.2.2 was also necessary. For reference periods i.e., before the change, it was selected the interval between the 29th of August and the 4th of September. For the study periods, the interval between the 7th and 12th of September was chosen. The results can be seen in Table C-2 in Annex C.

Once again, a difference of less than $\pm 2°C$ in every cooling unit proves that the superheat change did not affect substantially the temperature inside the stations.

4.3 Discussion and economic analysis

To better discuss the results, its best to synthesise them in a table comparing software results and real world results, which can be seen in Table 9.

TABLE 9: SUMMARY OF THE OBTAINED RESULTS

Ambient Temperature [º]	Percentual change per changed unit								
	P_{tank}			**MT suction Pressure**			**MT superheat**		
	Software		Real	Software		Real	Software		Real
	parallel	flashgas		parallel	flashgas		parallel	flashgas	
18	0.00%	0.10%	0.83%	3.32%	3.63%	3.82%	-0.17%	-0.08%	0.01%
19	0.00%	0.05%	0.67%	3.27%	3.55%	3.95%	-0.17%	-0.07%	-0.19%
20	0.00%	0.03%	0.79%	3.31%	3.62%	2.94%	-0.10%	-0.05%	-0.26%
21	0.00%	0.08%	0.83%	3.28%	3.63%	1.51%	-0.14%	-0.05%	-0.47%
22	0.00%	0.07%	1.37%	3.26%	3.64%	1.57%	-0.14%	-0.05%	-0.24%
Average	**0.00%**	**0.07%**	**0.90%**	**3.29%**	**3.61%**	**2.76%**	**-0.14%**	**-0.06%**	**-0.23%**

Being a dynamic system, even though the period of study was chosen in order to minimize changes and exterior influences, the real results will always differ somewhat to the theoretical. In the case of MT suction pressure and superheat, the software results are in the same order of magnitude, being considered valid. For the receiver pressure, the erratic results seen in Figure 4.20 may explain why the disparity in results. This value is highly sensitive and even in conditions of no store activity presented significant amplitude of results during the study, which may invalidate the results. Furthermore, there are always measuring uncertainties both in the software and in the real world measurements. From the software point of view, although it accurately accounts for compressor inefficiencies, the model won't be able to predict with 100% accuracy the real world scenario. From the real world measurements, there are also uncertainties associated with pressure, temperature, and energy usage readings from sensors which, at this magnitude of changes, can be significant. The possible error associated with the measurement of ambient and gas-cooler outlet temperatures may also contribute to a further study uncertainty.

A representative week during the studied period was chosen when no parameter change was applied in order to understand how much energy the whole system would spend in a typical day. The energy monitoring is divided in two different meters: one unit measures the refrigeration system + gas cooler spendings (then used for the EER calculation) and the other measures the total energy usage of the cooling units, including defrosting, lights and ventilation. A typical day has, on average, the following energy usage, with an overall constant electrical load:

- 480 kWh for the cooling units;
- 860 kWh for the refrigeration system.

It can be considered that a EER increase will only affect the refrigeration system energy spending. At a **0.22€/kWh** price (company reference values), the average daily spending on refrigeration system alone is, on average, **189.20€**.

The studied period, however, only reflects 20.83% of the whole day, meaning that only this period can be considered for the energy usage, for now. With this in mind, the energy savings from the EER increase can be calculated:

- For an average of 0.9% saving by increasing 1 bar of receiver tank pressure, during 20.83% of the day, an energy saving of up to 1.6 kWh daily;
- For an average of 2.76% saving by increasing 1 bar of MT suction pressure, during 20.83% of the day, an energy saving of up to 4.94 kWh daily;
- For an average of 0.23% saving by decreasing 1 K of MT superheat, during 20.83% of the day, an energy saving of up to 0.41 kwh daily;

In other words, with 35.83 kW consumption, or 7.8€ per hour spent, these saving would mean that, when ambient temperatures average 18ºC to 22ºC:

- Increasing receiver pressure by 1bar would save 0.07€ per hour;
- Increasing MT suction pressure by 1bar would save 0.22€ per hour;
- Decreasing MT superheat by 1K would save 0.02€ per hour;

These results may seem insignificant but extending them to the whole year reveals the total potential save. Although lacking conclusive data, to extend the study for the whole day and year, an extrapolation from theorical study data can be useful. For the receiver pressure increase it is expected that the average saving increases, further increasing the energy savings. Being a little more pessimistic, even assuming that the 0.9% saving is maintained for all temperatures, it still reflets in a 7.74 kw/h daily which expanded for the whole year is a saving of 2825 kWh, saving 621.52€. For the MT suction pressure, it is expected that the EER increase decreases with temperature, by up to half the studied value. Assuming a yearly average of 1.4%, it still represents a 4395kwh saving, reflecting on a 966.81€ save. For the MT superheat, it is unclear if the increase to higher temperatures brings advantages or not, complicating the extrapolation. On a most pessimistic approach, one could argue that superheat change won't significantly affect EER during the whole year, only during lower average ambient temperatures. Of course this last paragraph lacks conclusive data, as the validity of the theorical model for other temperature and/or store activities range is not validated. The receiver results should also be viewed as not completely valid, as the order of magnitude difference between real and theorical results is not the same.

5. Conclusions & Future work

CO_2 refrigeration systems are becoming increasingly popular due to their low GWP and zero ODP and are viewed as a sustainable and future regulation-proof refrigerant. Not only that, but CO_2 usage in refrigeration has some other practical advantages such as higher volumetric cooling capacity than traditional fluids such as ammonia, for example, which leads to smaller installations.

The challenges when trying to use this refrigerant as a viable solution comes from the fact that the critical point of CO_2 is at a relatively low temperature and high pressure, requiring high compressor ratios and, therefore high energy spendings, specially is warmer climates such as Portuguese cities. To combat this, transcritical systems with parallel compression and flash gas relieve were developed such that allow for competitive EER in climates where temperature is commonly above the refrigerant's critical point at 31.1ºC.

The chosen object of study was a refrigeration plant of a supermarket in Felgueiras, Portugal, with a booster R744 refrigeration system with parallel compression, of which the dissertation's objective was to optimize its EER without any structural change, only by changing chosen parameters. The chosen parameters were receiver pressure, suction pressure and superheat value. It was decided that only MT suction pressure and superheat would be changed, discarding LT parameters, as the firsts would yield best EER changes, due to the load ratio of 4.47.

The real installation's specifications were loaded into *Bitzer Software*, a program chosen because of its capacity of mimicking the real compressor's inefficiencies, which is crucial for this type of work. For ambient temperatures around 20 ºC, an increase receiver pressure of 1 bar could potentially increase EER by 0.0 to 0.1%. For temperatures of around 30ºC, this increase could be up to 0.5%, and for higher temperatures of 40ºC the increase could go up to 0.7%. For the MT suction pressure increase, the software calculated for ambient temperatures of around 20ºC,30ºC and 40ºC an increase in EER of up to 4%, 3% and 2%, respectively, when increasing the suction temperature by one degree, or approximately 0.8 bar. Regarding the MT evaporator superheat, mixed results were produced, where an increase in superheat by 1K would lead to a decrease in EER by up to 0.1% around 20ºC ambient temperature, a decrease from 0.1% to 0.0% in the 30ºC temperature range and a EER increase of up to 0.1% around the 40 ºC temperatures.

The real installation tests were conducted during August and September 2022, with analysis conducted from 00:00 to 05:00, time periods where loads were constant and no influence from the supermarket activity was present. Temperature ranges of 18ºC to 22ºC were analysed because they were the most common. Receiver pressure was changed between 38 bar and 40 bar and a EER increase of up to 1% per bar was observed, for situations of flash-gas only, with no parallel compressor working. This result differed by almost 10 times the theoretical values and produced scattered results, leading to a questionable validity. For the MT evaporation pressure/temperature, it was increased from -9ºC to -10ºC and EER changes were in the order of 3% increase per bar of pressure increased. During the considered study time, parallel compression was working for 1.2% of the total time, with the 98.8% of the rest corresponding to a flash gas only situation. The MT evaporator superheat influence was then studied by changing the superheat on 38 of the 41 evaporator units, corresponding to 91% of the total MT cooling load. The setpoint was changed from -10K to -9K, having obtained an average of -0.2% decrease in EER per degree of superheat increased. During the study period, the system was in parallel compression mode for less than 0.1%. Both MT suction pressure and MT evaporator superheat were changed without significant effect on cooling unit's ambient temperatures, with less than 1.0ºC difference between the changed conditions

It was concluded that, when ambient temperatures range from 18 to 22ºC, the system is running mostly on flash-gas only, with an average daily spending of $860\ kWh$ just for the refrigeration unit and gas-cooler and an average price per kwh of 0.22€, an increase in 1bar receiver pressure would save 1kW or 0.22€/hour. An increase of suction pressure by 1 bar would save 0.20kW or 0.07€/hour, and a decrease in MT evaporator superheat by 1K would save 0.09kW or 0.02€/hour.

An extension of this work should be developed during at least an entire year of operation, in order to fully document the influence of these parameter changes for all ambient temperatures and all working conditions, and to fully validate receiver pressure results, especially. With that information, dynamic setpoints could be set up to further increase optimization and energy saving beyond the suggested expectations. As an example, between temperature and load intervals, MT suction pressure could be increased to the maximum allowable limit where no significant temperature product is changed, running with a maximum EER, and return to initial conditions outside the determined intervals.

A future work approach could focus on the effect of combining the three parameters change and check whether the influence in EER is cumulative, or undesirable effects appear. Also, although not studied, the influence of LT suction pressure and superheat in EER could also be studied. Still in the optimization realm, without adding new components to the system, RPRV and High-Pressure Valve's PID constants optimization could also potentially bring new EER improvements.

Bibliography

[1] B. Krasner-Khait, “The Impact of Refrigeration,” [Online]. Available: https://history-magazine.com/refrig.html. [Accessed March 2022].

[2] C. Afonso, Sistemas Frigoríficos, 2019.

[3] Sandvik, “The History of the refrigerator,” [Online]. Available: https://www.materials.sandvik/pt/campaigns/fridge-of-the-future/the-history-of-the-refrigerator/. [Accessed March 2022].

[4] Museum of Applied Arts & Sciences, “GE ‘Monitor Top’ refrigerator,” 2015. [Online]. Available: https://collection.maas.museum/object/210813. [Accessed March 2022].

[5] Intenational Institute of Refrigeration, “The Role of Refrigeration in the Global Economy,” *38th Informatory Note on Refrigeration Technologies,* June 2019.

[6] R. Ciconkov, “Refrigerants: There is still no vision for sustainable solutions,” *International Journal of Refrigeration,* vol. 86, pp. 441-448, 2018.

[7] G. F. Hundy, A. R. Trott and T. C. Welch, Refrigeration, Air Conditioning and Heat Pumps, Butterworth-Heinemann, 2016.

[8] M. J. Molina and F. S. Rowland, “Stratospheric sink for chlorofluoromethanes chlorine atom-catalysed destruction of ozone,” *Nature,* vol. 249, pp. 810-812, 1974.

[9] UN Environment Programme, “About Montreal Protocol,” 2022. [Online]. Available: https://www.unep.org/ozonaction/who-we-are/about-montreal-protocol. [Accessed June 2022].

[10] European Union, “EU legislation to control F-gases,” 2022. [Online]. Available: https://ec.europa.eu/clima/eu-action/fluorinated-greenhouse-gases/eu-legislation-control-f-gases_en. [Accessed June 2022].

[11] Emerson, “CO2 as a Refrigerant,” 2015. [Online]. Available: https://emersonclimateconversations.com/2015/07/30/co2-as-a-refrigerant-r-744-advantagesdisadvantages/. [Accessed May 2022].

[12] Race S.A., “Race,” [Online]. Available: https://www.race.com.pt/pt/a-race. [Accessed March 2022].

[13] C. Afonso, Termodinâmica para engenharia, FEUP Edições, 2012.

[14] W. F. Stoecker, Refrigeration and Air Conditioning, Mcgraw Hill Higher Education, 1983.

[15] Intarcon, “CO2 refrigeration,” [Online]. Available: https://www.intarcon.com/en/co2-refrigeration/#Advantages. [Accessed April 2022].

[16] N. Purohit, D. K. Gupta and M. S. Dasgupta, “Energetic and economic analysis of trans-critical CO2 booster system for refrigeration in warm climatic condition,” *International Journal of Refrigeration,* vol. 80, pp. 182-196, 2017.

[17] B. T. Austin and K. Sumathy, “Transcritical carbon dioxide heat pump systems: A review,” *Renewable and Sustainable Energy Reviews,* vol. 15, no. 8, pp. 4013-4029, 2011.

[18] R. Cabello, D. Sánchez, J. Patiño, R. Llopis and E. Torrella, “Experimental analysis of energy performance of modified single-stage CO2 transcritical vapour compression cycles based on vapour injection in the suction line,” *Applied Thermal Engineering,* vol. 47, pp. 86-94, 2012.

[19] Y. T. Ge and S. Tassou, “Thermodynamic analysis of transcritical CO2 booster refrigeration systems in supermarket,” *Energy Conversion and Management,* vol. 52, no. 4, pp. 1868-1875, 2011.

[20] RACE S.A., *private comunication,* 2022.

[21] S. Sawalha, M. Karampour and J. Rogstram, “Field measurements of supermarket refrigeration systems. Part I: Analysis of CO2 trans-critical refrigeration systems,” *Applied Thermal Engineering,* vol. 87, pp. 633-647, 2015.

[22] Bitzer, “W...A Series,” 2020. [Online]. Available: https://www.bitzer.de/us/us/reciprocating-compressors/w...a-series/. [Accessed April 2022].

[23] J. Sarkar and N. Agrawal, “Performance optimization of transcritical CO2 cycle with parallel compression economization,” *International Journal of Thermal Science,* vol. 49, no. 5, pp. 838-843, 2009.

[24] Bitzer, “Ecoline Transcritical,” 2022. [Online]. Available: https://www.bitzer.de/gb/en/reciprocating-compressors/ecoline-transcritical/. [Accessed April 2022].

[25] Emerson, “Reciprocating Hermetic Compressors,” 2020. [Online]. Available: https://climate.emerson.com/en-us/products/refrigeration/commercial-refrigeration/reciprocating-hermetic-compressors. [Accessed April 2022].

[26] Danfoss Engineering, *Pack controller Type AK-PC 782A - User Guide,* 2021.

[27] Danfoss Engineering, *E-lesson: Expansion Devices Module 1 - Introduction,* 2022.

[28] Tecnac, “RV-CO2,” 2019. [Online]. Available: https://www.tecnac.net/products/rv-co2/. [Accessed May 2022].

[29] S. Bortolin, M. Rossato, S. Bernardinello and D. Del Col, “Investigation of Evaporator Performance with and without Liquid Overfeeding,” in *International Refrigeration and Air Conditioning*, 2016.

[30] SWEP, “B56,” 2019. [Online]. Available: https://www.swep.net/products/b56/. [Accessed July 2022].

[31] Danfoss Engineering, *Case/room controller (EEV): Type AK-CC55 Single Coil and AK-CC55 Single Coil UI - User Guide,* 2021.

[32] Carel, “Products - Boss Range,” [Online]. Available: https://www.carel.com/local-monitoring-systems/-/journal_content/56_INSTANCE_i4q5KIMLInKK/10191/497233. [Accessed May 2022].

[33] Danfoss Engineering, *AK-System Manager: AK-SM 800 Series - User Guide,* 2021.

[34] TECNAC, “RV-90BAR/130BAR Vertical CO2 reciever,” [Online]. Available: https://www.tecnac.net/en/products/liquid-receivers/co2-vertical-receivers-transcritical/rv-90bar-130bar/. [Accessed May 2022].

[35] A. Chesi, F. Esposito, G. Ferrara and L. Ferrari, “Experimental analysis of R744 parallel compression cycle,” *Applied Energy,* vol. 135, pp. 274-285, 2014.

Annex A: Object of Study definition

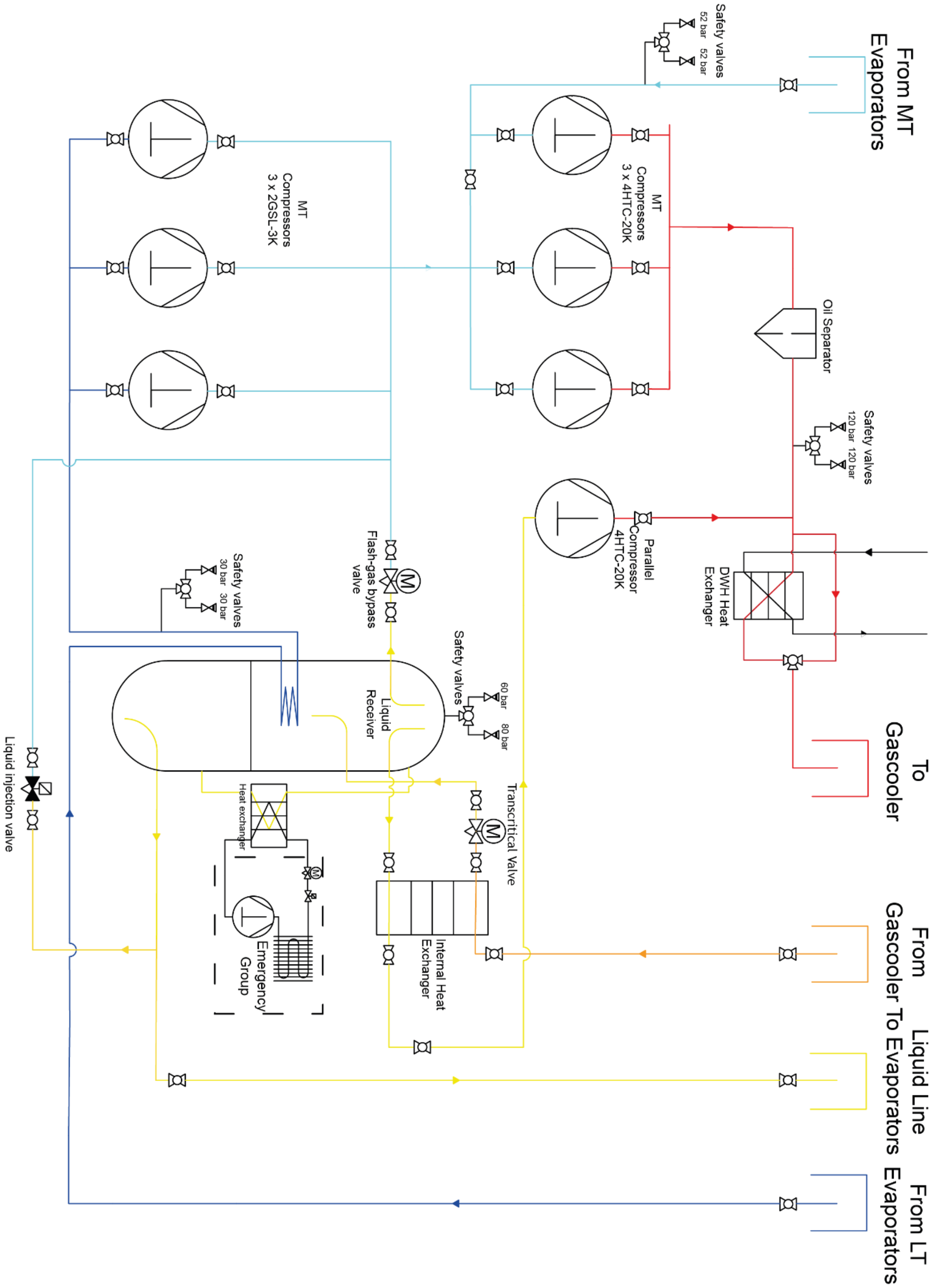

FIGURE A-1: DIAGRAM OF THE STUDIED REFRIGERATION SYSTEM

TABLE A-1: COOLING LOAD'S INITIAL CONDITIONS

Station Name	Ref.	Nominal Power [kW]	Superheat [K]	Temperature Setpoint [ºC]
LT units				
Ilha congelados - peixaria	PX01	0.9	8	-21
Mural congelados - Topo	CG15	15.1	10	-21
Mural congelados - linear	CG16		8	-21
Mural congelados - linear	CG17		8	-21
Mural congelados - linear	CG18		8	-21
Mural congelados - linear	CG19		8	-21
Mural congelados - topo	CG20		8	-21
Camara congelados 1	CC1	4.1	6	-21
Camara congelados 2	CC2	4.1	8	-21
Camara congelados padaria	CCP	3.0	10	-21
	Total:	27.2	-	-
MT units				
Mural talho aves	Tl01	3.4	10	1.7
Mural talho cpc	tl02	3.4	10	1
Vitrine talho atendimento	tl03	1.4	10	1
Vitrine talho atendimento	tl04	1.4	10	1
Vitrine charcutaria	CH02	1.1	10	2
Vitrine charcutaria	CH03	1.4	10	2
Vitrine charcutaria	CH04	2.7	10	2
Retrobalcão charcutaria	CH01	2.1	10	1
Mural Charcutaria	CH05	2.1	10	4
Mural legumes	FL01	14.4	10	2
Mural legumes	FL02		10	3.5
Mural legumes	FL03		10	4
Mural especialidades	TW01	3.2	10	3
Mural especialidades	TW02	3.0	10	2

Mural Charcutaria	CH06	13.0	10	2
Mural Charcutaria	CH07		10	2
Mural Charcutaria	CH08		10	2
Mural Charcutaria	CH09		10	2
Mural Charcutaria	CH10		10	2
Mural Iogurtes topo	LT01	28.2	10	2.2
Mural Iogurtes linear	LT02		10	2
Mural Iogurtes linear	LT03		10	3
Mural Iogurtes linear	LT04		10	2
Mural Iogurtes linear	LT05		10	2
Mural Iogurtes linear	LT06		10	2
Mural Iogurtes linear	LT07		10	2
Mural Iogurtes linear	LT08		10	2
Mural Iogurtes linear	LT09		10	2
Mural iogurtes topo	LT10		10	2
Camara peixe fresco	CP	5.8	10	0
Camara laticinios	CL	3.2	6	2
Camara aves	CA	3.0	10	0
Camara bacalhau	CB	4.3	11	5
Camara take away	CT	4.1	10	2
Laboratorio talho	LO1	4.0	10	12
Laboratorio charcutaria	LO2	1.5	10	12
Buffer frescos	BF	2.8	10	12
Camara talho	CT	5.7	10	0
Camara padaria	CP	3.6	9	2
Camara charcutaria	CC	2.8	10	2
Camara frutas e legumes	CF	4.5	10	2
	Total:	121.7	-	-

Annex B: Tables from theorical study

TABLE B-1: THEORETICAL EER VARIATION WITH TEMPERATURE AND RECEIVER PRESSURE, FOR A PARALLEL SYSTEM

Gas cooler	Receiver Pressure [bar]								
Temperature [ºC]	34	35	36	37	38	39	40	41	42
20	2.5	2.5	2.5	2.5	2.5	2.5	2.49	2.5	2.5
21	2.47	2.48	2.48	2.48	2.47	2.47	2.47	2.48	2.47
22	2.46	2.46	2.45	2.46	2.46	2.45	2.45	2.46	2.46
23	2.44	2.43	2.44	2.43	2.43	2.43	2.42	2.44	2.44
24	2.4	2.41	2.41	2.41	2.41	2.4	2.4	2.39	2.4
25	2.36	2.37	2.38	2.37	2.37	2.38	2.37	2.38	2.37
26	2.33	2.34	2.34	2.34	2.35	2.35	2.34	2.34	2.35
27	2.3	2.3	2.31	2.31	2.31	2.32	2.32	2.32	2.32
28	2.26	2.26	2.27	2.28	2.28	2.29	2.29	2.29	2.29
29	2.21	2.22	2.23	2.23	2.24	2.24	2.25	2.25	2.25
30	2.13	2.16	2.16	2.18	2.18	2.19	2.20	2.20	2.21
31	2.03	2.05	2.08	2.08	2.10	2.10	2.11	2.11	2.12
32	1.94	1.96	1.97	1.99	2.00	2.01	2.01	2.02	2.03
33	1.86	1.87	1.88	1.9	1.91	1.92	1.93	1.93	1.94
34	1.78	1.79	1.8	1.82	1.83	1.84	1.84	1.85	1.86
35	1.71	1.72	1.73	1.74	1.76	1.77	1.76	1.78	1.78
36	1.63	1.65	1.66	1.67	1.68	1.69	1.69	1.71	1.71
37	1.57	1.58	1.6	1.6	1.62	1.62	1.63	1.64	1.64
38	1.51	1.51	1.53	1.55	1.55	1.56	1.57	1.58	1.58
39	1.45	1.46	1.47	1.49	1.49	1.5	1.51	1.52	1.52
40	1.39	1.41	1.41	1.43	1.44	1.44	1.45	1.46	1.47

TABLE B-2 :THEORETICAL EER VARIATION WITH TEMPERATURE AND RECEIVER PRESSURE, FOR A FLASH GAS ONLY SYSTEM

Gas cooler Temperature [°C]	**Receiver Pressure [bar]**								
	34	**35**	**36**	**37**	**38**	**39**	**40**	**41**	**42**
20	2.23	2.23	2.24	2.24	2.24	2.24	2.24	2.25	2.25
21	2.21	2.2	2.2	2.2	2.21	2.21	2.21	2.21	2.21
22	2.17	2.17	2.17	2.17	2.17	2.17	2.17	2.17	2.18
23	2.13	2.13	2.13	2.13	2.14	2.14	2.14	2.14	2.14
24	2.09	2.09	2.09	2.1	2.1	2.1	2.1	2.1	2.1
25	2.05	2.05	2.05	2.05	2.06	2.06	2.06	2.06	2.06
26	2.01	2.01	2.01	2.01	2.01	2.01	2.01	2.02	2.02
27	1.96	1.96	1.96	1.96	1.96	1.96	1.97	1.97	1.97
28	1.91	1.91	1.91	1.91	1.91	1.91	1.91	1.91	1.91
29	1.84	1.84	1.84	1.84	1.85	1.85	1.85	1.85	1.85
30	1.76	1.77	1.77	1.77	1.77	1.77	1.77	1.77	1.77
31	1.67	1.67	1.68	1.68	1.68	1.68	1.68	1.68	1.68
32	1.59	1.59	1.59	1.6	1.6	1.6	1.6	1.6	1.6
33	1.52	1.52	1.52	1.52	1.52	1.52	1.52	1.53	1.53
34	1.45	1.45	1.45	1.45	1.45	1.45	1.45	1.46	1.46
35	1.38	1.39	1.39	1.39	1.39	1.39	1.39	1.39	1.39
36	1.32	1.33	1.33	1.33	1.33	1.33	1.33	1.33	1.33
37	1.27	1.27	1.27	1.27	1.27	1.27	1.27	1.28	1.28
38	1.22	1.22	1.22	1.22	1.22	1.22	1.22	1.22	1.22
39	1.17	1.17	1.17	1.17	1.17	1.17	1.17	1.17	1.17
40	1.12	1.12	1.12	1.12	1.12	1.12	1.13	1.13	1.13

TABLE B-3: THEORETICAL EER VARIATION WITH AMBIENT AND MT EVAPORATION TEMPERATURE, FOR A PARALLEL SYSTEM

Gas Cooler Temperature [ºC]	**MT Evaporation pressure/temperature**					
	24.3 bar	**25.01 bar**	**25.75 bar**	**26.49 bar**	**27.26 bar**	**28.03 bar**
	-13 ºC	**-12 ºC**	**-11 ºC**	**-10 ºC**	**-9 ºC**	**-8 ºC**
20	2.28[1]	2.35[1]	2.42[1]	2.50[1]	2.57[1]	2.66[1]
21	2.26[1]	2.33[1]	2.40[1]	2.47[1]	2.55[1]	2.63[1]
22	2.24[1]	2.31[1]	2.38[1]	2.46[1]	2.53[1]	2.61[1]
23	2.22	2.28	2.35	2.43	2.5	2.58
24	2.19	2.26	2.33	2.40	2.47	2.55
25	2.18	2.24	2.31	2.38	2.45	2.52
26	2.16	2.22	2.28	2.35	2.43	2.49
27	2.14	2.19	2.26	2.32	2.39	2.46
28	2.1	2.16	2.22	2.29	2.35	2.42
29	2.07	2.12	2.18	2.25	2.31	2.37
30	2.02	2.07	2.13	2.18	2.24	2.31
31	1.94	1.99	2.04	2.10	2.15	2.21
32	1.86	1.9	1.95	2.00	2.05	2.10
33	1.78	1.82	1.86	1.91	1.96	1.99[2]
34	1.7	1.75	1.78	1.83	1.86[2]	1.91[2]
35	1.64	1.68	1.71	1.76	1.79[2]	1.83[2]
36	1.57	1.61	1.64	1.68[2]	1.72[2]	1.76[2]
37	1.51	1.55	1.58[2]	1.62[2]	1.65[2]	1.69[2]
38	1.46	1.48[2]	1.52[2]	1.55[2]	1.58[2]	1.62[2]
39	1.4	1.43[2]	1.46[2]	1.49[2]	1.53[2]	1.56[2]
40	1.35	1.38[2]	1.41[2]	1.44[2]	1.47[2]	1.51[2]

[1]Smaller parallel compressor used; [2]Bigger parallel compressor used.

TABLE B-4: THEORETICAL EER VARIATION WITH AMBIENT AND MT EVAPORATION TEMPERATURE, FOR A FLASH GAS SYSTEM

Gas Cooler Temperature [ºC]	MT Evaporation pressure/temperature					
	24.3	**25.01**	**25.75**	**26.49**	**27.26**	**28.03**
	-13	**-12**	**-11**	**-10**	**-9**	**-8**
20	2.11	2.18	2.25	2.33	2.41	2.49
21	2.08	2.15	2.22	2.29	2.37	2.45
22	2.04	2.11	2.18	2.25	2.33	2.41
23	2.01	2.07	2.14	2.22	2.29	2.37
24	1.97	2.04	2.10	2.17	2.25	2.33
25	1.93	1.99	2.06	2.13	2.20	2.28
26	1.89	1.95	2.02	2.08	2.15	2.23
27	1.84	1.90	1.97	2.03	2.10	2.17
28	1.79	1.85	1.91	1.98	2.04	2.11
29	1.73	1.79	1.85	1.91	1.97	2.04
30	1.66	1.71	1.77	1.83	1.89	1.95
31	1.58	1.63	1.68	1.73	1.79	1.85
32	1.50	1.55	1.60	1.65	1.71	1.76
33	1.43	1.48	1.52	1.57	1.62	1.68
34	1.37	1.41	1.46	1.5	1.55	1.60
35	1.31	1.35	1.39	1.44	1.48	1.53
36	1.26	1.29	1.33	1.37	1.42	1.46
37	1.20	1.24	1.28	1.32	1.36	1.40
38	1.16	1.19	1.23	1.26	1.30	1.34
39	1.11	1.14	1.18	1.21	1.25	1.29
40	1.07	1.10	1.13	1.16	1.20	1.24

TABLE B-5: THEORETICAL EER VARIATION WITH AMBIENT AND MT EVAPORATION SUPERHEAT, FOR A PARALLEL COMPRESSOR SYSTEM, ALONG WITH PERCENTUAL CHANGE

Gas Cooler Temperature [°C]	MT evaporator superheat [K] / whole system superheat [K]									% change from 4K to 16K
	4 / 9	6 / 11	8 / 13	9 / 14	10/15	11/16	12/17	14/19	16/21	
20	2.52[1]	2.51[1]	2.50[1]	2.50[1]	2.50[1]	2.49[1]	2.49[1]	2.48[1]	2.47[1]	-2.0%
21	2.50[1]	2.48[1]	2.48[1]	2.48[1]	2.47[1]	2.47[1]	2.47[1]	2.46[1]	2.45[1]	-2.0%
22	2.47[1]	2.45[1]	2.45[1]	2.46[1]	2.46[1]	2.45[1]	2.45[1]	2.44[1]	2.44[1]	-1.2%
23	2.45	2.44	2.43	2.43	2.43	2.42	2.42	2.41	2.41	-1.7%
24	2.42	2.42	2.41	2.40	2.40	2.40	2.40	2.39	2.38	-1.7%
25	2.39	2.39	2.38	2.38	2.37	2.37	2.37	2.37	2.36	-1.3%
26	2.37	2.36	2.35	2.36	2.35	2.35	2.34	2.35	2.34	-1.3%
27	2.34	2.33	2.33	2.32	2.31	2.32	2.32	2.31	2.31	-1.3%
28	2.30	2.30	2.29	2.29	2.28	2.29	2.28	2.27	2.28	-0.9%
29	2.26	2.26	2.25	2.24	2.24	2.24	2.24	2.24	2.23	-1.3%
30	2.20	2.19	2.19	2.19	2.18	2.18	2.19	2.18	2.18	-0.9%
31	2.11	2.10	2.10	2.09	2.10	2.09	2.09	2.09	2.09	-1.0%
32	2.00	2.00	2.00	2.00	2.00	2.00	2.00	2.00	1.99	-0.5%
33	1.92	1.92	1.92	1.91	1.91	1.91	1.91	1.91	1.91	-0.5%
34	1.84	1.84	1.83	1.83	1.83	1.83	1.83	1.83	1.83	-0.5%
35	1.75	1.75	1.75	1.74	1.76	1.75	1.76	1.75	1.75	0.0%
36	1.68	1.68	1.67	1.68	1.68	1.67	1.68	1.67	1.68	0.0%
37	1.61	1.61	1.61	1.61	1.62	1.61	1.61	1.61	1.61	0.0%
38	1.55	1.55	1.55	1.55	1.55	1.55	1.55	1.55	1.55	0.0%
39	1.50	1.50	1.49	1.49	1.49	1.49	1.50	1.49	1.49	-0.7%
40	1.44	1.44	1.44	1.44	1.44	1.44	1.44	1.43	1.44	0.0%

[1]Smaller parallel compressor used.

TABLE B-6: THEORETICAL EER VARIATION WITH AMBIENT AND MT EVAPORATION SUPERHEAT, FOR A FLASH GAS ONLY SYSTEM, ALONG WITH PERCENTUAL CHANGE

Gas Cooler Temperature [°C]	MT evaporator superheat [K]								
	4	6	8	9	10	11	12	14	16
20	2.34	2.34	2.33	2.33	2.33	2.33	2.32	2.32	2.32
21	2.30	2.30	2.30	2.29	2.29	2.29	2.29	2.29	2.28
22	2.26	2.26	2.26	2.26	2.25	2.25	2.25	2.25	2.25
23	2.22	2.22	2.22	2.22	2.22	2.21	2.21	2.21	2.21
24	2.18	2.18	2.18	2.17	2.17	2.17	2.17	2.17	2.17
25	2.14	2.13	2.13	2.13	2.13	2.13	2.13	2.13	2.12
26	2.09	2.09	2.08	2.08	2.08	2.08	2.08	2.08	2.08
27	2.04	2.03	2.03	2.03	2.03	2.03	2.03	2.03	2.03
28	1.98	1.98	1.98	1.98	1.98	1.97	1.97	1.97	1.97
29	1.91	1.91	1.91	1.91	1.91	1.91	1.91	1.91	1.91
30	1.83	1.83	1.83	1.83	1.83	1.83	1.83	1.83	1.83
31	1.73	1.73	1.73	1.73	1.73	1.73	1.74	1.74	1.74
32	1.65	1.65	1.65	1.65	1.65	1.65	1.65	1.65	1.65
33	1.57	1.57	1.57	1.57	1.57	1.57	1.57	1.58	1.58
34	1.50	1.50	1.50	1.50	1.50	1.50	1.50	1.50	1.51
35	1.43	1.43	1.43	1.43	1.44	1.44	1.44	1.44	1.44
36	1.37	1.37	1.37	1.37	1.37	1.37	1.38	1.38	1.38
37	1.31	1.31	1.31	1.31	1.32	1.32	1.32	1.32	1.32
38	1.26	1.26	1.26	1.26	1.26	1.26	1.26	1.27	1.27
39	1.21	1.21	1.21	1.21	1.21	1.21	1.21	1.21	1.22
40	1.16	1.16	1.16	1.16	1.16	1.17	1.17	1.17	1.17

Annex C: Tables from real installation study

TABLE C-1: AVERAGE COOLING UNIT TEMPERATURE BEFORE AND AFTER MT SUCTION PRESSURE CHANGE

Station Reference	Average T before change [ºC]	Average T after change [ºC]	Difference
Tl01	1.29	1.61	**0.32**
tl02	0.53	0.80	**0.27**
tl03	5.90	6.00	**0.11**
tl04	5.66	5.75	**0.09**
CH02	0.91	1.16	**0.25**
CH03	2.31	2.31	**0.00**
CH04	2.26	1.88	**-0.38**
CH01	1.03	1.15	**0.12**
CH05	3.61	3.31	**-0.29**
FL01	4.25	4.03	**-0.22**
FL02	4.16	4.21	**0.05**
FL03	3.25	3.46	**0.21**
TW01	2.80	3.25	**0.45**
TW02	2.21	2.34	**0.13**
CH06	1.77	2.14	**0.38**
CH07	1.38	1.55	**0.16**
CH08	1.39	1.53	**0.14**
CH09	1.16	1.16	**0.00**
CH10	1.12	1.10	**-0.02**
LT01	2.72	3.01	**0.29**
LT02	2.08	2.43	**0.35**
LT03	2.95	3.05	**0.10**
LT04	2.13	2.35	**0.22**
LT05	2.12	2.48	**0.36**
LT06	2.19	2.72	**0.53**
LT07	2.06	2.43	**0.37**
LT08	2.23	2.37	**0.14**
LT09	2.48	2.99	**0.51**
LT10	3.12	2.93	**-0.19**
CP	4.70	5.25	**0.55**
CL	2.75	3.14	**0.39**
CA	1.12	1.44	**0.32**
CB	3.77	3.77	**-0.01**
CT	3.01	3.31	**0.30**
LO1	18.54	18.43	**-0.11**
LO2	20.37	19.06	**-1.31**
BF	12.05	12.16	**0.11**
CT	1.89	1.77	**-0.11**
CP	2.44	2.42	**-0.02**
CC	3.71	3.77	**0.06**
CF	2.91	3.08	**0.17**

TABLE C-2: AVERAGE COOLING UNIT TEMPERATURE BEFORE AND AFTER MT EVAPORATOR SUPERHEAT CHANGE

Station Reference	Average T before change [ºC]	Average T after change [ºC]	Difference
Tl01	1.32	1.19	-0.12
tl02	0.63	0.53	-0.11
tl03	5.66	5.51	-0.15
tl04	5.70	5.68	-0.02
CH02	0.97	0.97	-0.01
CH03	1.95	1.71	-0.24
CH04	2.07	2.34	0.28
CH01	1.53	1.20	-0.33
CH05	3.32	3.52	0.20
FL01	2.93	2.13	-0.79
FL02	3.94	3.86	-0.07
FL03	3.27	3.52	0.25
TW01	2.82	2.54	-0.28
TW02	2.96	3.03	0.06
CH06	1.43	1.45	0.02
CH07	1.53	1.41	-0.12
CH08	1.51	1.27	-0.23
CH09	1.18	1.23	0.04
CH10	1.10	1.23	0.13
LT01	2.72	2.49	-0.22
LT02	2.10	2.04	-0.06
LT03	3.00	2.88	-0.13
LT04	2.08	1.93	-0.15
LT05	2.13	1.91	-0.21
LT06	2.26	2.07	-0.19
LT07	2.06	1.92	-0.14
LT08	2.25	2.16	-0.09
LT09	2.51	2.40	-0.11
LT10	2.76	3.13	0.37
CP	4.40	4.93	0.53
CL	2.94	3.17	0.23
CA	1.29	1.30	0.01
CB	3.92	3.96	0.03
CT	3.30	3.08	-0.22
LO	19.78	18.81	-0.97
LO	15.74	15.76	0.03
BF	12.23	13.10	0.87
CT	1.58	1.71	0.14
CP	2.24	2.18	-0.06
CC	3.90	3.86	-0.05
CF	2.81	2.95	0.14